Bi-Level Optimal Control Algorithm for Climate Optimized Cruise Trajectory

With En-route Step Climb and Descent Flight Modes

Kaushik Radhakrishnan

Technische Universiteit Delft

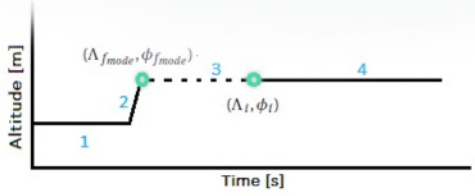

Switching Time (s)		
t_1	t_2	$t_3(t_f)$

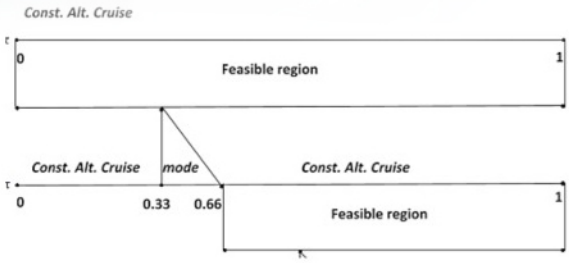

TU Delft Delft University of Technology

Challenge the future

Bi-Level Optimal Control Algorithm for Climate Optimized Cruise Trajectory

With En-route Step Climb and Descent Flight Modes

by

Kaushik Radhakrishnan

in partial fulfillment of the requirements for the degree of

Master of Science
in Aerospace Engineering

at the Delft University of Technology,
to be defended publicly on Thursday July 26, 2018 at 02:00 PM.

Student number:	4501497	
Project duration:	March 1, 2017 – July 5, 2018	
Thesis committee:	Prof. dr. ir. H. G. Visser	TU Delft, Chair committee and Supervisor
	Prof. dr. ir. S. Hartjes,	TU Delft, Air Transport and Operations
	Prof. dr. ir. M. Voskuijl,	TU Delft, Flight Performance and Propulsion

TU Delft Delft University of Technology

ABSTRACT

In the year 2050, global anthropogenic radiative forcing from aircraft emissions are projected to increase significantly. Recent studies have considered climate optimized flight trajectories to be a promising measure to mitigate non-CO_2 emissions' environmental impact, which is highly sensitive to locus and time of emissions. Estimating the maximum mitigation potential from these trajectories requires accounting of air traffic regulations. As designing regulated climate optimal trajectories necessitates solving a hybrid optimal control system with unknown mode sequence and associated switching times, there is a need to build an efficient and systematic control technique. In this thesis, a bi-level optimal control algorithm is proposed for designing climate optimal cruise trajectories, the lower level calculates the optimal switching times and control inputs of a fixed mode sequence and, the upper level updates the mode sequence with mode insertion which lower the cost locally. The problem for trajectory optimization is formulated here as a hybrid optimal control problem with a switched system and with a variable mode sequence, where step-climb and descent modes are included in the mode sequence. Optimal Control problems for minimizing operating cost and climate cost with fictitious climate cost functions (CCF), varying with altitude, are solved to study the performance of the algorithm. The algorithm is implemented within the Trajectory Optimization Module (TOM) by building a bi-level framework. The framework was validated by solving the operating cost optimal control problem. The maximum error between the cost reduction estimated by the algorithm and the actual cost reduction was found to be less than 15%. With high probability it can be stated that the bi-level framework is able to calculate an optimal mode sequence as the framework allow for zero entry modes in the mode sequence i.e. modes of zero duration. Although, careful consideration is required while selecting a mode for insertion as the framework is highly dependent on the sequence of the set of modes.

Despite a satisfactory performance of the bi-level optimal control technique there are few challenges which limits the scope of this technique. The maximum error was found to increase for optimal control problems with AirClim CCFs. The dependence of the AirClim CCFs on position of the aircraft influences the locus of the trajectory at each flight level. Because of this the the trajectories calculated in each iteration of the framework are found to be inconsistent. A flight trajectory guided by waypoints is proposed as solution for future studies to handle the inconsistency between trajectories. As future studies are expected to focus on finding optimal mode definitions for designing climate optimal trajectories, the bi-level optimal control algorithm can act as an intermediary tool with which the researchers can systematically investigate cost benefits along the trajectories.

Keywords: Aircraft Trajectory Optimization, Bi-Level Control Algorithm, Climate Optimized Trajectory, Hybrid Systems, Optimal Control Theory, Switched System

ACKNOWLEDGMENT

I would like to thank Mr. Benjamin Lührs and Institute of Air Transportation (DLR), Hamburg for offering an interesting and worthy project for my thesis. During my working days at DLR, Benjamin acted as my direct supervisor. His open door policy and enthusiasm in solving problems was a huge motivation in pursuing this study. He was always assuring and believed in my work. With his guidance I was able to ensure a constant progress within my work. The experience gained from DLR has taught me a lot and has inspired me to become a better professional.

The satisfactory completion of this thesis would not have been possible without the support of Prof. Dries Visser. The conclusions derived in this study are dedicated to his expert guidance. His thorough knowledge of the subject gave me an immense opportunity to learn and grow. He never hesitated to challenge my ideas and directed me patiently. He was always eager to help and was very understanding. I am grateful for Prof. Visser's input in my thesis.

Any work environment becomes unstable without a well functioning personal and social environment. All my friends in Delft, Hamburg and India kept me motivated and made me determined to see the end of it. A special mention goes to Lisa Harseim for her unfailing support. Indifferent of the circumstances, she was always ready to help. The project duration was made easy because of her acquaintance. She also deserves a special credit for making a significant contribution in designing the cover page of this thesis.

A final thanks goes to my family who are my strongest supporter. Their inexplicable confidence and trust in me encourages me to achieve excellence. I am indebted to my parents for their constant support regardless of my success or failure. I am forever grateful to have such an amazing family.

Kaushik Radhakrishnan
Delft, July 2018

CONTENTS

List of Figures

List of Tables

1

INTRODUCTION

Aviation emissions primarily consist of carbon dioxide (CO_2), Nitrogen Oxides (NO_x), water vapour (H_2O) and particles (aerosols and soot particles). With varying level in certainty, the global effect from the emission of these greenhouse gasses is predicted to warm up the Earth's surface. The Radiative Forcing (RF), a measure of the change in energy balance of Earth, measured (as of 2005) from global aviation is estimated to be positive, see figure 1.1. Besides CO_2, the best estimate of RF from NO_x emissions also indicate a positive contribution. Based on the current understanding, NO_x is considered responsible for the formation of the Ozone (O_3) and reduction of methane (CH_4) from the atmosphere. Further, the contribution of water vapour (H_2O) and soot particles is suspected to be positive, since these are predicted to enhance cirrus cloud from spreading contrails.[6]

In a span of 5 years, from 2000 to 2005, there has been a 14% increase in total RF. The total aviation RF in the year 2005 was 3.5% of the total anthropogenic forcing and by 2050 it is estimated to be around 4-4.7% of the total RF, where the highest percentage of RF would be due to the non- CO_2 emissions[7]. In the year 2050, aircraft emissions are projected to increase, the global CO_2 by 3% , ozone concentration by 13%, contrail cover by 0.5% and cirrus cloud cover by 0.8%. The environmental impact due to air traffic emission would further raise as the air connectivity demands are expected to grow at a rate of 4.1% annually, according to IATA [8]. In a report published by IPCC [9] in 1999, it was predicted that by 2050 the range of technologies developed will not significantly reduce the global anthropogenic RF caused by the increasing air traffic. Researchers around the world are working on finding mitigating steps to reduce the impact of air traffic emissions on global warming.

In the past, significant research has been done in designing optimized flight trajectories to reduce climate impact due to aircraft emissions. The main aim of developing these climate optimized trajectories is to enable the policy makers to make a trade-off between the climate impact mitigation and operating cost, while making decisions on aviation operations. Various climate models have been used previously to express emissions impact on climate quantitatively. Studies, such of Oliveira,R. et al.[10], represent the climate impact in terms of Emission Indexes. The Emission Index (EI), defined as grams of pollutant per kilogram of burnt fuel (g/kg), are calculated using methods such as the Advanced Emission Model or the Boeing Fuel Flow Method (designed by Eurocontrol). The results of [10] showed improvements upto 21% in reducing aircraft emissions by optimizing only the vertical flight profile of the departure procedures at Frankfurt Airport. Further, the study of Sridhar et al.[11] combines the temperature response with the EI, based on a linear dynamic system response model, for Trans-Atlantic cruise flight. The cruise trajectories are then optimized in presence of winds while considering the environmental impact caused due to CO_2 emissions and contrails. The results of the study estimated 38% and 20% reduction in temperature response with an increase of 3.1% and 3.7% fuel burnt for westbound and eastbound Trans-Atlantic flights respectively. With estimated climate mitigation potential being significant there has been an increased interest in designing climate optimized trajectories.

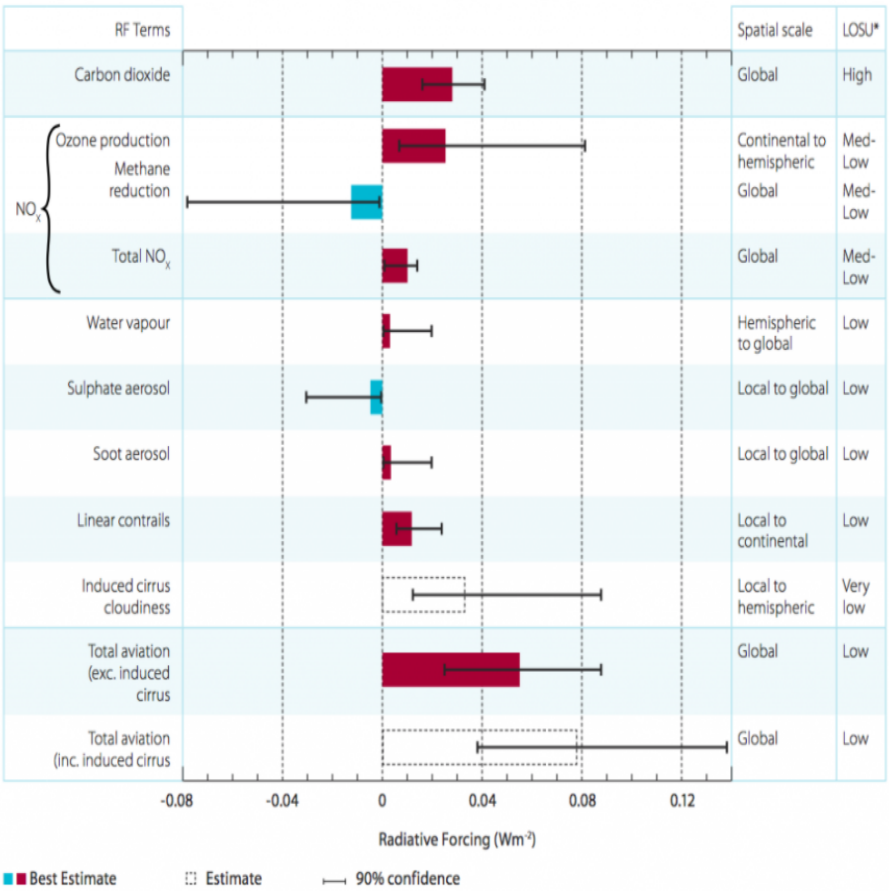

Figure 1.1: **Estimates for radiative forcing from global aviation in 2005. The error bars represent the 90% likelihood range for each estimate. The level of scientific understanding (LOSU) is shown on the right. Source: reproduced from [1].**

1.1. CLIMATE IMPACT AND AVIATION EMISSIONS

The increasing understanding of the climate system and improved climate simulation models has allowed researchers to reproduce the observed global temperature patterns and trends over many decades[6]. As mentioned previously and from figure 1.1,the non-CO_2 emissions are estimated to have a significant contribution in global climate change e.g. from changes in ozone, methane, cloudiness and others. According to the report published by IPCC[9], these non-CO_2 emissions are characterized to have temporal and spatial variability in their effects. The impact of these emissions on climate depends not only on the amount of emitted substances, as would be the case with CO_2 emissions, but also on the time and region where the emission takes place. Based on the qualitative assessment of the emissions variability the regions with high climate sensitivity have been identified. This aids in the development of possible strategies to minimize climate impact from optimizing aircraft trajectories. Further, efforts are made in modelling precise climate models for quantification of climate impact at regions with high climate sensitivity. This section will discusses the dependencies of individual emission and pin point prominent regions where the impact is significant.

1.1.1. CONTRAILS AND CIRRUS CLOUDS

Aircraft line-shaped contrails tend to warm the Earth's surface, similar to thin clouds. RF of contrails depends on their global cover and optical properties. Their formations are triggered from the water vapour emitted by the aircraft and their optical properties depends on the particles emitted and on ambient atmospheric conditions. A faster growth in contrail cover is expected due to increase in air traffic. The growth is mainly expected to increase in the upper troposphere, also where the contrails form preferentially. The contrail cover over Earth's surface is projected to grow from 0.1%, in 1992, to 0.5%, in 2050. It is also suspected that the contrail formation may occur with improvements in aircraft fuel efficiency.[9]

According to the current understanding of contrails, they are known to form at high altitudes where the

ambient temperature is low. In dry air the contrails dissolve quickly and in regions where the relative humidity with respect to ice is high they persist. As the expected effects of persistent contrails is predicted to be three to four times greater than that of carbon dioxide[12], recent studies have focused on developing strategies to optimize flight path for contrail avoidance.[13] To assess the potential of contrail mitigation through trajectory optimization, studies in [14] and [15] propose optimization algorithm with climate impact models to predict the formation of persistent contrail.

In ice-supersaturated air the contrails grow with the absorption of ambient water vapour and turn into contrail-cirrus. The increasing trend in cirrus/high cloud over congested air traffic regions are attributed with aviation activities. Cirrus formations are noticed to occur mainly in the regions of North America, North Atlantic and Europe. Over central Europe the cirrus coverage is estimated to increase by about 1-2% per decade. This has led to an increased interest in optimizing Trans-Atlantic flight routes for contrail mitigation e.g.[11]. However, due to limited understanding on cirrus clouds the RF of these are unknown presently.[13]

1.1.2. NO_x, H_2O AND PARTICLES

NO_x emissions are estimated to have increased the ozone concentrations at the cruise altitudes in northern mid-latitudes by up to 6% and are projected to rise to about 13% in 2050 from aircraft activities. Further, NO_x emissions are expected to decrease the methane concentration by 5% in the year 2050. The effect of ozone concentrations are effectively observed to increase through NO_x emissions in the upper troposphere mainly in the Northern Hemisphere. The largest increase in ozone concentration due to aircraft emission is calculated to occur near the tropopause where natural variability is high. It is also observed that the aircraft NO_x emissions have a stronger effect in the upper troposphere than an equivalent amount of emission on the surface. Although, the RF of methane and ozone are of similar magnitude and opposite in sign, the difference in latitudinal structure of the forcing does not cancel at regional level. However, the uncertainties in the sources and sinks of methane does not allow for a conclusive testing of the impact due to air traffic.[9]

Similar to previously discussed aircraft emissions, water vapour (H_2O) tends to increase the Earth's surface temperature. A smaller fraction of H_2O released in the lower stratosphere can build to large concentrations with time. Though the effect of H_2O is comparatively smaller than those of CO_2 and NO_x, the water emissions in stratosphere tend to partially off-set the NO_x induced ozone increase[9]. Further, as discussed in the previous section, based on the ambient atmospheric conditions the H_2O and particles emitted from aircraft in the troposphere region aids in the formation of persistent contrails.

As predominant effects of the latter discussed emissions are manifest in the upper stratosphere and troposphere region, studies with trajectory optimization for minimizing climate impact focus on developing optimal aircraft routes for cruise altitudes. As the cruise is the longest phase of a long range flights, increased interest lies in optimizing cruise trajectories to measure the maximum potential of climate mitigation through flight trajectory optimization. Although, few studies in the past have focused on calculating the mitigation of NO_x emissions for the cruise phase (e.g.[10, 16]), the climate impact models used in these studies do not include spatial and time variability. Thus, the results of these studies present a basic scope of climate mitigation with the purpose of motivating future studies to focus on developing climate optimized trajectories with improved climate models which can quantify climate impact based on variability of emissions.

1.1.3. CARBON DIOXIDE (CO_2)

In the year 1992, carbon dioxide emissions from all transportation sources accounted for 13% of the total anthropogenic carbon dioxide emissions. About 2% of the total CO_2 was contributed by the air traffic. As the RF from these emissions is resulting from emissions during the past 100 years, the concentration of CO_2 attributable to aviation in year 1992 is a little more than 1% of the total anthropogenic increase. By 2050 the projected accumulation of carbon dioxide due to aircraft accounts for 4% of that from all human activities[9]. Based on the understanding on the effects of CO_2 emissions, their accumulation in the atmosphere is predicted with high confidence to have a global impact raising the global mean surface temperature.[6]

CO_2 is the primary carbon gas emitted from aircraft engines because of complete combustion of aviation fuel. Since the total fuel consumption has a direct dependence on the operational cost, all previous studies of optimized aircraft routes for optimal operating cost have indirectly minimized the total aviation CO_2 emissions. Further, studies in [10, 17, 18, 16, 19] offer optimization frameworks for minimizing fuel consumption with cost models in presence of winds, wind shear and cross wind for different phases of the flight trajectory. The already available literature on the latter subject offers strong methodologies for predicting the reduction in carbon dioxide emission by optimizing flight trajectories. As the impact of the emission is global, these optimized trajectories could be extended to the global flight network.

1.2. CLIMATE COST FUNCTIONS

Based on the recent understandings of non-CO_2 emissions dependency on time, location and weather pattern studies are working on quantifying their variability. Within these studies climate cost functions (CCF) are calculated as a measure for the climate impact of individual aviation emissions depending upon the latter dependencies. These CCFs physically represent near surface temperature which is presumed to be a reasonable indicator for climate change. As the effects of the non-CO_2 emissions depends on individual weather situations different modelling approached are used for climate models. To the extent of author's knowledge, AirClim[20], a tool designed for climate evaluation of aircraft technology, and REACT4C[21], an European project developed to investigate the potential of climate optimized flight routing, offer climate models which are capable of quantifying the individual emission's spatial variability (CCF). Studies in Niklaß et al.[2] and Lührs et al.[4] have utilized AirClim tool and REACT4C climate model, respectively, for assessing the climate mitigation potential during cruise. Both studies have assumed a free airspace and constant speed cruise for North Atlantic flight routes and have reached similar conclusions, measuring large potential in climate mitigation.

1.2.1. CLIMATE MITIGATION WITH AIRCLIM CCFS

AirClim model is designed to be applicable for climate agents CO_2, H_2O, CH_4 and O_3 and contrails. The model linearises the complex functional chain from emissions to climate change including transport, chemistry, micro-physics, and radiation under consideration of climatological mean data. As climate-chemistry calculations are expensive in time and computational resources, AirClim combines pre-calculated atmospheric data with aircraft emission data. These pre-calculated data are derived from 25 steady-state simulations for the year 2050 with the climate-chemistry model E39/C, prescribing normalized emissions of NO_x and H_2O at various atmospheric regions. AirClim calculates the temporal evolution of atmospheric concentration changes, radiative forcing and temperature changes as a function of latitude and altitude, except contrails for which the climate changes are calculated as a function of latitude, longitude and altitude with minimal computational time.[20, 2]

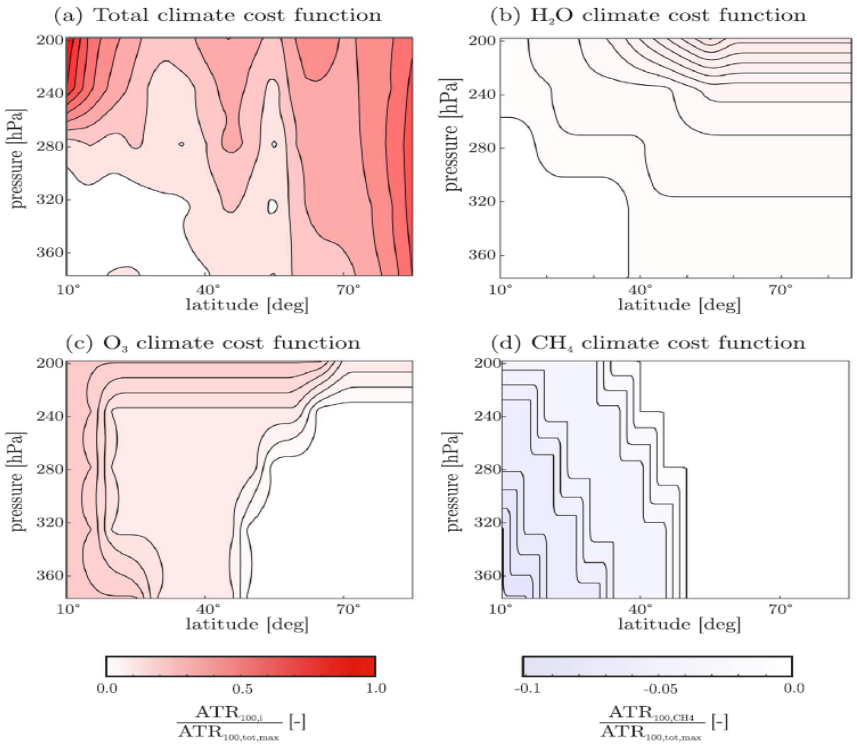

Figure 1.2: **Absolute climate change functions (CCF) at Greenwich meridian as function of altitude and latitude derived with AirClim. Figure show CCF of (a) all considered climate agents, (b)water vapor (H_2O), (c) ozone (O_3) and (d) methane (CH_4). Source: [2]**

The study in Niklaß et al[2] presents an interim climate mitigation strategy by defining climate restricted airspaces (CRA), regions with high climate sensitivity, characterizing the climate impact with CCFs calculated

from AirClim model. The restricted area are defined by selecting a threshold value (C_{thr}) which is based on the total climate costs. The total climate costs are determined from estimating the climate change, expressed as average temperature response over 100 years ($ATR_{100,i}$ for each climate agent i), over a defined time horizon caused by CO_2 and non-CO_2 emissions. The global mean surface temperature changes resulting from cruise emissions of each flight level is then investigated to define CRAs. The climate sensitivity calculated for climate agents, H_2O, O_3 and CH_4, between +15°and +80°northern latitude and between -130°and +30°eastern longitude for an altitude range of 7,610 m to 11,840 m is shown in figure 1.2.

The cruise trajectory between Helsinki (EFHK) and Miami (KMIA) is then optimized from re-routing the flights around the CRA. Within this study, the climate mitigation potential are investigated by calculating trajectories based on the percentage of overall airspace being closed. The study additionally also considers optimizing cruise trajectories by lowering the climate sensitivity along the trajectory. The overall mitigation potential for these trajectories are then investigated from varying climate mitigation weighting factor. The flight conditions for all trajectories calculated within this study assume a free flight with no ATM or ATS restrictions. The preliminary results of this study show potential to mitigate climate impact by 12% from climate optimized trajectories and 8.7% from CRA avoided trajectories with 28.8% of the total airspace closed, with no addition to the operational cost. The altitude variations in the flight path with time for climate optimized trajectories and CRA avoided trajectories calculated for varying climate weighting factors are shown in figure 1.3. Within these trajectories, it can be observed that with an increasing climate weighing factor (C_ψ) the flight altitude is altered such that regions with high climate sensitivity are avoided.

From figure 1.2 it can be observed that the climate sensitivity of all considered agents, except CH_4, is increasing with rising altitude. However, the combined climate sensitivity of these agents, see fig. 1.2 (a), is observed to be non-linear, without a strict increasing or decreasing gradient with altitude. The trajectories calculated with maximum weight factor for climate mitigation, see figure 1.3, also indicates this non-linearity, as these climate optimal trajectories cannot be categorized with only climb or descent flight profiles.

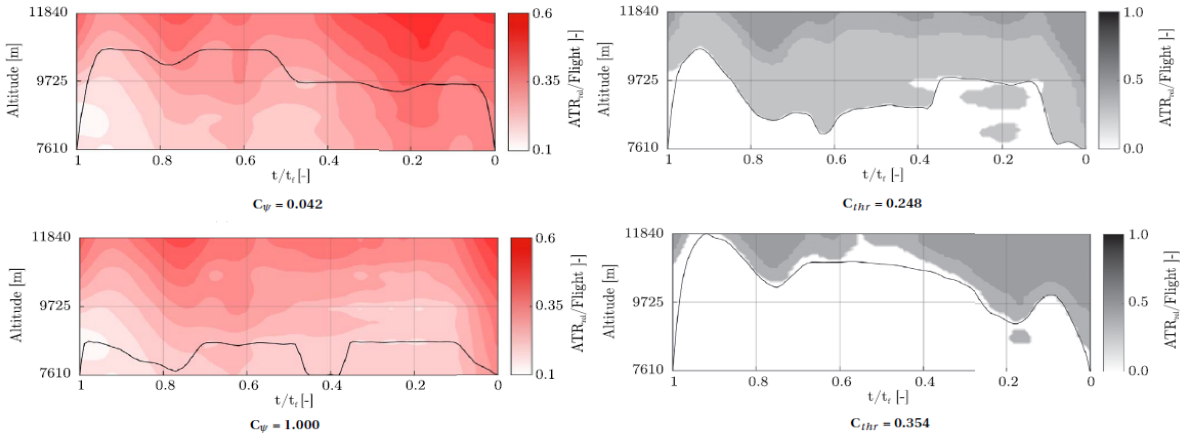

Figure 1.3: **(1)Altitude variation with flight time, on the left, for climate optimized trajectory, where C_ψ is the climate weighting factor and (2) Altitude - longitudinal plot for CRA avoided trajectory, on the right, with CRA are pictured along the cross-section of lateral path and C_{thr} represents total airspace available for air traffic for cruise trajectories from Helsinki (EFHK) to Miami (KMIA). Source [2]**

1.2.2. CLIMATE MITIGATION WITH REACT4C CCFS

REACT4C is an EU project which focuses on quantifying emission impact variability by first concentrating on frequently occuring daily weather patterns. The modelling approach of REACT4C uses Atmospheric Chemistry model (EMAC) to calculate climate cost functions. In REACT4C, the CCFs calculation includes the contribution of primary aviation emissions to atmospheric concentration and contrail properties. Further, the radiative impact is calculated over a time period of weeks leading to an approximate annual mean instantaneous RF. The model uses a correlation between instantaneous and adjusted RF to obtain a reliable basis for the expected climate change.[21]

Within the REACT4C project, the climate modelling approach provides CCFs for a defined weather situation. The most important aviation emissions are measured as a function of location, altitude and time. The calculation of climate cost function includes the calculation of the emission induced atmospheric changes

such as the perturbations of NO_x, O_3, CH_4, H_2O and the formation of contrails and their optical properties. In [3] the CCFs are calculated for the North Atlantic region. The study considered typical weather situations and released aviation emissions at 7 latitudes between 30°N and 80°N, at 6 longitudes between 75°W and 0°W, at four pressure levels between 200 and 400 hPa, and at 3 times between 6:00 and 18:00. Figure 1.4 (**A**) show the CCF calculated for H_2O and CH_4, as a function of latitude and altitude, at 30°W. Also, figure 1.4 (**B**) show the CCF calculated for contrail and O_3, as a function of latitude and longitude, at an altitude of 200 hPa. The contours of figure 1.4 show the RF, which serves as the basis for other possible metrics like global warming potential or global temperature potential. The results of the study estimate the RF value to increase with altitude for H_2O and is predicted to have longer lifetime, before dissolving, for stratospheric emission. The RF from CH_4 is predicted to increase from the tropopause towards mid-tropospheric altitudes and O_3 RF is estimated to increase with altitude. For the formation of contrail, it was predicted that at a specific altitude (200 hPa) there are regions with positive and negative RF and with large areas with no contrail formation. The distribution of the contrail is based on the extent of the ambient conditions i.e. ice super saturated regions which are suitable for contrail formation.

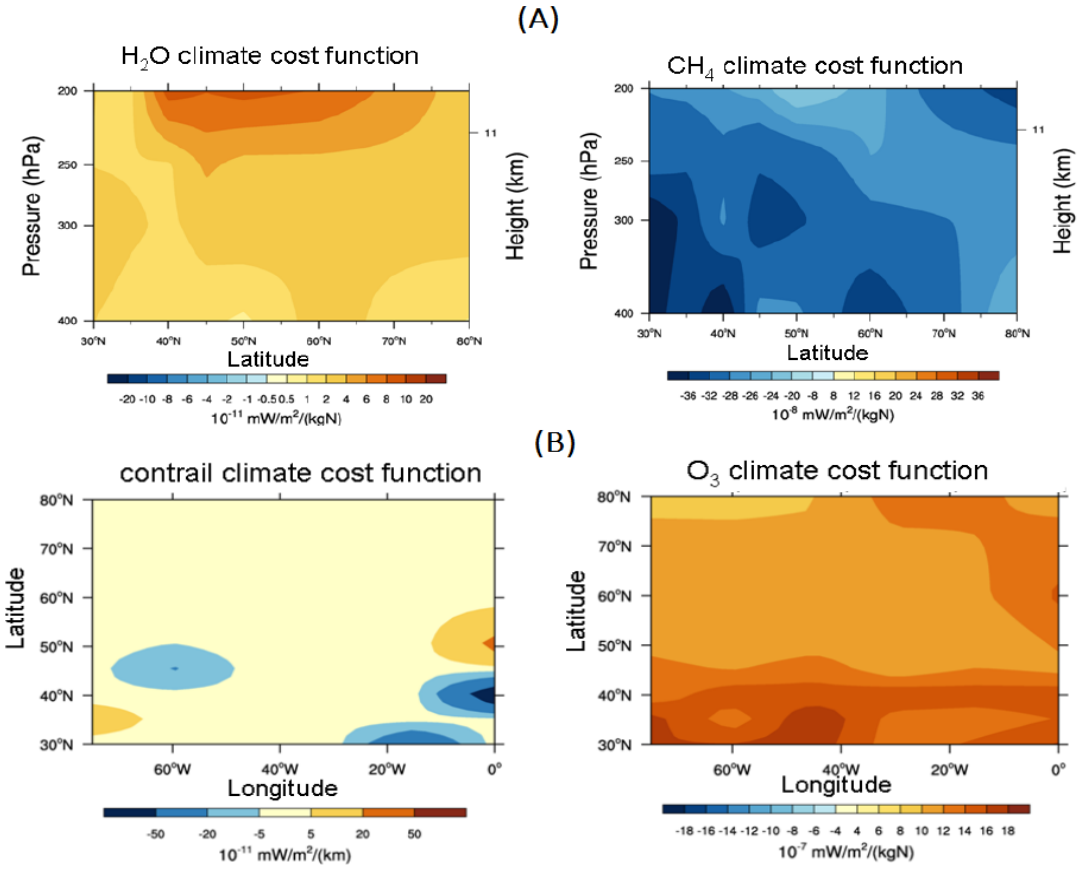

Figure 1.4: **A: H_2O and CH_4 climate cost functions in terms of net radiative forcing represented as a function of altitude (pressure) and latitude at 30°W. B: Contrail and O_3 climate cost functions in terms of net radiative forcing represented as a function of latitude and longitude at 200 hPa. Source [3]**

The climate mitigation potential with REACT4C CCFs were estimated by Lührs et al. [4] from investigating nine fictitious North Atlantic routes in the presence of winds for westbound and eastbound flights. The climate costs were expressed as average temperature response integrated over a time period of 20 years. The results of the study showed approximately 15% reduction in average temperature response from optimization with the horizontal plane (2D) for 2% rise in operating cost and 20-35% higher reduction for a similar rise in cost in case of 3D optimized trajectories. Similar to the study in [2], this study also calculates the climate mitigation potential for a constant speed cruise flight assuming free flight conditions without air traffic restrictions. Figure 1.5 show the altitude variations with longitude for 3D climate optimized cruise trajectories calculated from REACT4C CCFs.

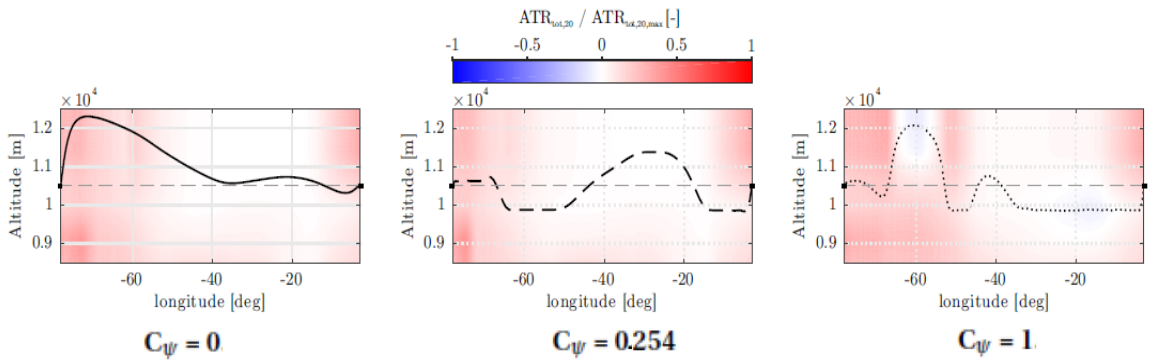

Figure 1.5: **Altitude variation with longitude plots of vertical and lateral optimized trans-Atlantic cruise flight investigated over fictitious flight routes for varying climate weighting factors (C_ψ). Source [4]**

The result of the study [4] demonstrated the influence of wind presence, in addition to climate sensitive regions, while determining the climate mitigation potential of climate optimized trajectories. The trajectories calculated were observed to have a constant altitude cruise in regions with weak winds and climb was encouraged in regions with strong headwinds. In addition to the wind direction and strength, the vertical profile of the trajectories were observed to climb or descent, if the reduction in climate sensitivities predominates the additional emissions caused by headwinds, increased cost from climb or descent phases, additional flight distance and off-design altitudes.

From the results of the studies, discussed in this and the previous section, it can observed that the vertical flight characteristics of the climate optimal trajectories are dependent on the CCFs of climate agents and wind conditions. Since, both CCF and wind conditions do not follow a strict increasing or decreasing gradient with altitude, the vertical profiles of the climate optimized trajectories are observed to include a climb or descent phase based on the estimated climate cost benefits.

1.3. CLIMATE TRAJECTORIES VS. ATM TRAJECTORIES

All climate optimized trajectories discussed in the previous section are calculated assuming free flight conditions and constant speed. However, actual flight profiles are regulated by Air Traffic Management (ATM) and Air Traffic Service (ATS) constraints and consist of different flight modes. The flight path and the sequence of flight modes are planned either by an Air Traffic Controller (ATC) or a pilot. This is fixed for most part of the flight until a variation in the sequence is deemed necessary due to operational or emergency reasons. Thus, unlike the altitude variations observed in case of free flight climate optimized trajectories, ATM regulated trajectories are restricted to pre-assigned Flight Levels (FL) and a change in altitude is achieved through step climb/descent procedures which are constrained by ATM and aircraft flight envelope. Further, to ensure safe flight strict restrictions on vertical separation between aircraft are imposed, called Semi-Circular rule[22], based on the course of the aircraft (westbound or eastbound).

1.3.1. SEMI-CIRCULAR RULE

To limit the possible conflicts with another aircraft coming from the opposite direction, the semi-circular rule defines a basic vertical separation for conventional airspace and between same types of aircraft. The basic rule for the flight levels or altitude selection is defined as a function of the aircraft course, separating the available flight levels into two categories; the even and odd flight level. The flight levels represent the altitude in feet rounded off to the nearest 100 or 1000 for altitude below and above 10,000 ft. respectively, e.g. FL 40 corresponds to 4000 ft. and FL 330 corresponds to 33,000 ft. All flight levels with an even number before the final 0 are termed as even flight levels (FL 40, 60, 120...) and flight levels with odd number before the final 0 are termed as odd flight levels (FL 50, 70, 90, 130...). For a conventional airspace, the semi-circular rule defines the flight levels based on East/West orientation, where the aircraft track with heading angles between 0°to 179°is assigned odd flight level and for heading angles between 180°to 359°is assigned even flight levels. Further, the available flight levels between FL 290 and FL 410 are defined by the semi-circular rule as RVSM (Reduced Vertical Separation Minimum) airspace where 1000 ft. separation between two aircraft are provided.[22] Figure 1.6 show a visual example of the semi-circular rule followed in conventional airspace.

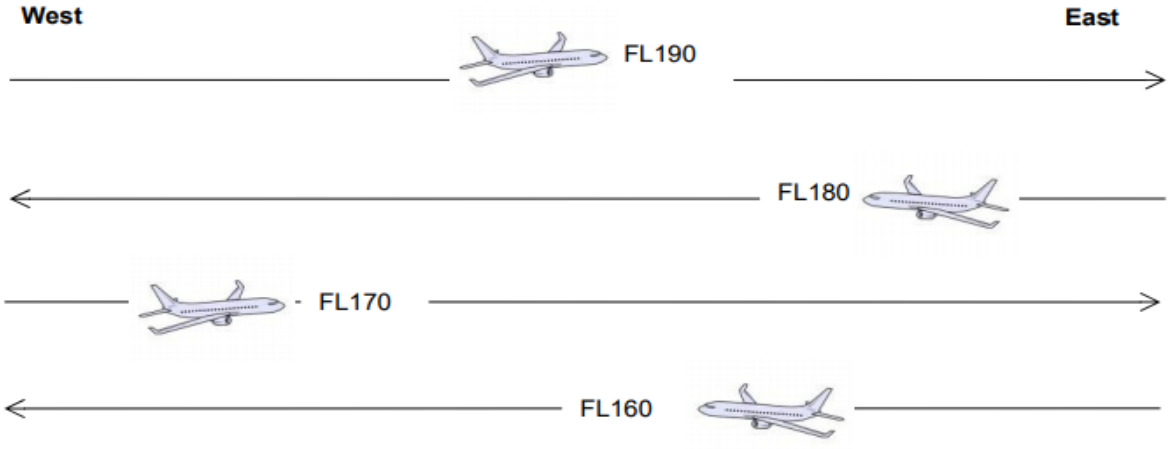

Figure 1.6: **Vertical separation between eastbound and westbound flights defined by semi-circular rule for a conventional airspace, restricting available airspace to even and odd flight levels.**

Previous studies that have estimated the potential of climate optimized trajectories for climate mitigation have observed a difference in the plausible reduction of climate impact for the same routes depending on the flight orientation. The difference in overall potential with orientation is observed for CO_2 and non-CO_2 emissions alike (ref. [11, 4]. Thus for the realization of the maximum potential for climate mitigation through climate optimized trajectories in an ATM airspace would require optimized flight profiles to be constrained by semi-circular rule. Further, it is also important to note that the flight levels refers to the pressure altitude and not the geometric altitude. This is mainly because the performance of an aircraft is based on pressure altitude for different reasons such as, the geometrical altitude provided by GPS becomes unreliable at higher altitudes, to and to have a redundant system.

1.3.2. STEP CLIMB AND DESCENT

The climb mode of an aircraft characterizes the flight motion that calls for an increase in altitude. In the cruise phase of the flight, climbing in steps to an optimum altitude is proposed as one of the best practices for fuel economy (according to ICAO[23]). Further, apart from fuel efficiency, a climb in cruise phase is also carried out upon ATC request to maintain a specific cruise speed or for turbulence avoidance. A climb in all phases of flight should abide by the semi-circular rule where the aircraft can climb only to the designated flight levels (odd or even). The maximum altitude to which civil aircraft is allowed to climb is FL 411, although the ceiling altitude of most civil aircraft are lower than this. During climb, the safety envelope of the flight restricts the speed requirement and the climb is carried out in vertical speed mode where the vertical speed takes precedence over the true air speed of the aircraft[24].

Similar to climb, the descent mode characterizes the flight motion for decrease in altitude. However, descent during cruise is not a common practice but is only included into the sequence of flight modes for emergency situation or to avoid incoming traffic. A descent in altitude for either of the latter reasons still abides by the semi-circular rule unless the pilot declares a Mayday emergency situation. Further, the speed mode selected and speed restrictions imposed during descent are conceptually similar to that of the climb mode.

For an estimation of the maximum potential of the climate optimized trajectories, a study would require to develop aircraft routes constrained by ATM regulations. As climate optimized trajectories discussed previously include non-linear altitude variations, an extension of these trajectories in a conventional airspace would pose a serious challenge to safety of airspace as potential conflicts may arise between aircraft routes. A study for climate optimized trajectories with ATM constraints imposed would serve as a comparison to the potential climate mitigation between free flight conditions and a conventional airspace. The results of such a study would allow future research to consider improved methodology in developing aircraft routes through any perceived modifications to the ATM restricted airspace. This study considers A330-200 type aircraft in all future references, as this aircraft has been selected in the studies discussed in section 1.2

2

Optimal Control Problem

The optimization of flight trajectories is possible with the application of optimal control theory which can consider dynamic effects of the new generation high performance aircraft. In optimal control theory the governing physical principles of the system, referred as system-state, are described with a set of parameters called state variables. The evolution of the system state in time is influenced by the inputs (control variables). The main objective of the optimal control problem is to steer the system by means of it's control variables in such a way as to achieve the best value for the specified performance index (eg.: maximize range, minimize fuel consumption), without violating any constraints imposed on the system. Solving these control problems employ analytical methods which are iterative and require high computation time. To reduce the computational complexity, efforts are made to generate near-optimal solution based on simplified system models. [25]

The flight of an aircraft can be distinguished with several flight phases such as climb, cruise and descent, where each phase is associated with a dynamical model and set of constraints (or boundary conditions). Since, cruise is the longest phase of the flight, for a long-haul flight, most studies with optimal control theory have focused on optimizing the cruise part of the flight. Studies such as [26] have optimized cruise trajectories with multiple cruise altitudes, where each cruise segment is followed by a climb mode. The optimal control problem for trajectories with multiple flight modes are formulated as a hybrid control system as the state of the flight is defined as a combination of continuous dynamics and discrete switches between modes. Solving an hybrid control problem is highly complex and hard as the optimization is expected to calculate both, the optimal mode sequence and their corresponding switching times. This complexity is often handled by assuming the mode sequence to be known and thus solving only for their discrete switching times. The hybrid control problem with known mode sequence is then solved with multi-phase framework.

A multi-phase framework approach in trajectory optimization allows to split the trajectory into phases. Each phase can then be defined with different dynamics, constraints and performance index, allowing the inclusion of ATM constraints into the problem formulation. However, based on the trajectories calculated for minimizing climate impact, discussed in section 1.2, assuming a phase sequence is not straightforward as the trajectories are dependent on the temporal and spatial variability of emissions. Few studies in the past have proposed improved analytical approaches for calculating the mode sequence for climate optimized trajectories. All of these approaches were found to be highly complex and required high computation time. Alternately, to overcome such complexities Gonzalez et al.'s[27] proposes a bi-level hierarchical algorithm to solve control problems with variable mode sequence, where the lower level minimizes the performance index for a given mode sequence and the higher level updates the mode sequence based on a single mode insertion technique.

For calculating climate optimized cruise trajectories with ATM regulated climb and descent modes, this chapter focuses on developing a control technique based on a bi-level optimization. Initially, a brief description of the hybrid control system is given and available literature on optimization techniques for solving optimal control problem for hybrid systems are reviewed. To describe the scheme of the bi-level optimization a numerical interpretation is presented. Finally, the necessary characteristics of the bi-level control technique are discussed with the purpose of extending it's scope of application for designing climate optimized trajectories.

2.1. HYBRID CONTROL SYSTEM

Hybrid control systems are dynamical system which comprise both discrete and continuous state variables. The discrete component involves the sequence of the modes and the continuous components corresponds to both the mode duration and continuous inputs of each mode. The class of hybrid dynamical systems whose state exhibit continuity while switching between modes are called switched dynamical systems. A general model of the switched system includes both controlled and autonomous switches. A controlled switch between modes occur in response to certain control input and an autonomous switch takes place as certain region of the state space are reached. An optimal control problem for the switched system thus seeks for the optimal sequence, switching instants and continuous inputs. [5]

The flight of an aircraft intrinsically has the characteristics of a switched system, where the sequence of the flight modes are fixed either by the pilot or ATC controller. Studies in the past have designed trajectories for aircraft from solving optimal control problem for a switched system, where the mode sequence is assumed to be given. With recent focus on planning environmentally sustainable flight profiles there has been a growing interest towards solving hybrid control problems with variable mode sequence. The efficient nonlinear optimization techniques and high-performance computers have enabled the development of numerical methods for such problems. These methods include a two stage (bi-level) optimization, where the stage 1 seeks the optimal continuous inputs and optimal switching instants, and stage 2 seeks optimal sequence [28]. However, numerical complexities of these methods have limited their applications in designing flight trajectories because of large computation time.

In this section available literature on optimization techniques are reviewed to frame a bi-level optimization which can determine the optimal sequence and switching instants of discrete modes in a computationally efficient manner.

2.1.1. VARIABLE MODE SEQUENCE

For various formulations of optimal control problems with switched systems, Dynamic Programming (DP) is selected as an optimization technique to calculate mode sequence. The DP method utilizes a optimal value function for evaluating the impulse effect on cost from switching. This allows to determine the switching instant for a discrete mode at which the cost is minimum and thus enabling the determination of the position of the discrete mode in the mode sequence. The computation time with this approach is very high since the optimal solution is computed at each state. In the study of Ng,H. et al.[11] climate optimal cruise trajectories are developed with the concept of DP, where the optimal aircraft turning and step climbing locations are optimized based on the climate cost associated with each extremal generated by forward or backward integrations.

DP discritizes the state space from possible combination of transitions which enables the calculation of global minimum and since it does not contain any iterative calculations the computational time is predictable. However, combinatorial explosion problems may occur as the number of state variables increases. Furthermore, the representation of the value function becomes increasingly complex with increasing modes. The accuracy of the solution with the DP method depends on the discritezation grid and often needs adjustment to generate solutions suitable for practical use which may result in increased computational time. [29]

Xu et al.[29] consider stage wise optimization in which the maximum principle approach is utilized for providing sufficient condition to determine an optimal mode sequence. Gonzalez et al.[27] extends this method further and proposes a descent technique to find an optimal sequence while considering constraints. In the latter study an optimal control algorithm with two stages is developed where the higher level constructs a new lower cost mode sequence by employing a single mode insertion technique. This algorithm guarantees calculation of a locally optimal mode sequence by systematically evaluating cost reduction from mode insertions at candidate times. To demonstrate the advantages of the latter approach, in designing flight trajectories, the study in [30] calculates a mode sequence with climb and descent flight modes for weather avoidance. The results of this study suggest quick convergence to a solution, compared to the DP method discussed previously.

2.1.2. MULTI-PHASE OPTIMIZATION

In all of the two stage optimization approaches developed for hybrid control system, the lower level is constructed with an optimal control problem which solves for the optimal continuous inputs and optimal switching instants for a given mode sequence. The problems formulated for these control problems can described

as finding control inputs to steer the aircraft route from an initial waypoint to the final waypoint such that the performance index is minimized. The decision making process in these control problem arises while determining the optimal time at which a mode is activated. Studies which formulated control problems with known mode sequence have frequently used multi-phase formulation, often solved using the pseudo-spectral methods (eg. [31, 5]).

The multi-phase optimal control formulation splits the flight trajectory into phases (or modes) and each phase can then be associated with different dynamics, constraints and performance index. To enforce continuity across different phases the multi-phase problem needs interior point constraints and linkage conditions. Defining the latter conditions becomes very difficult for trajectories which are modeled to minimize performance indices that are represented with functions external to the aircraft dynamical system (for example climate cost). In order to relax the trigger conditions for switches between phases, studies in [5, 32] considered translating the multi-phase problem into a non-linear control problem, where the problem is converted to a conventional optimal control problem.

The multi-phase problem is converted to a conventional optimal control problem by making the unknown switching times of the phases part of the state variables and introducing an independent variable to model the decision making process. In the reformulated control problem a linear relation between the switching time and independent variable is established to represent the independent variable as time scaling factors from which the optimal switching times are calculated.

In general, non-linear control problems are the most challenging class of problems in computational optimization. However with advanced computer programs such as IPOPT[33], nonlinear solvers are developed which have proven effective in calculating locally optimal solution.

2.2. BI-LEVEL CONTROL ALGORITHM

Based on the literature, discussed in the previous section, this study develops a bi-level control technique with the algorithm proposed in the study [27] as the base. The control technique is defined as a two stage optimization such that the hybrid control problem is divided into two constrained optimization problem, for continuous dynamics and discrete switches respectively. The lower stage of the algorithm is defined such that a conventional optimal control problem is formulated for a given mode sequence and the higher stage updates the mode sequence from calculating a mode insertion which lowers the overall cost. The basic working principle of the bi-level optimization is presented below:

- *Stage 1*: A mode sequence is specified and then the optimal continuous input and switching times are calculated; using a multi-phase formulation.
- *Stage 2*: A new mode sequence is determined by inserting a mode into the mode sequence of Stage 1, which decreases the overall cost. If no such sequence can be found, the algorithm stops else it repeats stage 1 with the new sequence until the algorithm cannot determine a new sequence that would decrease the overall cost.

The following sections elucidates the bi-level optimal control algorithm with a mathematical representation of the optimization.

2.2.1. STAGE 1 - LOWER LEVEL

A hybrid switch system contains a set of n differential equations describing the dynamic system of the aircraft for different flight modes.

$$\dot{\boldsymbol{x}}(t) = f_q(\boldsymbol{x}(t), \boldsymbol{u}(t)), \quad q \in Q = \{1, 2, ..., N_q\} \tag{2.1}$$

Where $\boldsymbol{x} \in R^n$ represents the continuous state and Q represents all the discrete modes along the flight path. The control input $\boldsymbol{u}$ belongs to set of functions $\{\boldsymbol{u} : [0,\infty) \rightarrow U | \boldsymbol{u}$ is measurable$\}$, with $U \subset R^m$ a compact set, where m is the range of control inputs. The continuous dynamics for each discrete mode q in $Q = \{1, 2, ..., N_q\}$ is given by the vector field $f_q : R^n \times R^m$.

The bi-level algorithm at each iteration provides a mode sequence, with varying number of total modes. It is assumed that the mode sequence space is finite, let's say, N+1 number of mode sequences. The mode sequence space is represented as

$$\{\boldsymbol{\sigma} \in Q^{N+1} | \boldsymbol{\sigma}(j) \in Q \quad j \leq N+1\} \tag{2.2}$$

The notation t_i is introduced to indicate the switching times at which the mode changes from $\sigma(j-1)$ to $\sigma(j)$ and the corresponding dynamics changes from $f_{q'}$ to f_q, where $\sigma(j-1) = q'$ and $\sigma(j) = q$. The time t_i $\in [t_0, t_f]$ where i $\in$ {1,2,...,N} for a mode sequence with N+1 modes and, t_0 and t_f represents the initial (start) and final time of the sequence.

The hybrid optimal control problem can be formulated, for each mode, considering a switched system, where the state and control inputs are subjected to a set of M_j constraints, represented as,

$$\{\boldsymbol{h}_j(\boldsymbol{x}(t), \boldsymbol{u}(t)) \leq 0, j = 1, 2, ..., M_j\} \tag{2.3}$$

Find a σ which minimizes the following objective function or the cost functional, while satisfying the constraints 2.3.

$$J(\boldsymbol{\sigma}, \boldsymbol{u}) = \phi(x(t_f), x(t_0), t_0, t_f) + \int_{t_0}^{t_f} L(\boldsymbol{x}(t), \boldsymbol{u}(t))dt \tag{2.4}$$

The term L is called Lagrangian running cost and ϕ is the penalty term.

The first stage of algorithm finds optimal control inputs $\boldsymbol{u}$ and optimal switching times $\{t_1, t_2, ..., t_N\}$ for a given mode sequence σ, with N+1 flight modes. In this the number of switches and mode sequence are known. This multi-phase problem with unknown switching times can be solved by converting the problem into a conventional optimal control problem i.e. making the unknown switching time part of the state vector. An independent variable τ is introduced, with respect to which the switching times are fixed, as in the study [5].

Without loss of generality, it is assumed that $t_0 = 0$ and $t_f = t_{N+1}$. The switching times are introduced as new state variables $x_{n+1}, ...x_{n+i}, .., x_{n+N}$, corresponding to switching times t_i, where n represents the number of state vectors excluding the switching times. The final time t_f is also included in the state variable as x_{n+N+1}.

$$x_{n+i} = t_i \tag{2.5}$$

$$\dot{x}_{n+i} = 0 \tag{2.6}$$

There is a linear relation between the independent variable, τ, and switching times. The slope of this linear relation changes between two switching times intervals, $[t_i, t_{i+1}]$. The slopes are time scaling factors which are also a part of the optimal control problem solution. The linear relation between time, t, and independent variable, τ, is established such that at any fixed point, $\tau_i = \frac{i}{N+1}$, where t equals t_i for switching times and t_f for final time. The relation is defined as in eq. 2.7 and a graphical interpretation of the relation is shown in figure 2.1.

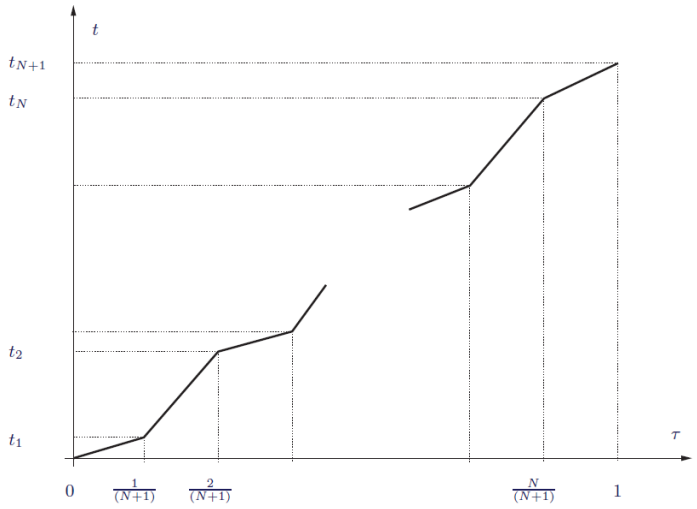

Figure 2.1: **Graphical representation of the relation between independent variable τ and real (unscaled) time t, Source: [5]**

$$t = \begin{cases} (N+1)x_{n+1}\tau & : \quad 0 \leq \tau \leq \frac{1}{N+1} \\ (N+1)(x_{n+i+1} - x_{n+i})\tau + (i+1)x_{n+i} - i x_{n+i+1} & : \quad \frac{i}{N+1} \leq \tau \leq \frac{i+1}{N+1}; \quad i \in [1, N] \end{cases} \tag{2.7}$$

The reformulated optimal control problem with extended state is as follows:

$$J = \phi(x(\tau_{N+1}), x(\tau_0), \tau_{N+1}) + \int_0^{N+1} L(\boldsymbol{x}(\tau), \boldsymbol{u}(\tau))d\tau \tag{2.8}$$

subject to

$$\dot{\boldsymbol{x}}(\tau) = f_{q_i}(x(\tau), u(\tau)), \quad \tau \in [i, i+1], i = 0, ..., N \tag{2.9}$$

$$\dot{\boldsymbol{x}}_{n+i+1}(\tau) = 0, i = 0, ..., N \tag{2.10}$$

$$\boldsymbol{h}_j(\boldsymbol{x}(\tau), \boldsymbol{u}(\tau)) \leq 0, j = 1, 2, ..., M_j \tag{2.11}$$

Since the duration of each mode is constant with respect to the introduced variable, the unknown switching times can be obtained from solving the above control problem.

2.2.2. STAGE 2 - HIGHER LEVEL

The difficulty with determining the discrete modes is that the trajectories obtained with a given mode sequence may be far from nominal one and hence not comparable in computationally efficient manner. However, if one considers a variation in which the modified sequence differs from the original one by modes whose durations are sufficiently small, one can then analyze the differences in the resulting trajectory and cost function [30]. The idea of the stage 2 described in [27] is to analyze these differences and calculate a lower cost mode sequence.

Consider insertion of a mode $\alpha \in Q$ initiated at a time $\hat{t} \in [t_0, t_f]$ for a duration $\lambda \geq 0$ into the mode sequence $\boldsymbol{\sigma}$. The mode dynamics are active in the interval $(\hat{t}, \hat{t}+\lambda)$. The mode characteristics are defined as $\boldsymbol{\eta} = (\alpha, \hat{t}, \hat{\boldsymbol{u}}) \in Q \times [t_0, t_f] \times U$, where $\hat{\boldsymbol{u}}$ is the inputs of the inserted mode. The insertion function $\rho^{\boldsymbol{\eta}}$: $\lambda \rightarrow (\hat{\boldsymbol{\sigma}}, \hat{\boldsymbol{u}})$ is defined to describe the insertion of mode α into sequence $\boldsymbol{\sigma}$. The definition of the insertion function is given in eqs. 2.12 and 2.13. In eq. 2.13, $u(t)$ is the continuous inputs of the mode sequence $\boldsymbol{\sigma}$.

$$\rho_\sigma^{\boldsymbol{\eta}}(\lambda) = (\sigma(1)_{(t_1)}, ..., \sigma(j)_{(\hat{t})}, \alpha_{(\hat{t}+\lambda)}, \sigma(j)_{(t_j+\lambda)}, ..., \sigma(N+1)_{(t_N+\lambda)}) \tag{2.12}$$

$$\rho_u^{\boldsymbol{\eta}}(\lambda) = u(t) + (\hat{u} - u(t))\|_{[\hat{t}, \hat{t}+\lambda]}(t) \tag{2.13}$$

To consider the variation in cost from the mode insertion the directional derivative is defined, see eq. 2.14. This evaluates the cost variation as λ approaches zero. If the directional derivative is negative then the insertion of mode α for a duration λ would decrease the cost.

$$\left.\frac{dJ(\rho^{(\boldsymbol{\eta})}(\lambda))}{d\lambda}\right|_{\lambda=0} = \lim_{\lambda \rightarrow 0} \frac{J(\rho^{(\boldsymbol{\eta})}(\lambda)) - J(\boldsymbol{\sigma}, \boldsymbol{u})}{\lambda} \tag{2.14}$$

Considering the control problem in hand, the discrete modes are cruise, step climb and step descent. Since the entire control problem is defined for a cruise phase, cruise is removed from the set of Q. The step climb and descent, both are a two point boundary value problem. The separation distance between the initial and final altitudes for both modes is fixed. This means that the insertion duration is finite, say $\bar{\lambda}$. In this study, the directional derivative will be evaluated for an insertion of finite duration $\bar{\lambda} \in [\lambda_{min}, \lambda_{max}]$, see equation 2.15. The duration range λ_{min}, λ_{max} are the minimum and maximum bound set on the mode duration respectively.

$$\frac{dJ(\rho^{(\boldsymbol{\eta})}(\bar{\lambda}))}{d\lambda} = \frac{J(\rho^{(\boldsymbol{\eta})}(\lambda)) - J(\boldsymbol{\sigma}, \boldsymbol{u})}{\bar{\lambda}} \quad ; where \quad \bar{\lambda} \in [\lambda_{min}, \lambda_{max}] \tag{2.15}$$

In addition to evaluating the cost variation, it is also important to ensure if the insertion is feasible i.e. if the physical constraints are not violated. An additional set of path constraints i.e. boundary conditions which are not included within the set of constraints imposed on state and control vectors, are defined as $\boldsymbol{h}_j(\boldsymbol{x}(t)) \leq 0, j = 1, ..., M$ and $t \in [t_0, t_f]$. Define a variable ψ, where $\psi = \max \boldsymbol{h}_j(\boldsymbol{x}(t))$. For the feasibility of the inserted mode in satisfying the constraints, it is sufficient to have

$$\frac{d\psi(\rho^{(\boldsymbol{\eta})}(\bar{\lambda}))}{d\lambda} < 0 \tag{2.16}$$

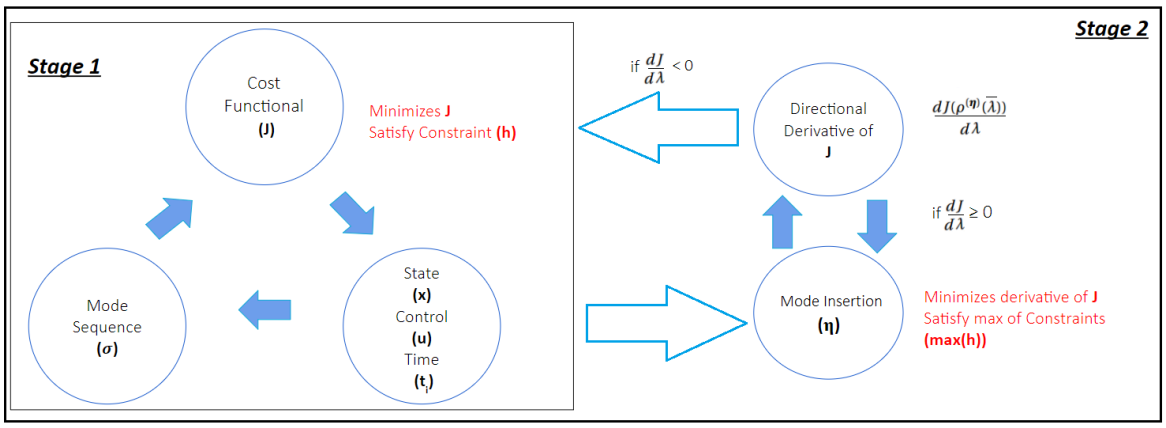

Figure 2.2: **A schematic representation for the bi-level optimization with the flow diagram explaining the algorithm within an optimizer**

Based on the variation of cost, the stage 2 of the algorithm selects a mode insertion which has maximum reduction in cost while ensuring the constraints remain feasible. It is important to note that the minimum of the directional derivative does not necessarily coincide with the global minimum as the cost variation calculated are discontinuous and are susceptible to changes with changes in mode inputs. Additionally, as this approach does not consider removing of a mode from the mode sequence, it is important that the feasible mode insertions at initial insertion times are given higher preference such that an optimal mode sequence could be calculated. The final optimality function constructed for stage 2 of the algorithm is given in eq. 2.17. The resulting mode sequence after insertion of the mode, characterized by $\boldsymbol{\eta}$, is the solution of the stage 2 optimization problem:

$$minmax\left\{\frac{dJ(\rho^{(\boldsymbol{\eta})}(\bar{\lambda}))}{d\lambda}, \psi(\boldsymbol{\sigma}, \boldsymbol{u}) + \frac{d\psi(\rho^{(\boldsymbol{\eta})}(\bar{\lambda}))}{d\lambda}\right\} \tag{2.17}$$

To implement stage 2 one should solve eq. 2.17 for every candidate mode $\alpha \in Q$, over the variable $\boldsymbol{\eta}$. Finding $\boldsymbol{\eta}$ at each insertion times requires solving a min-max problem. Once a $\boldsymbol{\eta}$ which lowers the overall cost is found, stage 2 would exit with a new mode sequence. The optimal switching times for this sequence is then calculated in stage 1. This loop between stage 1 and 2 is continued until no mode insertion can be found to decrease the cost.

2.3. STUDY OBJECTIVE

The bi-level algorithm, discussed in the previous section, provides a systematic technique to investigate a mode selection for a climate optimized trajectory based on the mode's feasibility to lower the climate cost. The algorithm was previously utilized in study [30] for solving simple weather avoidance control problem as means to demonstrate the algorithm's validity. However, because of discontinued study on the algorithm the maximum potential of such a technique remains unknown. Thus, before this control technique could be used in an optimization setup for solving the climate cost hybrid control problem, it is essential to first evaluate the algorithm's performance in more detail. An investigative study is selected to answer the questions on reliability of such an optimization method. This would lead to an increased understanding of the developed control technique and would allow to reach conclusive decision on the possibilities of designing ATM regulated climate optimal trajectories with bi-level technique. The study conducted herein restricts the hybrid control problem to a cruise phase with climb and descent modes. With a focus on investigating the bi-level algorithm's suitability for designing climate optimized trajectories, the results of this study are dedicated towards answering the following question, henceforth referred as the objective question:

> *Can ATM regulated climate optimized trajectories be designed from solving an optimal control problem with variable mode sequence using a bi-level control algorithm?*

The case studies in [27, 30] discusses the bi-level optimization scheme by transforming the hybrid control problem into one where the optimization of the trajectories are designed to avoid certain target points

within airspace. The objective function in these studies includes these target points in their final cost term. Since the overall cost was calculated from measuring the difference between the position of the aircraft and the target points, validating a feasible mode insertion calculated by the algorithm becomes simpler for the latter cases. However, for the optimal control problems with climate impact models, discussed in section 1.2, such transformations are difficult because the climate cost functions are determined using highly non linear differential equations, which makes defining target points very hard.

Since defining target points within advanced climate model is hard, validating the mode sequence calculated by the bi-level control algorithm becomes difficult. Thus, before evaluating the performance of the algorithm with advanced climate models, this study considers extensively studied control problem and fictitious climate models to measure the performance of the selected control technique. The optimal mode sequence for these control problems are calculated using the bi-level algorithm. Once the algorithm's performance with such simple climate models are validated then the algorithm can be extended to control problems with advanced climate models.

The future scope of this study requires evaluating the cost benefit potential, i.e. raise in operating cost vs. climate mitigation potential, from climate optimized trajectories. To obtain such a multi-objective optimization the cost functional needs to integrate the climate and operational cost. A simple yet efficient selection of the mathematical model, which describes the control problem, is required as the available computational resources are limited. Further, a flexible computational framework needs to be developed which enables fast debugging and also reduces the computation time.

In the following chapters, optimal control problems are formulated and solved with bi-level control algorithm to find an answer to the objective question. A mathematical model which describes the cruise regime of the flight is defined with cruise, climb and descent modes such that the trajectories designed are comparable to realistic ATM regulated flight paths. For formulating the control problems a computational framework is designed with the bi-level algorithm implemented. The performance measure in each of the control problem considered is tailored to represent the individual parameters which directly contribute to the climate cost functions calculated from advanced climate impact models. Finally, the optimal solutions obtained from solving the control problems along with the performance of the bi-level control technique are discussed. Based on this conclusions are drawn and future work of this is stated.

3

Mathematical Model and Computational Framework

A mathematical description used for solving an optimal control problem determines the applicability of the acquired solutions to the real world control problems. The objective thus of defining a mathematical model for optimizing trajectories is to adequately predict the response of a physical system such that the conclusions drawn from it remain valid for conventional airspace. Further, the inadequate understanding of the bi-level algorithm, discussed in section 2.3, requires a model which does not unnecessarily complicate the analysis of the results.

The set of parameters (state and control variables) which represent the state of the system in a mathematical model requires careful selection such that the system is neither oversimplified nor made too complex. A flexible system is essential for studying the performance of the proposed algorithm. This requires the identification of the parameters from each flight modes, i.e. cruise, climb and descent, which can adequately represent the characteristics of an airplane. It is also important that the behaviour of these identified parameters in each mode are previously known or understood through analytical studies. The latter becomes essential for validating the solution obtained from solving the control problem with a bi-level optimization framework.

Within the mathematical model the state-evolution with time is given using equations of motion. These equations of motion describe the state-evolution using a set of differential equations. These equations are a function of aircraft performance parameters (e.g. lift, drag, engine thrust), state variables and control variables. Further, the set of parameters and state-evolution are constrained by performance limitations, ATM regulations and operational procedures. Determining the state-equations and selecting a performance model which best represents the performance parameters and all latter mentioned constraints would complete the formulation of a mathematical model for aircraft trajectory optimization using control theory.

The objective of the control problem considered in this study is to evaluate the performance of the bi-level algorithm in calculating mode sequences based on the feasibility of a mode to minimize the performance criterion. As the future prospects of this study are focused on estimating the cost benefit potential in developing climate optimized trajectories, a performance measure which can quantify both simple and complex models of operating cost and climate impact is preferred. This flexibility of the performance criterion will allow to formulate a control problem which is effective for conducting a feasibility study with the algorithm.

For solving a control problem using a bi-level algorithm, a computational framework is to be designed. As the function defined for inserting a mode into the mode sequence, η, is highly sensitive to control inputs, a framework which would formulate a new control problem for each stage, every iteration of the algorithm is considered. Such a framework offers the advantage to visualize the system behaviour by individually studying and comparing the state and control responses obtained from both stages of the algorithm.

3.1. State, Inputs and State-Equations

The motion of an aircraft in a control system is described by a vector of state variables ($\mathbf{x}$(t)) and control variables ($\mathbf{u}$(t)). As this study characterizes the 3D (lateral and vertical) flight motion, longitude (Λ), latitude (φ) and altitude (H) are included in the state vectors to define the physical state of the system. Further, the mass

of the aircraft and accumulated mass of engine emissions, m_i ($i \in CO_2$, H_2O, NO_x), are also included in the state vectors as the purpose of the control problem being formulated is to calculate trajectories with optimal operating cost and/or climate impact mitigation. The computational resources required for solving a control problem depends on the dimensions of the state and control vectors. Thus, to improve the computational efficiency and to ensure a safe flight characteristics, limited to the flight envelope (eg: maximum Mach number, max pressure altitude, etc..) , an additional path vector (P) is introduced. The path variables cover the additional boundary conditions which cannot be covered by the state and control limitations. The set of parameters which correspond to control and path vectors are determined based on the flight characteristics in each mode (cruise, climb and descent) and their corresponding ATM restrictions.

3.1.1. CRUISE

The cruise phase is the segment of each flight which has a dominant influence on the global characteristics of the flight, such as time, fuel consumed and distance covered. Accordingly, the design of the cruise profile is based on Long-range cruise regime (for maximum distance), Maximum endurance cruise regime (to maximize time). High speed cruise regime (for a constant Mach cruise) and Economy cruise regime (for minimizing operational cost). With a focus on designing trajectories to measure benefits between cost and potential climate impact mitigation, this study considers economy cruise regime. Within this regime the flight characteristics are categorized as follows:

- *Constant Pressure Altitude:* When a constant altitude restriction is imposed, an aircraft may change it's Mach number based on the ratio of time and fuel costs.
- *Constant Mach:* A restricted Mach cruise flight will result in a continuous increase in altitude to maintain the lowest possible fuel consumption.
- *Absolute Economy:* A cruise phase with no restrictions would result in increase in flight altitude and Mach number as the aircraft weight is reduced, in order to maintain economic flight.

All the above categories are considered for designing cruise trajectories to offer a comparative study with the algorithm. Assuming that the flight plan is free and the change in altitude or heading is brought about with the approval or instruction from ATC, a constant altitude cruise is assumed for most part of the flight. It is important to note that the flight altitude refers to the pressure altitude and not the geometric altitude. Based on the latter assumption both constant altitude and constant Mach cruise are defined as constant pressure altitude cruise with variable and constant Mach respectively. The absolute economy cruise is defined with no altitude restrictions for both variable and constant Mach. The absolute economy trajectories are used as reference trajectories to find the maximum altitude change for a given performance criterion and to validate the mode sequence calculated by the algorithm.

In a cruise phase the Mach number is calculated targeting for the best economy based on the cost index. The thrust is adjusted automatically to maintain the calculated Mach number (also referred as target Mach) and the true airspeed is calculated from the target Mach[24]. Both pressure altitude (H_p) and Mach number (Ma) are included in the set of path variables as these parameters are conditionally restricted based on the definition of the phase. Further, as pressure altitude does not equal geometric altitude the vertical speed ($\dot{H}$), and path angle (Γ) are also considered as path variables to represent the deviation between both altitudes. This ensures that the definition of the control problem remains unaltered irrespective of the phase definition. The relative thrust, T, and true airspeed, v_{TAS}, are defined as control inputs. However, since calculating the vertical speed from the total energy model requires acceleration ($\dot{v_{TAS}}$) as an input (see eq 3.1), thus airspeed is represented as a state variable. To account for the changes in lateral profile, the heading angle, χ_H, is considered as an additional control input with the assumption that the change in heading is instantaneous.

$$\dot{H} = \frac{(T \cdot (Th_{max} - Th_{min}) + Th_{min}) - D) \cdot v_{TAS}}{m \cdot g} - \frac{v_{TAS} \cdot \dot{v_{TAS}}}{g} \tag{3.1}$$

Where T is the relative thrust, Th_{min} and Th_{max} are minimum and maximum thrust respectively, D is the aerodynamic drag. It is assumed that the thrust is always aligned to the velocity vector.

3.1.2. CLIMB AND DESCENT

During climb the vertical speed (or target speed) mode is selected and accordingly the auto thrust adjusts the thrust settings to the maintain the target speed. The pitch (or path angle) control is an additional parameter which allows an aircraft to maintain the target speed. In case of lateral deviation, the climb mode

is engaged as an open climb with no restrictions till a specific waypoint after which the vertical speed mode is reengaged.[24] Assuming an instantaneous change in heading, the open climb and vertical mode are integrated as a single phase step climb in this study. To ease the formulation of the control problem, the climb phase is defined with similar control and path variables as the cruise phase. Since path angle acts as an important control in the climb phase, the path angle (γ) is calculated and constrained in terms of true airspeed (v_{TAS}) and vertical speed ($\dot{H}$), see equation 3.2.

$$sin\gamma = \frac{\dot{H}}{v_{TAS}} \tag{3.2}$$

The descent mode of the flight is conceptually similar to the climb mode. In case of a descent required by ATC, the descent mode would be selected and the descent path and descent speed is determined based on the altitude constraints and wind. The thrust is managed in order to maintain the descent speed and in case of lateral deviations the aircraft would maintain the current vertical speed irrespective of the effect on the aircraft which may trigger a warning. However, assuming instantaneous change in heading the latter effect is ignored.

The vertical speed for both climb and descent modes in an economy flight regime is calculated on the basis of weight, atmospheric conditions and cost index. In this study, both modes are defined as a variable Mach flight mode with limits on vertical speed for a safe flight envelope.

3.1.3. STATE-EQUATIONS

From the flight characteristics defined in the previous sections the state variables in all three phases are defined as $\mathbf{x} = [\Lambda, \varphi, H, m, m_i, v_{TAS}]$, where Λ represents the longitude, φ is the latitude, H is the altitude, m_i is the accumulated mass of the engine emission ($i \in CO_2, H_2O, NO_x$) and v_{TAS} is the true airspeed.

The control inputs are chosen as $\mathbf{u} = [\chi_H, \dot{v_{TAS}}, T]$, where χ_H represents the heading angle, $\dot{v_{TAS}}$ is the acceleration and T is the relative thrust i.e. $T = 0$, for minimum thrust and $T = 1$, for maximum thrust.

In regular cases the control variables are computed as a function of state and co-state variables. Finding a complete solution to an optimization problem in general is extremely difficult as the control problem may not always provide a unique control. The complete solution to an optimal control problem may be found in low dimensions unless the system presents a lot of symmetries [34]. Further, the control problem always presents a possibility of bang-bang control behaviour with subsequent introduction of numerical interpolation noise in the final solution. Accounting for all the latter difficulties, the previously chosen control parameters are represented as state variables while the control inputs are modified to represent the change in control variables.

The complete set of state vectors after modifying the control inputs are $\mathbf{x} = [\Lambda, \varphi, H, m, m_i, \chi_H, v_{TAS}, T]$. The modified control inputs are $\mathbf{u} = [\dot{\chi}_H, \dot{v_{TAS}}, \dot{T}]$.

Finally, the additional path variables are defined as $P = [H_p, Ma, v_{CAS}, C_{L,rel}, \dot{H}, \gamma]$, where H_p represents the pressure altitude, Ma the Mach number, v_{CAS} the calibrated airspeed and $C_{L,rel}$ the relative lift coefficient ($C_{L,rel} = 1$ for maximum lift) which are introduced into the set of parameters for monitoring the buffeting limitations of the aircraft, $\dot{H}$ is the vertical speed and γ is the flight path angle .

Table 3.1 show the assumptions made in each phase and the state-equations used to define the aircraft dynamics, assuming a point mass model with variable aircraft mass and three degrees of freedom.

Within the state equations, R_E is the radius of the Earth and the wind speeds in eastward and northwards directions are represented as u_w, v_w. The flight path angle γ is related to the true airspeed and vertical speed as defined in eq. 3.2. The performance parameters such as the aerodynamic drag D, Thrust maximum Th_{max}, and Thrust minimum Th_{min} are obtained from the performance model. The engine performance within the performance model yields fuel flow FF. The fuel flow FF is multiplied with emission index EI_i to estimate the accumulated mass m_i ($i \in CO_2, H_2O, NO_x$). The emission indices are obtained from the calculation performed in Eurocontrol modified Boeing Fuel Flow Method 2[35].

The flight time for the entire cruise is bounded by estimating the time required to cover the total flight distance on ground with lower and upper bounds of true airspeed. The true airspeed itself is bounded dependent on the bounds on set Mach number.

3.2. PERFORMANCE MODEL AND CONSTRAINTS

Depicting realistic flight motion with state-equations requires accurate prediction of aircraft performance and defining an operational flight envelope, by imposing limitations on performance parameters and path

Table 3.1: **The assumptions made in each fight mode (Cruise, Climb and Descent) along with the state-equations.**

	Constant Altitude Cruise	**Step Climb/Descent**
Assumptions	H_p = Constant Instantaneous change in heading	Instantaneous change in heading
State-Equations	$\dot{\Lambda} = \frac{v \cdot cos\gamma \cdot sin\chi_H + u_W}{(R_E+H)\cdot cos\varphi}$ $\dot{\varphi} = \frac{v \cdot cos\gamma \cdot sin\chi_H + v_W}{R_E+H}$ $\dot{H} = \frac{(T\cdot(Th_{max}-Th_{min})+Th_{min}-D)\cdot v_{TAS}}{m\cdot g} - \frac{v_{TAS}\cdot \dot{v_{TAS}}}{g}$ $\dot{\chi}_H = \dot{\chi}_H$ $\dot{v_{TAS}} = \dot{v_{TAS}}$ $\dot{T} = \dot{T}$ $\dot{m} = -FF$ $\dot{m}_i = FF \cdot EI_i$	

variables. Selecting a performance model which provides performance parameters over the entire flight envelope with increased level of precision enables modelling aircraft trajectories replicating real life trajectories. Recent studies have chosen BADA Aircraft Performance Model (APM) for efficient modelling of aircraft trajectories as the model provides accurate coefficients for calculating aircraft specific performance and also defines operational limitations. This model is used in this study for performance calculation of Airbus A330-200 type aircraft. Additionally, physical constraints on the path variables are imposed based on ATM regulations and manufacturers recommended operational procedures.

3.2.1. BADA PERFORMANCE MODEL

Base of Aircraft Data (BADA) is an aircraft performance model database which is developed and maintained by the Eurocontrol Experimental Center (EEC) with the purpose of modelling and simulating aircraft trajectories for ATM research and strategic ground planning. The model is based on a kinetic approach to aircraft performance modelling and contains aircraft specific coefficients necessary to calculate performance parameters. The newly developed BADA model, BADA Family 4, covers 70% of the aircraft types in ECAC (European Civil Aviation Conference) area and provides coefficients for the entire flight envelope. In this study, BADA 4.0 version of the BADA Family 4 is used for calculating the necessary performance parameters.[36]

BADA 4.0 is capable of supporting accurate computation of the geometric, kinematic and dynamic aspects of the aircraft behaviour. The design of this model is based on an in-depth review of flight dynamics, use of dimensional analysis techniques and employment of object oriented modelling. Geometric, kinematic, dynamic and environmental limitations are also incorporated within the model in order to ensure realistic representation of the aircraft performances. The geometric limitations include the maximum altitudes (with and without high-lift devices) and maximum pitch angle. The kinematic limitations include the maximum airspeed and Mach number for different combination of landing gear and high lift devices, as well as a buffet model which represents the aerodynamic limitations derived from maximum lift coefficient (C_L). The dynamic limitations cover the maximum aircraft weight for different phases of the flight and the maximum and minimum load factors. The environmental limitations include the valid range of temperatures at different altitudes.[37]

An error analysis made from comparing the performance values obtained from BADA model to the average values of actual flight performance parameters presented an average error below 5% in vertical speeds, 10% in drag coefficients and thrusts, and 5% in fuel consumption. Apart from providing a precise APM, the BADA model also offers the advantage of computing accurate trajectories with different weather conditions and under any atmospheric conditions.[36]

3.2.2. PATH CONSTRAINTS

Although the BADA model provides the operational limitations for the entire flight envelope there are additional limitations which are imposed on a flight path based on ATM regulations, see section 1.3. Further, taking the manufacturer, Airbus's, recommendation on few practices within each flight mode will introduce few more limitations on the flight path. With the objective to design realistic trajectories, the latter mentioned ATM regulations and recommended practices are translated into a set of constraints which bound the path variables.

As discussed in section 1.3, the cruise phase of a flight is regulated by the semi-circular rule in a conventional airspace. This categorizes the available cruise altitudes into even and odd flight levels for east and westbound flights respectively. Abiding by this rule, a step climb or descent mode during cruise should terminate at even or odd flight altitudes depending on the flight direction. Based on this the total altitude variation in each flight mode (climb and descent) is restricted to a minimum of 2000 ft. (or 609.6 m). Since the flight levels are represented by pressure altitudes, the final pressure altitude ($H_{p,f}$) is set to initial cruise pressure altitude ($H_{p,f}$) ± 2000 ft. for climb and descent mode, respectively. This final altitude then would become the initial altitude of the next mode in the flight sequence.

In the entire cruise phase the optimum Mach number is variable depending on several factors. For A330-200 type aircraft the thrust inputs allows for a small variation from the target Mach (v_{TAS}± 4kt.) before a thrust adjustment occurs. In order to save flight time the Mach number is managed between target Mach (or Green dot speed) and M0.84. In this study, a constant Mach cruise phase is considered. For the constant Mach cruise the target Mach is set to M0.82 which is recommended as the optimum cost index cruise Mach for Long-range flights by the A330 flight manual[24]. For step climb and descent modes, the Mach number is bounded by the operational limitations provided by the BADA model.The target speed for climb and descent modes are managed by the bounds on the vertical speed.

The vertical speed (V/S) takes precedence over speed requirements in both climb and descent modes. Selecting high V/S would lead to higher thrust requirement allowing the aircraft to decelerate to VLS (Lowest Selectable Speed) during climb and in case of descent the speed will increase till the aircraft reaches VMAX (Maximum Allowable Speed) after which the aircraft would pitch up. The rate of climb calculated using eq. 3.1 would result in slow rate of climb over the entire flight duration. This is understandable because the most optimal cost trajectories, in ISA conditions, can be discretized into several step climb of infinitesimally small duration. For convenience in formulating a computational framework, the vertical speed is bounded based on the ADS-B (Automatic Dependent Surveillance- Broadcast) data provided by Flightradar24 (see Appendix A). The V/S during climbs and descent of a Trans-Atlantic flight (YVR-MUC) at high altitudes were studied. Appendix A show the altitude plot of the entire flight and vertical speeds of the aircraft during step climb at Top of Climb(TOC), around Mid cruise and near Top of Descent (TOD) phases of the flight. For rate of descent, the vertical speed from TOD is shown. The average V/S from all climbs were found to be in the range of 500-750 ft/min and for descent around -1000 ft/min. According to [38] the recommended maximum descent rate is -1000 ft/min. Considering these, the vertical speed is limited between 0 and ± 1000 ft/min for climb and descent respectively. As the time to climb does not significantly affect the cost index (up to 3 minutes for A330 [38]), the total mode duration for the climb mode is limited between 200-500 seconds assuming a minimum average V/S of 250-500 ft/min. Since, the limits imposed on the mode duration bound the descent rate sufficiently, the mode duration is restricted equally for both climb and descent mode.

3.3. PERFORMANCE CRITERIA

Understanding the performance of the bi-level algorithm in calculating mode sequences based on the feasibility of a mode to minimize the performance criterion requires a performance measure for which the optimal solution is known beforehand. Selecting a performance criterion which has been previously studied offers the advantage of determining the scope of the algorithm in modelling aircraft trajectories. As this study considers cruise phase with constant altitude cruise, climb and descent modes, a performance measure or cost functional which can individually measure the performance index for each of these modes is considered. Further, the cost functions which summarizes the latter cost functional are defined in a manner such that the algorithm's capabilities are measured against fuel consumption (or accumulated masses of CO_2,H_2O and NO_x emissions) and spatial variability of emissions.

3.3.1. COST FUNCTIONAL

For measuring the operating cost-benefit from climate optimized cruise trajectories a cost functional (J) consisting of a penalty function (Υ) and a temporal integral function (Ψ) is defined in the study of Lührs,B.[4], see equation 3.3 and 3.4. In it's general form, the penalty function represents the operating cost (COC) of the flight which is dependent on the final and initial time (t_0 and t_f) as well as on the aircraft's initial and final mass (m_0 and m_f) and the temporal integral represents the climate cost integrated over time. The climate cost itself is defined as a function of the climate cost functions (CCF). The magnitude of Υ and Ψ are scaled by corresponding weighting factors C_Υ and C_Ψ, respectively, and are normalized with COC_{ref} and $ATR_{tot,ref}$ which corresponds to the reference trajectory with minimum COC.

$$\begin{aligned} J =& C_\Upsilon \cdot COC(t_f - t_0, m_0 - m_f) \cdot COC_{ref}^{-1} \\ &+ C_\Psi \cdot \underbrace{\left(\sum_i \int_{t_0}^{t_f} CCF_i(x,t) \cdot \dot{m}_i \, dt + \int_{t_0}^{t_f} CCF_{CiC}(x,t) \cdot v_{TAS}(t) dt \right)}_{ATR_{tot}} \cdot ATR_{tot,ref}^{-1} \end{aligned} \tag{3.3}$$

$$\begin{aligned} with \quad i \in [CO_2, H_2O, NO_x] \\ C_\Upsilon + C_\Psi = 1 \quad with \quad C_\Upsilon, C_\Psi \in [0,1] \end{aligned} \tag{3.4}$$

Considering the similarity in the objective of this study and that of Lührs,B., the cost functional for the control problem being formulated is defined from equation 3.3. Further, to account for the individual effect of each mode, in the mode sequence, on the performance measure the temporal integral function is rewritten. within the cost functional the temporal integral is represented as a summation of the climate cost calculated in each mode integrated over the mode duration. Additionally, a damping function is inserted into the cost functional which damps the bang-bang control behaviour and interpolation noises, see section 3.1.3. This function represents the control change rate squared and integrated over the entire flight time. It is important that the magnitude of the damping function is smaller compared to the overall performance measure. To ensure this the function is scaled with coefficients $\alpha_{\dot{T}}$, $\alpha_{\dot{\chi}_H}$ and $\alpha_{\dot{v}_{TAS}}$. The magnitude of these coefficients are based on the magnitude of the original cost functional obtained from equation 3.3. The augmented cost functional is expressed in equation 3.5, where n denotes the mode index in the mode sequence with N modes, t_n represents the corresponding switching time and term within '*'denotes the damping function.

$$\begin{aligned} J =& C_\Upsilon \cdot COC(t_f - t_0, m_0 - m_f) \cdot COC_{ref}^{-1} \\ &+ C_\Psi \cdot \sum_{n=1}^{N+1} \underbrace{\left(\sum_i \int_{t_{n-1}}^{t_n} CCF_i(x,t) \cdot \dot{m}_i \, dt + \int_{t_{n-1}}^{t_n} CCF_{CiC}(x,t) \cdot v_{TAS}(t) dt \right)}_{ATR_{tot}} \cdot ATR_{tot,ref}^{-1} \\ &+ \left[\alpha_{\dot{T}} \int_{t_0}^{t_f} (\dot{T})^2 dt + \alpha_{\dot{\chi}_h} \int_{t_0}^{t_f} (\dot{\chi}_h)^2 dt + \alpha_{\dot{v}_{TAS}} \int_{t_0}^{t_f} (\dot{v}_{TAS})^2 dt \right]^* \end{aligned} \tag{3.5}$$

3.3.2. COST FUNCTIONS

Advanced climate models such as Airclim express the emission dependency in terms of Average Temperature Response (ATR) per unit emission for CO_2, H_2O, NO_x emissions and, per unit distance flown for contrail induced cloudiness (CiC). From section 3.1.3, it is known that the emission flow rates $\dot{m}_i$ are estimated from multiplying the fuel flow with the corresponding emission index EI_i. Thus the climate cost per emission, calculated from the cost functional defined in equation 3.5, can be expressed as a function of fuel flow and locus (latitude, longitude and altitude) except from CiC, for which the cost is only a function of locus (see eq. 3.6). Based on the latter, this study determines the cost functions such that the individual effect of minimizing fuel flow and optimizing locus can be measured along with the bi-level algorithm's ability to calculate an optimal mode sequence.

$$\begin{aligned} CCF_{CO_2,H_2O,NO_x} &= f(\Lambda, \varphi, H) \left[\frac{K}{kg} \right] \\ CCF_{CiC} &= f(\Lambda, \varphi, H) \left[\frac{K}{km} \right] \end{aligned} \tag{3.6}$$

Since the operational cost have a direct dependence on the fuel consumed, a monetary cost function is selected to measure the algorithm's performance with minimizing fuel consumption. Further, from advi-

sories released by Airbus[38] it is known that a climb during cruise is beneficial in reducing the overall fuel consumption. This additional knowledge with regard to climb allows for the investigation of the algorithm in calculating mode sequence for cruise phase with climb mode insertion to minimize the fuel consumption. A description of the selected monetary cost function is presented below:

Monetary Cost Functions (COC): Monetary cost are calculated by the direct operating cost method developed by Liebeck et al.[39] The costs (based on US dollars) are scaled up from year 1993 to the year 2012 with the average inflation rate (between 1993 and 2012). The included costs are for fuel, crew, maintenance, navigation and landing fees. The calculated costs are specific to each aircraft type and are a function of flight time and fuel.

As the algorithm defines a mode's feasibility based on the sign of the directional derivative, solving for minimum monetary cost offers the possibility to understand the dependency of the directional derivative with fuel flow and climb flight characteristics. Similarly to understand the derivatives dependency with spatial variation (or locus) and descent mode, a fictitious CCF with 1D spatial variability in altitude is defined. The rate of change of these CCFs are expressed as a linear function in altitude (H), see equation 3.7, such that the overall climate cost decreases with decrease in altitude. The variables k_{11} and k_{12} are arbitrary constants.

$$\begin{aligned} \dot{CCF}_i = k_{11} + k_{12} \cdot H, \quad where \quad k_{11}, k_{12} > 0 \\ with \quad i \in [CO_2, H_2O, NO_x] \end{aligned} \tag{3.7}$$

Additionally, to extend the algorithm's investigation towards calculating a mode sequence with both climb and descent modes, a fictitious CCF with 2D variability in space (altitude) and time (t) is defined. Equation 3.8 expresses the rate of change of CCFs in 2D such that the climate cost decreases with decreasing altitude in the first half of the flight duration (T) and vice-verse in the second half. The variables k_{11}, k_{12}, k_{21} and k_{22} are arbitrary constants.

$$\dot{CCF}_i = \begin{cases} k_{11} + k_{12} \cdot H: & t \leq \frac{T}{2}, \quad where \quad k_{11}, k_{12} > 0 \\ k_{21} + k_{22} \cdot H: & t \geq \frac{T}{2}, \quad where \quad k_{21} > 0 \quad and \quad k_{21} < 0 \end{cases} \tag{3.8}$$

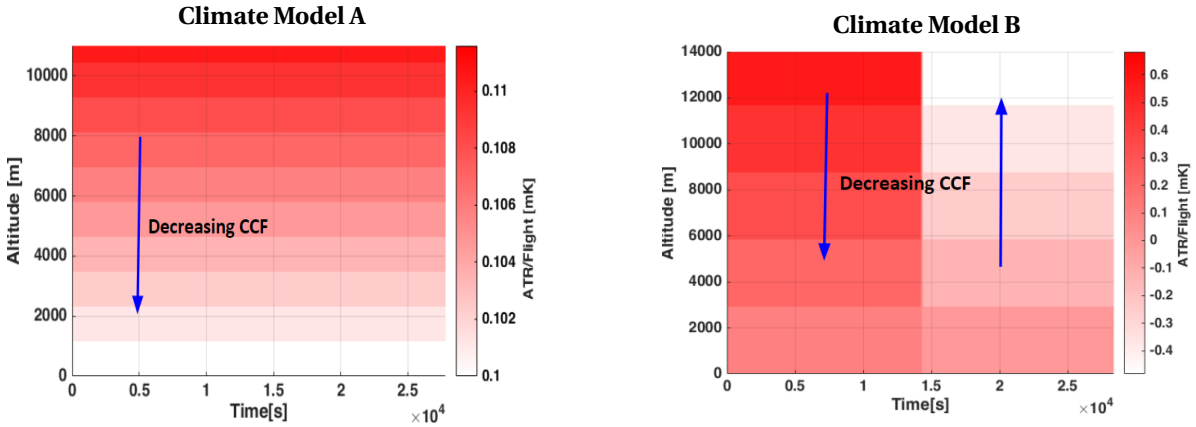

Figure 3.1: **Average temperature response with altitude plots for climate models with linear dependence on altitude, on the left the climate model A represents decreasing climate effect with decreasing altitude and on the right the climate model B represents decreasing climate effect with decreasing altitude in the first half of the flight duration and vice-verse in the second half.**

Figure 3.1 shows the ATR with altitude plots for both fictitious CCFs, equation 3.7 (Climate Model A) and 3.8 (Climate Model B). The values set for all arbitrary constants are given in Appendix B. Further, ATR with altitude plot obtained from AirClim CCF is shown in figure 3.2. This offers a comparison between spatial variation of emissions with actual CCF and fictitious CCFs proposed in this study. Based on the latter comparison, the proposed cost functions are considered to be the most straightforward and effective approximation of real-life climate chemistry. The trajectories calculated with these fictitious models are expected to offer sufficient understanding of the algorithm which will enable this study to reach conclusions in regard to the applicability of the bi-level algorithm for developing climate optimized trajectories.

Finally, the bi-level algorithm is implemented to calculate optimal mode sequence with AirClim CCFs. The AirClim CCFs express the climate response per flight as average temperature response over 100 years ($ATR_{100,i}$) for each climate agent i:

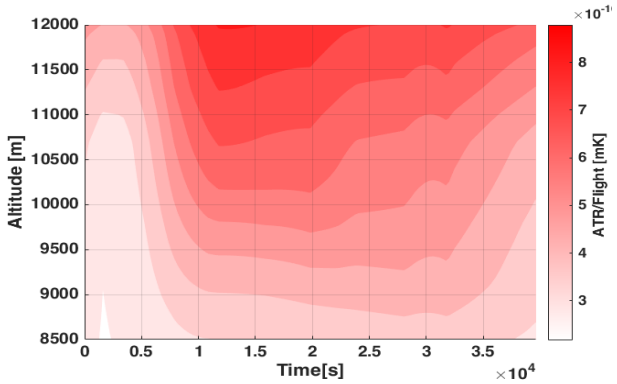

Figure 3.2: **Average temperature response with altitude for great circle trajectory between ORD-FRA, calculated using AirClim climate model with ISA conditions.**

$$ATR_{100,i} = \frac{1}{100}\int_{t}^{t+100} \Delta T_i(t) \cdot dt \tag{3.9}$$

Where t is time and T is temperature.

The spatial distribution of $ATR_{100,i}(z)$ is normalized by the emissions of corresponding flight level m_i(FL) (or distance for CiC) to generate emission based climate change function ($eCCF_i$) according to eq: 3.10-3.11.

$$eCCFi(x) = \frac{ATR_{100,i}}{m_i(FL)} \quad i \in CO_2, H_2O, NO_x \tag{3.10}$$

$$eCCF_{CiC}(x) = \frac{ATR_{100,i}}{d(FL)} \quad i \in CiC \tag{3.11}$$

The cruise emissions are simulated for an Airbus A-330-200 with varying flight levels (FL250-FL390) based on BADA 4.0. This serves as the input data for AirClim. The total CCF of a specific month is determined by superposition of eCCFs.[2]. In this study, the single mission assessment of the climate optimized trajectory is discussed for a cruise flight between Lisbon, Portugal (LIS) to Miami, USA (MIA). The latter control problem has already been studied in [40] with free flight cruise conditions. The CCFs for this flight path is based on the annual average conditions.

3.4. TRAJECTORY OPTIMIZATION MODULE (TOM)

Determining flight trajectories which minimize the performance criterion, defined in the previous section, requires a computational framework which can formulate and solve non-linear optimal control problems. The Trajectory Optimization Module (TOM) developed at DLR performs multi-objective optimization and calculates optimized flight trajectories based on optimal control approach.[4] As the current framework of TOM enables solving control problems with a multi-phase control technique, TOM is extended with the bi-level algorithm for the purpose of this study. In order to analyze the sensitivity of control inputs on the performance of the algorithm, a bi-level framework which formulates individual control problem for each stage iteration, is designed within TOM. Additionally, to reduce computational time the set of discrete modes with which the algorithm calculates the optimal mode sequence are defined outside the bi-level framework.

3.4.1. OPTIMIZATION WITH GPOPS-II SOLVER

TOM uses the Matlab toolbox GPOPS-II in order to solve a control problem. GPOPS discretizes the cost functional and state-equations of a multi-phase control problem using the Gauss-pseudospectral method. The Gauss-pseudospectral method uses global polynomials to approximate the state and control vectors with orthogonally collocated points which enables the solution to converge faster.[41] The phases are linked based on the conditions imposed on state and time. GPOPS then transforms the continuous control problem into a non-linear programming problem (NLP) which is solved using the NLP solver IPOPT. IPOPT guarantees convergence for NLP as the barrier method adopted within the solver accepts trial points which either improves the cost functional or the constraint violation.[33]

The control problem in it's general form is represented as Mayer problem in GPOPS, where the Lagrangian function is assumed to be zero. Since the Mayer problem only comprise of end cost terms, each CCF term within the Lagrangian function of eq. 3.5 is represented as state variables within GPOPS. These state variables are defined in addition to the set of state variables defined in section 3.1.3. The new set of state variables defined within GPOPS is given in eq. 3.12 and the dynamics for these state variables are given in eqs. 3.13-3.14. It is important to note that the state-equations defined below represent a general form of the performance criteria. However, while formulating optimal control problems with the fictitious CCFs, defined in section 3.3.2, the latter state equations will be replaced with eqs. 3.7 or 3.8. The damping function in eq. 3.5 is defined as an integral (I) within GPOPS. For computing the integral, the integrand ($\dot{I}$) is calculated at each time step and in each phase. The integrand is similar to the state-equations and are defined for each term within the damping function (see eqs. 3.15). The final objective function defined in GPOPS is shown in eq. 3.16.

$$\boldsymbol{x} = [\Lambda, \varphi, H, m, m_i, \chi_H, v_{TAS}, T, CCF_{(m_i,i)}, CCF_{(v_{TAS},CiC)}] \quad with \quad i \in [CO_2, H_2O, NO_x] \tag{3.12}$$

$$C\dot{C}F_{(m_i,i)} = CCF_i(x,t) \cdot \dot{m}_i \tag{3.13}$$

$$C\dot{C}F_{(v_{TAS},CiC)} = CCF_{CiC}(x,t) \cdot v_{TAS} \tag{3.14}$$

$$\dot{I}_1 = \alpha_{\dot{T}} \cdot \dot{T}^2; \quad \dot{I}_2 = \alpha_{\dot{\chi}_H} \cdot \dot{\chi}_H^2; \quad \dot{I}_3 = \alpha_{\dot{v}_{TAS}} \cdot \dot{v}_{TAS}^2; \tag{3.15}$$

$$\begin{aligned} J = & C_\Upsilon \cdot COC(t_f - t_0, m_0 - m_f).COC_{ref}^{-1} \quad + \\ & C_\Psi \cdot ATR_{tot}(CCF_{(m_i,i)_f}, CCF_{(v_{TAS},CiC)_f}) \cdot ATR_{tot,ref}^{-1} \quad + \\ & [I_1 + I_2 + I_3]^* \end{aligned} \tag{3.16}$$

The formulation of control problem in GPOPS requires writing an endpoint function and continuous function. The endpoint function defines the start and/or terminus for all phases in the problem, the cost to be minimized and the integral (the damping function). The continuous function defines the evolution of the dynamics and path constraints for each phase and the integrands required for computing the integrals. The latter two functions along with the limits for the following quantities completes the formulation of the control problem in GPOPS.

- the time at the start and end of each phase;
- the state at the start, during, and end of each phase;
- the control during each phase;
- path constraints

As the phase switching time is unknown for all multi-phase control problems considered within this study, a set of static parameters (t_s) are introduced into the optimization setup to determine the optimal switching times. Static parameters are variables defined within GPOPS optimization setup which are independent of the phase definition. The time itself is represented with the independent variable as discussed in section 2.2. within the continuous function the set of static parameters are related to the actual flight time using the relation defined in equation 2.7. Additionally, to link the phases and to ensure continuity of the problem, event constraints are computed in the endpoint function. In this study, the event constraints are defined to ensure continuity of independent variable (τ) and state variables ($\boldsymbol{x}(\tau)$). To ensure that the switching times computed with static parameters represents real time, the set of static parameters are also included in the event-group definition such that the phase duration always remains positive. Equation 3.17 expresses the event constraints that links two corresponding phases of the problem, where the subscript '0' and 'f' represent the start and end of a phase respectively and 'p' denotes the phase index (p ∈ [1,2...N]). Further, for implementing the limits on duration of climb or descent phase, as discussed in section 3.2.2, event constraints with static parameters are defined as expressed in eq. 3.18.

$$\begin{aligned} & \tau_{(f,p)} - \tau_{(0,p+1)} = 0 \\ & \mathbf{x}(\tau_{(f,p)}) - \mathbf{x}(\tau_{(0,p+1)}) = 0 \\ & t_s(p+1) - t_s(p) \geq 0 \end{aligned} \tag{3.17}$$

Where $p, p+1 \in \{Const.Alt.Cruise, Climb, Descent\}$ in eq. 3.17

$$\begin{aligned} 200\,s \leq t_s(p+1) - t_s(p) \leq 500\,s, \quad & p+1 \in \{Climb, Descent\} \\ & p \in \{Const.Alt.Cruise\} \end{aligned} \tag{3.18}$$

GPOPS also allows to specify initial guesses for time, state, control and static parameters. The closer the guess is to the actual solution, the faster the solver converges to a solution. The computational time can further be controlled based on the type of NLP solver and the expected accuracy (Primal and Dual infeasibility). The run time of GPOPS is also dependent on the number of collocation points defined by the solver before it converges to a solution. This can be manipulated within the optimization setup by defining the maximum number of iterations allowed per mesh, maximum number of mesh iterations, and the mesh refinement accuracy. In the current framework of this study, the solver computes derivatives based on numerical differentiation method. The GPOPS-II solver settings defined for solving control problem in this study are shown in table 3.2. Detailed explanation of the GPOPS solver can be found in GPOPS manual[41].

Table 3.2: **GPOPS-II solver setup for trajectory optimization in TOM.**

GPOPS Parameters	***Values***
Linear Solver	*'ma57'*
Derivatives	*'sparseFD'*
Mesh Method	*'hp-PattersonRao'*
Setup Method	*'RPM-Differentiation'*
Max Iterations per Mesh	*500*
Max Mesh Iterations	*3*
Primal and Dual Infeasibility	*5e-4*
Mesh Tolerance	*1e-3*

3.4.2. COSTATE ESTIMATION

The costate variable ($p(t)$) in an optimal control problem is related to the sensitivity of the objective function to perturbations in the system dynamics. The costate is essentially the derivative of the objective function with respect to a perturbation in the system dynamics[42]. For an infinitesimal mode insertion the cost variation (see eq. 2.14) can be evaluated by considering the costate ($p(\hat{t}_i)$), where $\hat{t}_i$ is the insertion time, and changes in dynamics (Δf). The costate variable is the solution to the differential shown in eq. 3.19. The definition of the The directional derivative of the cost function with respect to costate is given in eq. 3.20. The definitions of the parameters in the following equations are same as in section 2.2.

$$\begin{aligned} \dot{p}(t) &= -\frac{\delta f}{\delta x}^T(x(t), u(t)) \cdot p(t) - \frac{\delta L}{\delta x}(x(t), u(t)) \\ p(t_f) &= \frac{\delta \phi}{\delta x}(x(t_f)) \end{aligned} \tag{3.19}$$

$$\frac{dJ(\hat{t}_i + \lambda)}{d\lambda}\bigg|_{\lambda=0} = \Big(p(\hat{t}_i)\Big)^T \Delta f(x(\hat{t}_i + \lambda), u, \eta) + [\hat{u} - u(\hat{t}_i)]^T \frac{\delta L}{\delta u}(x(\hat{t}_i), u(\hat{t}_i)) \tag{3.20}$$

$$Where, \quad \Delta f(x(\hat{t}_i + \lambda), u, \eta) = f_\alpha(x(\hat{t}_i + \lambda), \hat{u}) - f(x(\hat{t}_i), u(\hat{t}_i))$$

Within GPOPS-II, an approximate solution for costate is estimated using the Gaussian quadrature collocation method. The default method used is Legendre-Gauss-Radau (LGR) collocation. The costate can be produced either in integral or differential form. In [42] the mathematical description for the costate approximation methods adapted in GPOPS is described in detail. Achieving a specific mesh error tolerance with integral dynamics is known to be much more stable and reliable than the differential form. However, the current version of GPOPS is only able to produce reliable costate in differential form. This method was implemented within the computational framework after consulting with the creators of GPOPS. The setup method in table 3.2 indicates the method selected for costate approximation, where RPM stands for Radau Points Method.

For calculating an optimal solution the control needs to chosen so as to minimize the Hamiltonian H, expressed in eq. 3.21. If the Lagrangian L and state dynamics f are not explicit function in time then the

Hamiltonian evaluated along the optimal trajectory must be a constant [25]. Since the control problems considered in this study are not explicitly dependent on time, the Hamiltonian evaluated for each optimal trajectory must be a constant. This information is used to validate the costate estimated within GPOPS. Note that the Lagrangian function within eq. 3.21 will evaluate to zero for a Mayer problem.

$$H(x,u,p) = L(x,u) + p^T f(x,u) = constant \tag{3.21}$$

Within the scope of this study, the utilization of the costate variable is limited to evaluating the Hamiltonian along the trajectory. This will be presented in chapter 4 as a means to promote GPOPS-II RPM-Differentiation costate estimation method for future studies.

3.4.3. BI-LEVEL FRAMEWORK

The purpose of the bi-level framework in TOM is to calculate the optimal mode sequence for all control problems which are based on optimizing flight trajectories. Within TOM a reference trajectory is calculated for all control problems considered. The reference trajectory is designed as an absolute economy cruise trajectory for which the final altitude boundary condition is set free. The main aim of defining a reference trajectory is to determine the maximum optimum altitude to which the aircraft climbs or descents. As all control problems formulated within this study are simple and have distinct regions which can be identified either with climb or descent modes, the reference trajectory allows to restrict the set of discrete modes to a finite number. This additionally also enables the validation of the mode sequence calculated by the bi-level algorithm. Further, determining the maximum number of modes in the mode sequence allows to optimize the maximum number of iterations needed. This saves considerable amount of computational time and enables quick validation of the algorithm.

Since all trajectories designed with TOM are limited to the cruise phase of the flight, the initial mode sequence is defined as a constant altitude cruise over the entire flight path. To verify the definition of the control problem in TOM, the solver settings and optimization setup are stored in a variable called debugger. Once the solver finds an optimal solution for the initial sequence, the time, state and control variables corresponding to the solution are stored in memory. For enabling stage 2 to calculate a new sequence, 'n' time steps are selected from the solution of the initial sequence. These time steps are then introduced as candidate set of insertion times, $\hat{t} \in (t_0, t_f)$. The climb and descent modes are considered within the set of discrete modes. It is important to note that neither the solution calculated by the solver nor the minimum evaluated by the algorithm necessarily represent the global minima. Hence, a careful consideration is required while selecting the time steps at which the algorithm evaluates the feasibility of a mode to reduce the cost functional. This is however not crucial for the first iteration of the bi-level framework as all time steps are valid candidate points for mode insertion. After the first iteration, when a climb or descent mode is inserted into the initial sequence, the cruise phase which lie after the terminus of the inserted mode and before the end is defined as the feasible region for evaluating the next mode insertion. This is because, considering time steps previous to the inserted mode would alter the sequence which was calculated in the previous iteration. This will lead the algorithm into an infinite loop. Figure 3.3 shows the selection of feasible regions for the first two iteration of the bi-level framework. Note that the time is represented in terms of independent variable (τ) and the scale of the axis is selected such as to represent the duration of the modes in real time.

To calculate the most optimal sequence the first time step at which the evaluated cost variation is less than zero should be considered as the initial guess within the solver. This provides an initial direction to the solver which would determine the closest solution to the guessed switching time and thus enabling the calculation of a mode sequence which may represent the global minimum within the considered domain. However, since the focus is to validate the performance of the algorithm, the bi-level framework is defined with flexibility in selecting the insertion time. This flexibility is computationally expensive but will allow this study to obtain cost variations for the entire domain of insertion time. Further, with different optimal solutions at different insertion times the sensitivity of the algorithm with respect to actual solutions can be obtained.

To avoid two modes of climb and/or descent being inserted in succession, the time steps selected for evaluating mode insertion always exclude the switching times, thus always separating the climb and/or descent modes with a constant altitude cruise mode. However, if the solution requires two modes in succession, for calculating a minimum, then the duration of the cruise mode can be set to zero by the optimizer. Figure 3.4 shows the general flow chart of TOM integrated with the bi-level framework (in red box). The definition of the set of discrete modes is separated from the bi-level framework such that the progressive loop of the algorithm could be controlled by limiting the number of mode insertions for which the loop is executed. This enables fast debugging of the computational framework.

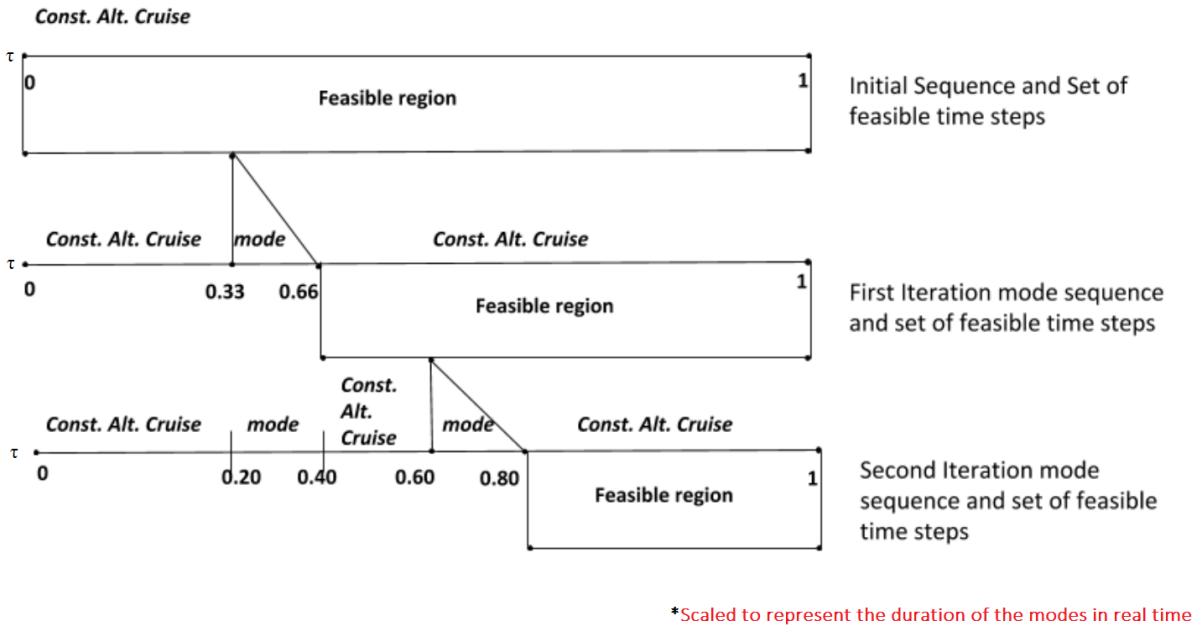

Figure 3.3: **Figure illustrating the transition from initial sequence to consecutive sequence calculated using bi-level framework along with the feasible region from which 'n' time steps are selected.**

For the 'n' time steps the stage 2 of the bi-level framework builds the mode characteristics function η, see sec. 2.2. Since a min-max problem is required to determine the control inputs ($\hat{u}$) of the mode, a control problem is formulated for each insertion time $\hat{t}_i$, where i ∈ [1,n]. The objective of the control problem is to find an optimal flight path, with the dynamics and limits corresponding to the mode α, which minimizes the cost functional. As the solver verifies the feasibility of the control problem, no further work is required in evaluating the constraint validation. As the algorithm is sensitive to the control inputs, the initial state boundary conditions for these control problems are set to the previous sequence state vector at $\hat{t}_i$. This ensures that the mode is represented as a continuous phase of the previous sequence.

Once the mode characteristics function η is defined, the value of the cost functional till the inserted mode ($\hat{t} + \bar{\lambda}$) can be easily obtained. The cost till $\hat{t}$ is obtained from the solution of the previous sequence and the additional cost due to the mode is obtained from the solution of the control problem described in the previous paragraph. A database is created with the optimal solutions of constant altitude cruise, at different flight levels, to interpolate the cost of the final cruise phase of the new sequence. Remember that the final phase is always a cruise mode which follows after the inserted mode in the new sequence. A cumulative sum of all the above mentioned costs provides the overall cost for the new sequence ($J(\rho^{\eta}(\bar{\lambda}))$. Now the cost variation can be obtained by comparing the overall cost of the previous sequence with the overall cost of the new sequence as defined in eq.2.15.

For the database, a cruise phase is simulated at a given altitude and speed. The cruise is initiated with maximum fuel (initial weight) and is terminated when the fuel tanks are empty (final weight). From the simulated result, time, range, fuel consumed and/or climate cost are recorded for a range of weights (between initial and final weight). The flight time, fuel consumed and/or climate cost for the phase after the climb/descent mode is then interpolated from this database. The required range to reach destination is calculated as a great circle trajectory from the final position of the inserted mode. The maximum possible range of the final cruise phase is interpolated with respect to the available fuel. If the required range is less than the maximum range then the flight time, fuel consumption and/or climate cost are interpolated for the required range. Based on this the cost from $\hat{t} + \bar{\lambda}$ to t_f is estimated. The latter method of interpolation is used for all control problems in which the cost functional are independent of the aircraft's position. For performance index with AirClim CCFs, which are dependent on location, the climate cost is estimated by interpolating a flight path which connects the inserted mode to the closest point on the trajectory of the previous sequence. The climate cost for the final phase of the new sequence is then evaluated by combining the cost of the in-

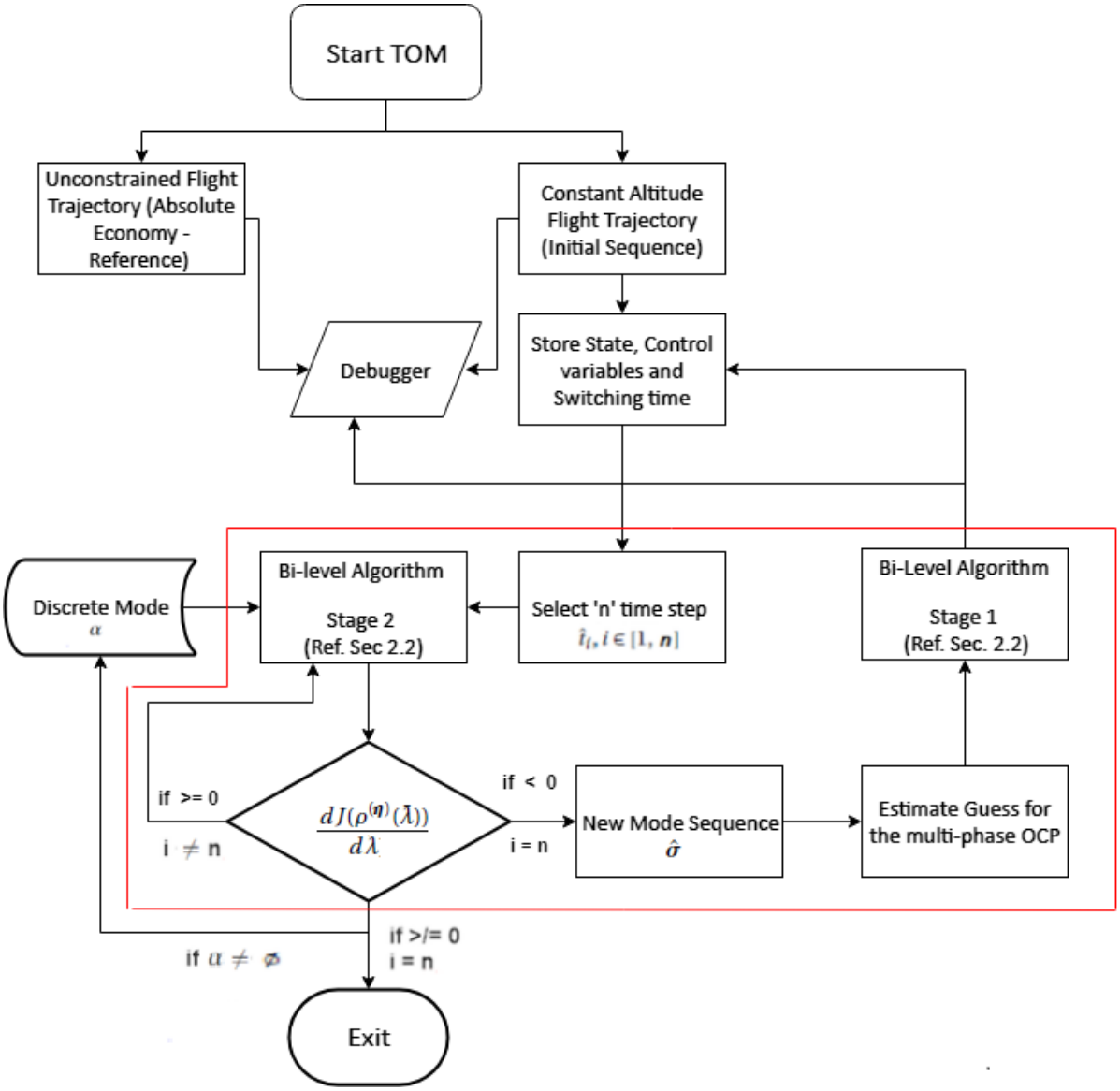

Figure 3.4: **Optimization flow chart of TOM with bi-level framework (in red box), built for an hybrid optimal control problem with variable mode sequence.**

terpolated flight path with the remainder cost. The remainder cost is estimated from the overall cost of the previous sequence. This will be further elaborated in chapter 4.

Within stage 2 an internal loop calculates the cost variation at each time step by solving a control problem for the mode and interpolating the cost for cruise phase after the mode. This loop is executed for each mode in the set of discrete modes. The cost variation corresponding to each insertion time $\hat{t}$ is stored in a variable. If at any insertion time, from the set of insertion times, the evaluated directional derivative is negative i.e. the new sequence cost is lower than the initial sequence, then the bi-level framework defines a new sequence $\hat{\sigma}$ by selecting an insertion time from the set of feasible insertion times. More often than not, this insertion time corresponds to the insertion at which the cost reduction is maximum. However, this maybe violated in this study for validation purposes. After the new sequence is defined, stage 1 will calculate their optimal switching times. For calculating the optimal switching times a multi-phase problem for the new sequence is formulated and solved within stage 1. The guess for this multi-phase problem is determined based on the time step at which the cost reduction was found to be negative, the solution corresponding to the previous mode sequence, and the mode solution from stage 2.

The directional derivative is calculated in the above manner for all the modes defined within the set of modes. However, if both climb and descent modes are defined within the set of discrete mode then the final optimal mode sequence depends on the order in which the discrete modes are inserted. The differences in the optimal mode sequence calculated with different set of discrete modes will be discussed in chapter 4. Figure 3.5 illustrates the bi-level framework with stage 1 and stage 2 of the algorithm highlighted.

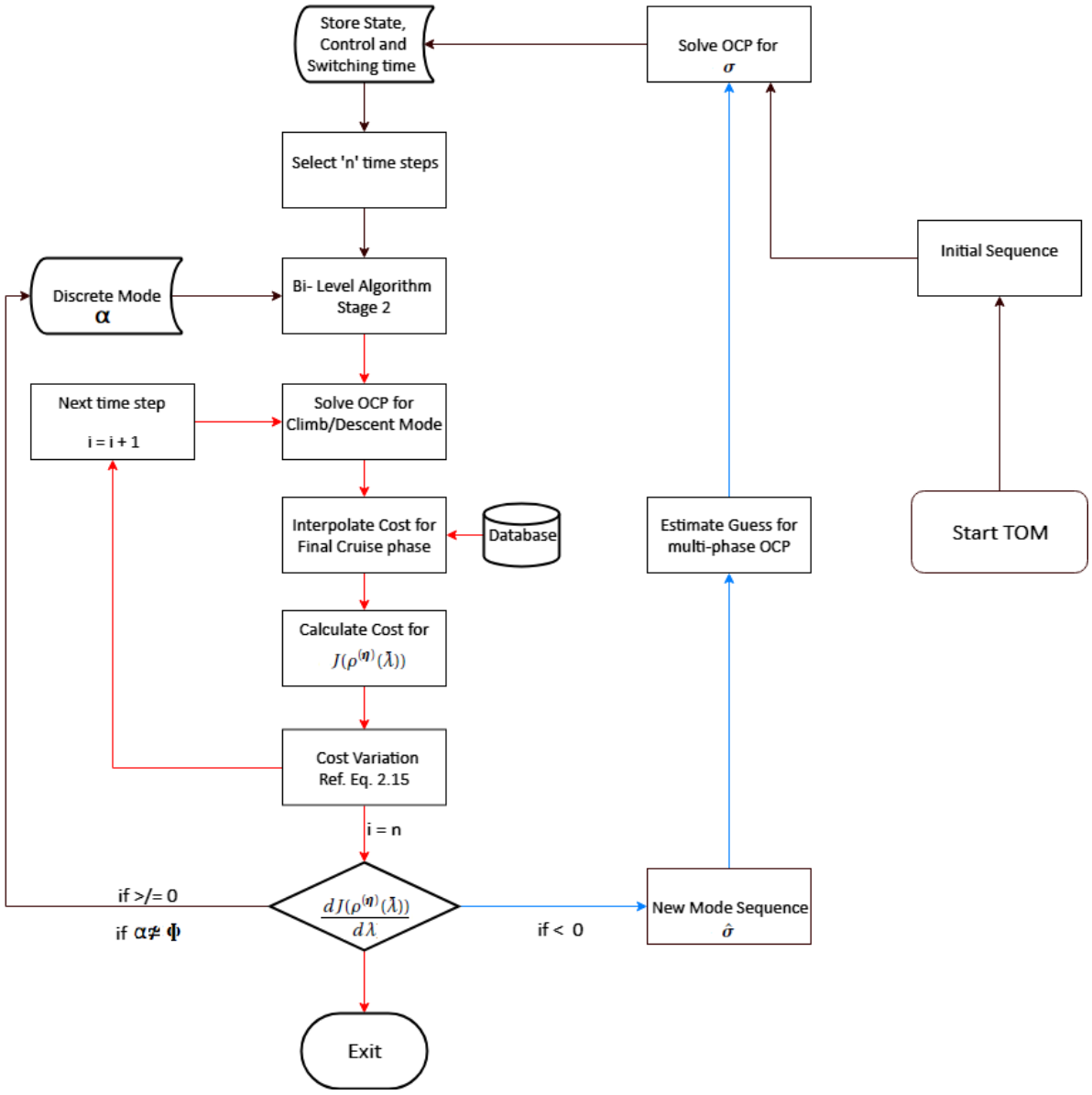

Figure 3.5: **Flow chart of the Bi-level framework in TOM, highlighting the loops of stage 2 (with red arrows) and stage 1 (with blue arrows)**

4

Designing Trajectories with the Bi-level Algorithm

As identified previously in section 3.3.2, the climate impact due to aviation emissions is dependent on fuel burnt and spatial variability of emissions. With the objective to investigate the algorithm's ability to calculate the optimal mode sequence for climate optimal trajectories, this chapter considers control problems for minimizing operating cost (or fuel consumption) and climate cost (with climate models defined in section 3.3.2). The optimal sequence for all control problems are calculated using the bi-level framework described in section 3.4.3.

The control problem for minimizing the operating cost of the cruise phase is extensively studied within the field of flight trajectory optimization. In this chapter this control problem is solved using the bi-level technique and an optimal mode sequence is calculated. Since it is known from literature that climb during cruise minimizes the operational cost [38], the bi-level framework is validated with climb mode insertions. For each feasible insertion time the fluctuation in estimated switching time and error between the actual (stage 1) and estimated (stage 2) cost reduction are calculated. Based on this the precision of the algorithm to determine feasible insertion times and cost reduction is estimated.

Since limited knowledge is available with regard to descent during cruise, mode sequences with descent modes are calculated for cruise trajectories designed within climate model A and B (shown in figure 3.1). Extending the bi-level technique to control problems with fictitious climate models, the set of discrete modes is defined with both climb and descent modes. The directional derivative will be evaluated for both modes in each iteration of the stage 2. The fictitious CCFs are defined to represent distinct regions of feasibility for both modes. After each iteration the mode sequence calculated by stage 2 is compared to the optimal sequence. From these comparison, the accuracy with which the algorithm can calculate the optimal mode sequence for a spatially varying cost functional is determined.

All fictitious climate models considered in this study have uni-dimensional (altitude) dependency in space. The fictitious CCFs and directional derivative, both are measured along the altitude. This is necessary to understand the performance and characteristics of the bi-level algorithm. However, for AirClim CCFs or any other realistic climate model the CCFs are dependent on exact emission position (longitude, latitude and altitude). Calculating an optimal flight path within such advanced climate model require three degrees of freedom in space. By discretizing the cruise phase into modes of constant altitude cruise, climb and descent, the bi-level algorithm is only able to evaluate the cost variation from changes in altitude. This limits the algorithm from calculating potential trajectories with maximum climate mitigation. In the final section of this chapter, a control problem to calculate the optimal mode sequence for a cruise phase between Lisbon (LIS) and Miami (MIA) is studied with AirClim CCFs. The trajectories are designed for minimizing the climate cost and the results of this section are validated with the results of study [40], where this control problem was first solved with free flight conditions. With this, the limitations of the bi-level control technique is highlighted.

All cruise trajectories designed in this chapter correspond to Trans-Atlantic flight routes. Control problems are formulated and solved using a standard PC featuring Intel i7 2.5 GHz processor and 12GB RAM.

4.1. OPTIMAL OPERATING COST CRUISE

In this section constant Mach cruise trajectories are designed for a fictitious North Atlantic flight route between Illinois, Chicago (ORD) and Frankfurt, Germany (FRA). To generate the optimal trajectories the operating cost is measured as the performance index. The climate weighing factor C_Ψ in the performance criterion (defined in equation 3.5) is set to zero while formulating the control problem. The initial sequence for the cruise phase is defined as a constant altitude cruise at FL 310 (10,363), assuming a constant Mach number of 0.82. For calculation of subsequent mode sequences, the variation in flight path is considered with the insertion of step-climb mode. The maximum altitude variation per mode insertion is set at +2000 ft.(609.6 m). An optimization is set up within TOM, using the mathematical model described in chapter 3, and the optimal mode sequence is calculated by the bi-level framework. The bi-level framework calculates the mode sequence from inserting a climb mode into the initial sequence such that a new sequence which lowers the cost is calculated in every iteration of the algorithm, till one of the exit conditions defined in section 3.4.3 is satisfied. The boundary conditions for the calculated trajectories are based on the BADA performance model (Airbus A330-200 aircraft) and the ATM constraints discussed in section 3.2. The atmospheric conditions are set to ISA conditions. The bounds imposed on the state and path vectors for solving this control problem are given in Appendix A.

4.1.1. REFERENCE TRAJECTORY AND COSTATE ESTIMATION

The reference trajectory is designed as an absolute economy cruise trajectory between ORD-FRA with the initial cruise altitude set to FL 340 (10,363 m) and the final altitude set free. The reference optimal trajectory is a flight path which gradually climbs until the ceiling altitude is reached, see figure 4.1. The final altitude of the reference trajectory results from a steep descent. The reason for the latter can be attributed to high speeds during descent, from converting potential energy to kinetic energy, which minimizes the fuel burnt in the final leg of the cruise. For convenience, the results of this section will only consider mode sequence with step-climb mode insertions. The maximum climb altitude is limited to the maximum altitude (FL 390) of the reference trajectory.

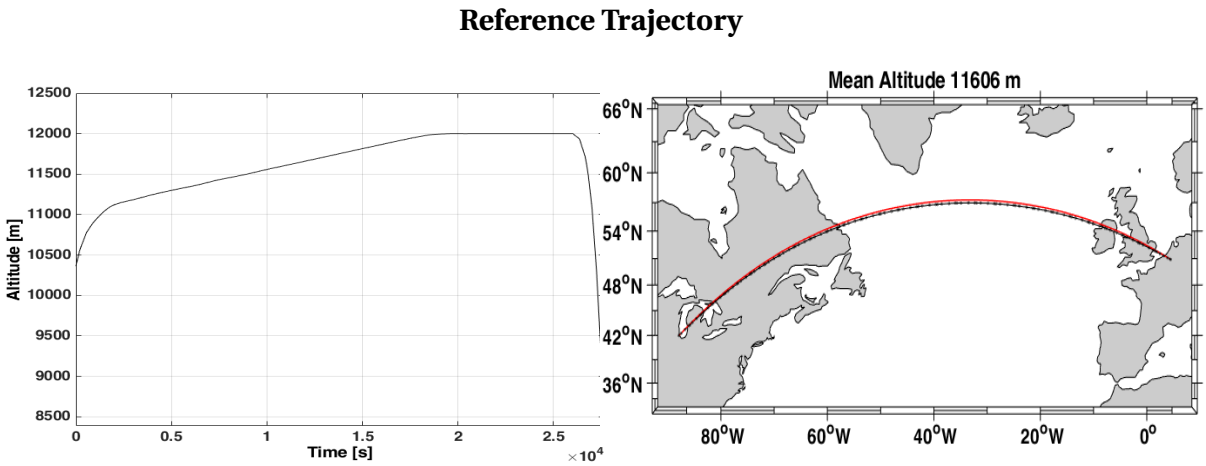

Figure 4.1: **Absolute economy cruise trajectory between ORD-FRA. Left: altitude with flight time plot. Right: latitude-longitude plot. The trajectory in red correspond to optimal cost and trajectory in black represent the Great Circle trajectory.**

Since the difference between the initial altitude and maximum altitude is approximately 5000 ft. (1524 m), the final optimal sequence calculated by the bi-level framework is expected to comprise of at most two step climbs. To save computational resources the maximum number of mode insertions is limited to two. In each insertion the flight trajectory will climb to flight level which is 2000 ft. higher than the initial altitude. Based on this the cruise trajectories are simulated at FL 360 (10,973 m) and 380 (11,582 m) and stored as a database for interpolating the operating cost of cruise mode in stage 2 of the algorithm. At a range of weights (between the take-off and zero fuel weight of the aircraft) the available fuel, range and flight time are recorded. The fuel consumption is calculated per distance covered. The recorded data for cruise at both flight levels is given in Appendix D.

To validate the costate estimated by GPOPS-II, the Hamiltonian is evaluated with the costate variables obtained from solving the constant altitude cruise control problem. Since the performance index only measures the operational cost, the number of state variables which contribute to the overall cost is reduced to four, longitude (Λ), latitude (ϕ), altitude (H) and the mass of the aircraft (m). The Hamiltonian is evaluated along the trajectory using eq. 3.21. At each time step the product of the costate (p_x) and state derivative ($\dot{x}$) is evaluated for each state variable. The Hamiltonian is then expressed as the cumulative sum of the latter product and plotted for all time steps, see figure 4.2. As expected, the Hamiltonian was found to be constant along the trajectory. This confirms that RPM-differentiation method used within GPOPS-II for costate estimation is reliable.

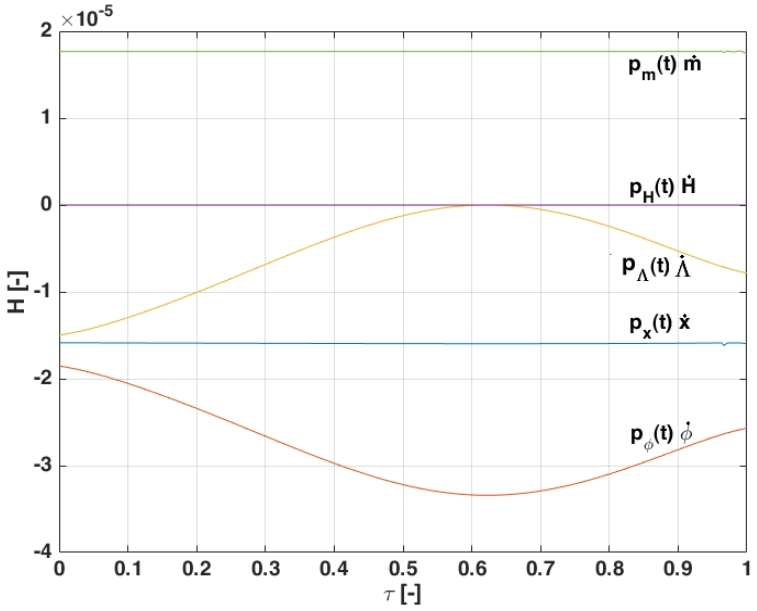

Figure 4.2: **Hamiltonian evaluated from the costate variables calculated within GPOPS-II. The costate estimation method is RPM-Differentiation.**

To initiate the bi-level framework, the optimal solution of the initial sequence is calculated. The continuous state and control vector obtained from solving the initial sequence is stored in memory. As only climb is considered in this section, the set of discrete modes is limited to step-climb. The initial and final Mach number of the climb mode is set to 0.82, for ensuring continuity between phases. The directional derivative is evaluated to determine the feasibility of the climb mode insertion. For each feasible mode insertion the optimal switching time calculated in stage 1 is bounded with a slack of $\pm$ 1000 seconds the estimated insertion time. This ensures that the optimal switching times calculated by the solver are closest to the estimated insertion times.

4.1.2. FIRST ITERATION

From the solution of the initial sequence 30% of the overall time steps are selected to represent set of insertion times in stage 2. For each insertion time a insertion function needs to be defined and a control problem for climb needs to be solved. Evaluating cost reduction for 100% time steps would increase the precision of the algorithm but would also increase the computational time significantly. Thus an appropriate percentage of insertion time is selected such that a fair compromise is made between the required precision and computation time.

In stage 2, the mode insertion is defined at each insertion time by solving a control problem to find the optimal climb. The initial boundary conditions for the control problem is set to the state vector from the solution of the initial sequence, corresponding to the insertion time. The final altitude at each insertion time is set to FL 340 and final Mach number is fixed to 0.82. Once the optimal climb is calculated the corresponding cost is stored. From the final position of the aircraft (after the climb), a great circle trajectory is assumed till the destination. The cost for this trajectory is then interpolated from the database corresponding to cruise at FL 340. The feasibility of the interpolated cruise phase is ensured by evaluating the maximum range with the available fuel. If the great circle distance is lower than the maximum range then the mode insertion is

determined to be infeasible and the corresponding cost variation is disregarded. The overall cost for the new sequence is calculated by combining the cost to cruise till the insertion time ($\hat{t}$), the cost to climb and the interpolated cost. The directional derivative is then evaluated using eq. 2.15.

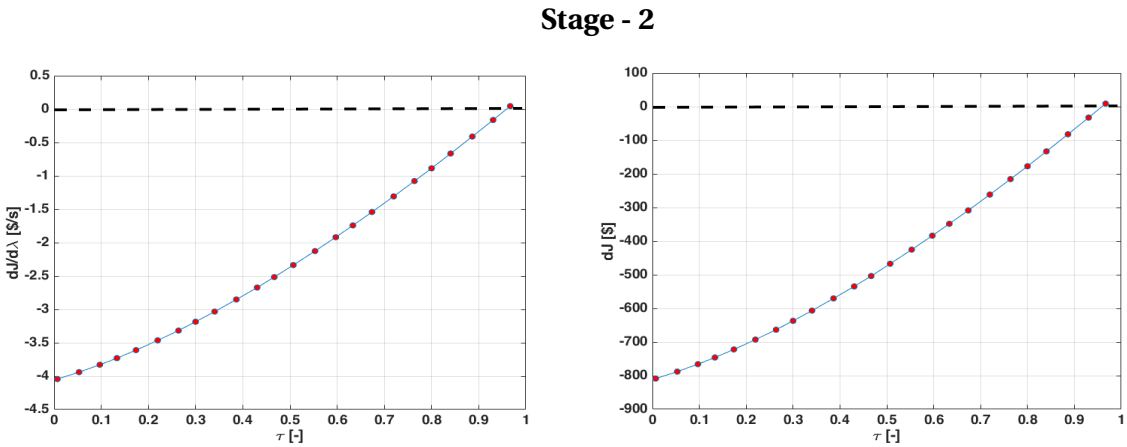

Figure 4.3: **Directional derivative Vs. insertion time plot, with increasing mode duration, (λ) for climb mode insertion in the initial sequence.**

Table 4.1: **Table to express the differences between the stage 2 and stage 1 calculations for optimal switching time and cost reduction, for all trajectories shown in figure 4.4.**

Trajectory	Estimated Switching time (s)	Optimal Switching Time (s)	Estimated Cost Reduction ($) (dJ($\rho^{\eta}(\tilde{\lambda})$))	Actual Cost Reduction ($) (dJ)	Error in Cost reduction(%)
A	193	869	808.7	727	11.23
B	6,020	6,673	692.7	650	6.56
C	10,088	9,289	570.3	595	4.20
D	15,363	15,063	383.7	437	12.19

The directional derivative evaluated in stage 2 along with the estimated cost reduction (dJ) is shown in figure 4.3. The flight time is represented in terms of the independent variable (τ), see definition in eq. 2.7. From the directional derivative plot it can be observed that a step-climb at all insertion times will lower the overall operating cost. This result is in agreement with the reference behaviour. Since the new sequence comprises three modes, their switching times will be represented as t_0, t_1, t_2, $t_3(t_f)$. The initial time t_0 is zero for all optimal trajectories calculated in this study. To evaluate the precision of the algorithm the optimal sequences are defined with the step-climb mode inserted at each of the insertion time in $t_1 = [193, 6020, 10088, 15363]$ seconds. The optimal switching times for the respective mode sequence is then calculated by solving the multi-phase problem in stage 1. The optimal trajectories along with their switching times, for each of the considered mode sequence, is shown in figure 4.4. Note that the optimal time to climb ($t_2 - t_1$) is limited by the upper bound set on duration to climb. This indicates that the bounds specified on duration to climb is insufficient to calculate an optimal climb. However, since the climb mode is relatively short, when compared to the overall flight time, the climb mode itself does not significantly affect the overall cost. Hence, a sub optimal climb solution is considered sufficient to continue this study.

From the optimal solutions of the trajectories shown in figure 4.4, the final time (t_f) is observed to increase with earlier insertions of climb. The true airspeed decreases with increasing altitude while flying at a constant Mach number. This characteristics of the airspeed increases the total flight time as the climb mode insertion approaches insertion times close to the initial time. However, the overall cost reduction is dependent on both time and fuel consumption. Flying at higher altitudes result in lower rate of fuel consumption. The total fuel burnt contribute significantly to the overall cost. Thus, the overall cost reduction from climbing should increase as the insertion time approaches the initial time. Based on this the characteristics of the evaluated directional derivative is validated. The maximum error within the algorithm's estimated cost reduction is less than 15%. The error between the estimated cost reduction (stage 2) and actual cost reduction (stage 1) is shown in table 4.1.

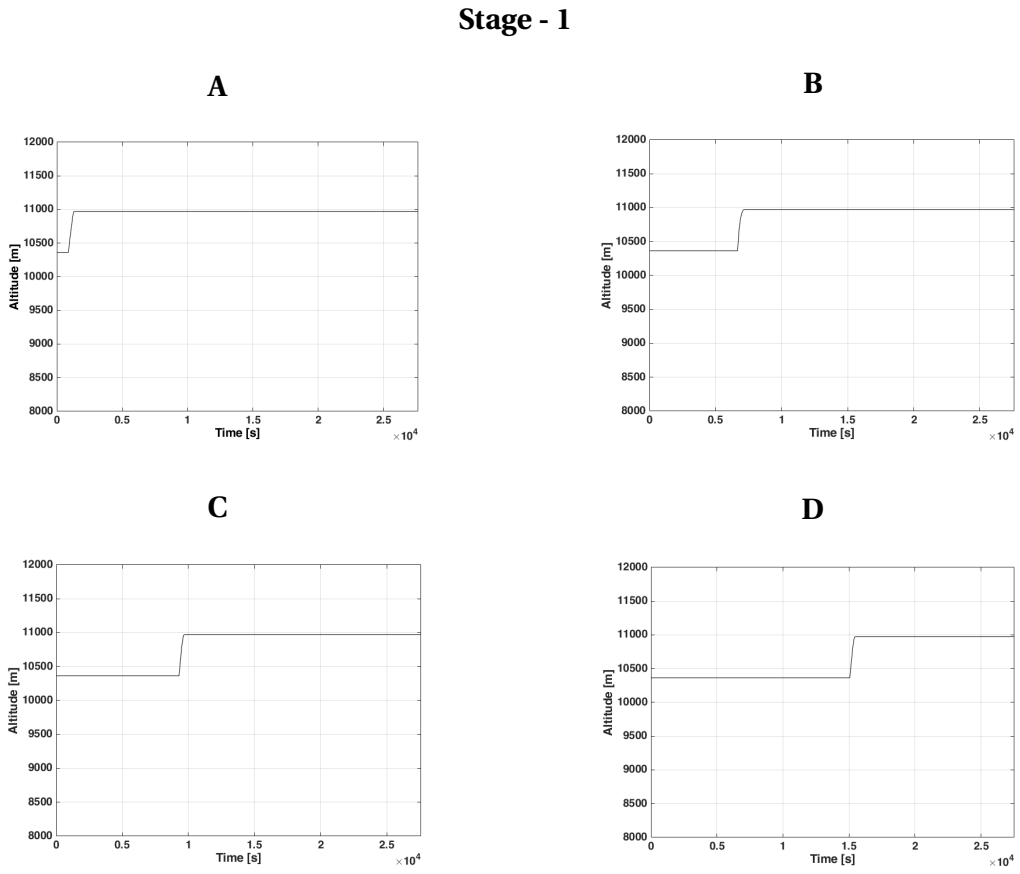

Optimal Trajectory	Switching Time (s)		
	t_1	t_2	$t_3(t_f)$
A	869	1,369	27,654
B	6,673	7,173	27,603
C	9,289	9,789	27,579
D	15,063	15,563	27,524

Figure 4.4: **Altitude-real flight time plots for a constant altitude cruise with a step-climb and their corresponding switching times calculated in stage 1 of the bi-level framework.**

To calculate the optimal sequence, the switching times corresponding to trajectory A in figure 4.4 are selected as the optimal switching times of the next mode sequence. Further insertions will be calculated by evaluating cost variation with respect to the final cost of this sequence.

4.1.3. SECOND ITERATION

Remember that for subsequent iterations the feasible set of insertion times are selected from the final cruise mode of the previous sequence, see section 3.4.3. In the second iteration of the stage 2, the second climb mode is inserted into the final cruise mode of the sequence determined in the first iteration. Similar to the first iteration, the number of candidate insertion times are limited to 30% of the time steps. The set of candidate insertion times is defined from the final phase solution, which is obtained after solving the multi-phase problem in stage 1. The inner loop within stage 2 calculates the optimal climb and sequence cost by solving a control problem and interpolating the cruise cost, from the database, at each candidate insertion time. The directional derivative and cost reduction both are evaluated at each insertion time. Figure 4.5 shows the directional derivative and cost reduction (dJ) plot for the second climb mode insertion. The independent variable axis of the plots represent the insertion times between 1,369 seconds (t_2) and 27,654 seconds (t_f).

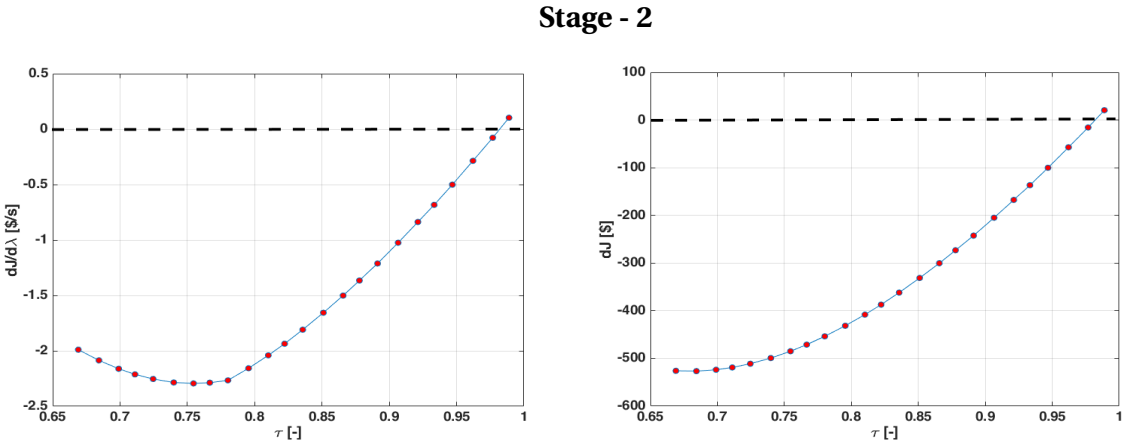

Figure 4.5: **Directional derivative and cost reduction with independent variable (τ) plot for the second climb mode insertion.**

From the cost reduction plot it is observed that the maximum cost reduction occurs at an insertion time closest to $\tau = 0.66$ (1,369 seconds). However, based on the directional derivatives, the cost reduction per second of climb is found to be maximum for an insertion at $\tau = 0.7546$ (7,803 seconds). For clearing the discrepancy between both the plots, a new sequence with two step-climbs is defined and the multi-phase problem is formulated. The switching time (t_3) of the second step-climb is bounded within [1369, 7803] seconds. The optimal stitching times for this mode sequence is then calculated in stage 1. It was observed that for insertion times less than 7,000 seconds the solver was not able to calculate an optimal solution, i.e. the problem remains in-feasible. Because a single phase climb control problem is used as an approximate solution for the climb phase of the multi-phase cruise problem, the infeasiblity at initial insertion times could not be captured in stage 2. From comparing the control inputs of climb mode, of stage 1 and stage 2, it is observed that the available thrust is over estimated while calculating climb in stage 2. As the bi-level algorithm is sensitive to the mode inputs, the switching time calculated in stage 1 and stage 2 can thus be significantly different.

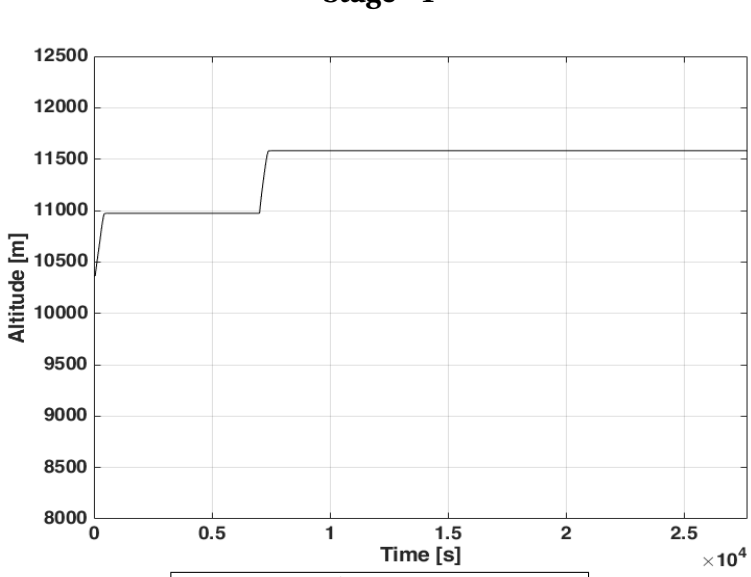

Switching Time (s)				
t_1	t_2	t_3	t_4	$t_5(t_f)$
54	554	7,015	7,515	27,680

Figure 4.6: **Altitude-real flight time plots for a constant altitude cruise with two step-climb and their corresponding switching times calculated in stage 1 of the bi-level framework.**

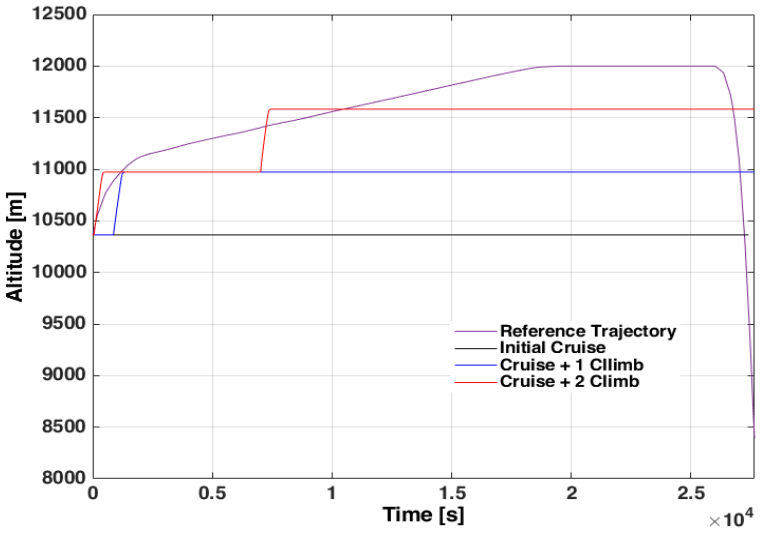

Figure 4.7: **Altitude-flight time plot for the reference trajectory, initial constant altitude cruise and trajectories calculated in each iteration of the bi-level framework, for cruise phase between ORD-FRA with no bounds on Mach.**

Table 4.2: **Normalized operating cost, fuel and flight time for mode sequence calculated within TOM for calculating the operating cost optimal cruise trajectory.**

Optimal Sequence	**COC [-]**	**Fuel [-]**	**Time [-]**
Reference Trajectory	1	1	1
Initial Sequence	1.021	1.059	0.991
Cruise + 1 Climb	1.011	1.025	0.999
Cruise + 2 Climb	1.004	1.008	1.001

For the mode sequence with two step climbs, the optimal switching time for performing the second climb is calculated at t_3 = 7,015 seconds. Further, the switching time of the step-climb calculated in the first iteration shifts backwards from t_1 = 869 seconds to 54 seconds, approaching the initial time. The optimal switching times and altitude plot for the new mode sequence is shown in figure 4.6. Based on the above results it can be suggested that the measure of cost difference can only provide sufficient information to determine whether a mode insertion will lower the cost. But, for estimating the optimal switching time evaluating the directional derivative maybe more efficient.

After the second iteration the bi-level framework terminates as the optimal mode sequence within feasible bounds is calculated. The optimal trajectories calculated in both iterations of the framework and that of the reference solution is shown in figure 4.7. The normalized operating cost (COC), fuel burnt and overall flight time for all the optimal trajectories shown in figure 4.7 are given in table 4.2. Based on the results it is concluded that for a cruise phase with step-climb the overall fuel burnt decreases and the flight time increases. Increasing the number of step-climb will further decrease the overall cost i.e. the cost will approach the reference cost.

4.2. FICTITIOUS CLIMATE OPTIMAL TRAJECTORIES

To calculate fictitious climate optimal trajectories, the cruise phase mode sequence with climb and descent mode insertions are calculated for the flight route between ORD-FRA. In the cost function equation the monetary cost weighing factor is set to zero for all control problems formulated in this section. Similar to the previous section, the cruise phase is defined assuming a constant Mach flight and the cruise mode is defined as a constant altitude cruise mode. Within the cruise phase, a beneficial deviation in flight path can only be brought about by performing either a climb or descent. The cruise phase is initiated at FL 350 (10,668 m). For both climb and descent modes the final boundary conditions are fixed for altitude (± 2000 ft.) and Mach number (0.82). The flight envelope and performance parameters are calculated from the BADA performance model. The flight conditions are calculated assuming ISA conditions.

In the following two sections, the cruise phase trajectories are calculated from minimizing the climate

cost. The CCFs to calculate the climate cost are determined from the fictitious climate model A and B, discussed in 3.3.2. The control problems are formulated within TOM and the optimal cruise mode sequence and corresponding switching times are calculated using the bi-level framework. The mode sequences are calculated from considering both climb and descent mode insertions in stage 2 of the algorithm.

4.2.1. MODE SEQUENCE FOR CLIMATE MODEL A

The 1D spatially varying CCFs of Climate model A are defined to reduce the climate impact with decreasing cruise altitude. The objective of this climate model is to determine mode sequences for cruise phase with the descent mode lowering the overall cost. The rate of change of climate cost is represented using eq. 3.7. The arbitrary constant k_{11} and k_{12} are chosen using trial and error such as to ensure that the climate impact remains sensitive to small variations in altitude. The values of these constants are given in Appendix C. The reference cruise trajectory calculated for minimizing cruise phase climate impact within climate model A is shown in figure 4.8. From the reference trajectory it can be observed that lowest climate impact in the fictional climate model results from cruising at the lower bound of the cruise altitude. With free flight conditions, the flight path for the optimal cruise descends from the initial cruise altitude FL 350 (10,668 m) to the minimum cruise flight level FL 270 (8,353 m). The time to descend is minimized such that the aircraft covers maximum flight distance from flying at the lowest cruise altitude. Based on this, the optimal mode sequence for a cruise within this fictitious climate model is expected to consist of successive descent modes until the lower bound of the cruise altitude is reached.

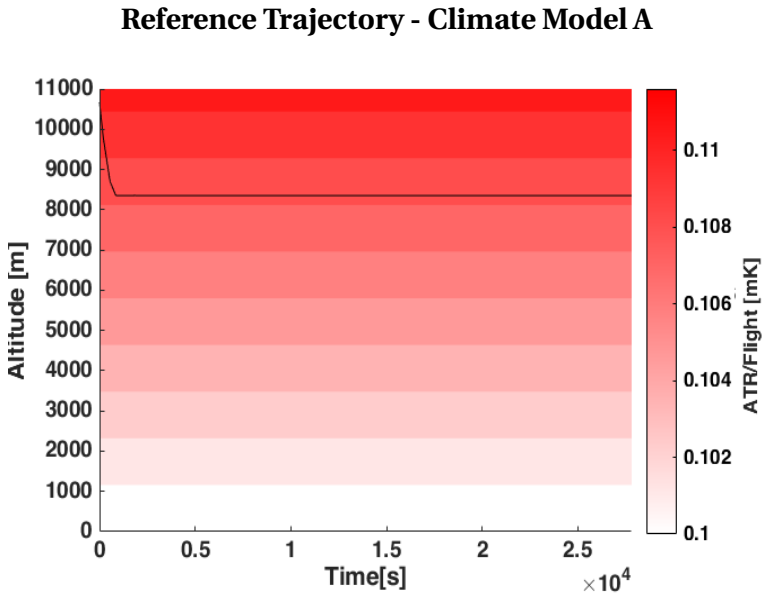

Figure 4.8: **Absolute minimal climate cost reference trajectory calculated from climate model A.**

For calculating the optimal cruise phase mode sequence the control problem to minimize climate cost is set up with the bi-level framework. The framework is initiated with the initial sequence set to constant altitude cruise at FL 350. Similar to the operating cost control problem, the candidate set of insertion times is limited to 30 % of the overall time steps of the initial solution. Constant altitude cruise trajectories are simulated at FL 370 (11,278 m), 330 (10,058 m), 310 (9449 m) and 290 (8839 m) for interpolating the climate cost of cruise mode in stage 2. In stage 2 the climate cost is interpolated for the cruise mode which follows after the inserted mode. Since the CCFs of climate model A are directly related to flight time and altitude, the climate cost is estimated from calculating the required flight time to cover the required range at a given altitude. The database used for solving the control problem formulated in this section is given in Appendix E.

In the first iteration of the bi-level framework the mode sequence is calculated from considering both, climb and descent mode insertions. At each insertion time an optimal control problem is solved for both climb and descent mode. The climate cost of the new sequence is then estimated from combining the cost from the initial sequence until the insertion time, cost during climb/descent and the interpolated cost of the cruise phase at the new cruise altitude. The directional derivative is then evaluated for each sequence cal-

culated within stage 2. The directional derivative plots evaluated from inserting climb and descent modes are shown in figure 4.9. As expected, the climate cost is observed to reduce for descent mode insertions. The maximum cost reduction is observed for a descent insertion at time $\hat{t} = 0$. Since the directional derivative evaluated for climb mode insertions are positive at all insertion times,a new mode sequence with only descent mode insertion is calculated in stage 2. In stage 1 the optimal switching times for this new mode sequence is then calculated. The optimal solution calculated in stage 1 is shown in figure 4.10.

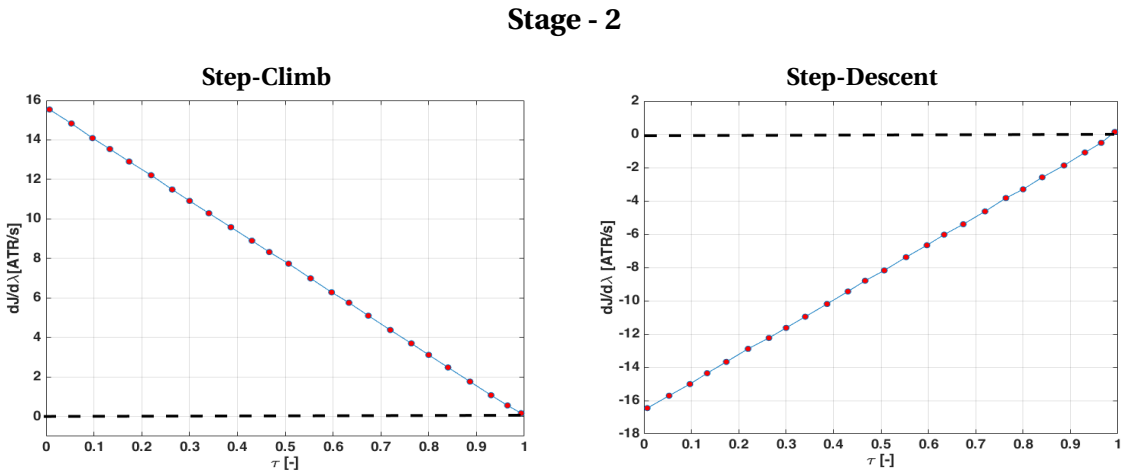

Figure 4.9: **Directional derivative- independent time plots for climb (left) and descent (right) mode insertions for lowering the climate cost of the cruise trajectory within climate model A.**

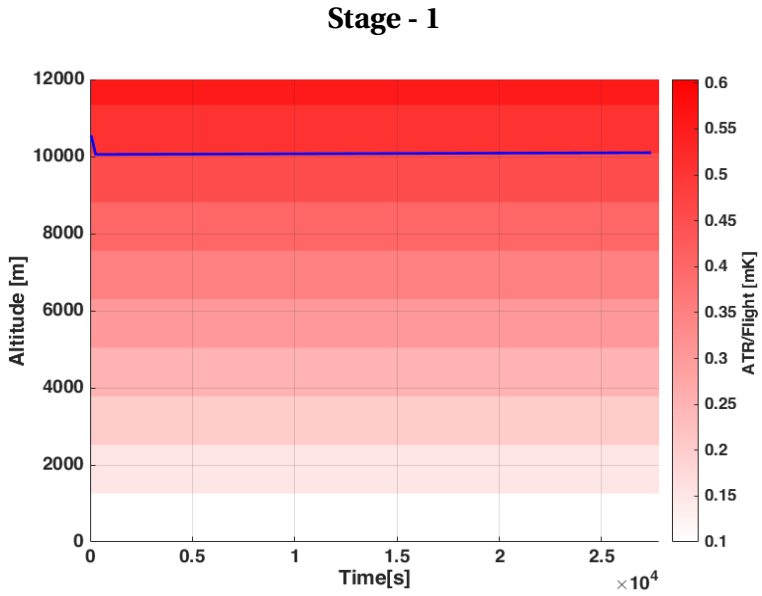

Switching Time (s)		
t_1	t_2	$t_3(t_f)$
0	500	28,485

Figure 4.10: **Altitude-real flight time plot for a constant altitude cruise with step-descent and switching times calculated in stage 1 of the bi-level framework.**

In each iteration of stage 2, a new mode sequence is calculated from inserting a descent mode into the mode sequence of the previous iteration. While calculating the new sequence, the stage 2 discretizes the cruise mode and inserts a descent mode based on the rule mentioned in figure 3.3. Due to limited memory, the number of bi-level framework iterations is restricted to a maximum of three mode insertions. In every iteration the algorithm successfully calculated the new mode sequence in stage 2 and their optimal switching

times are calculated in stage 1. The final optimal solution and switching time calculated by bi-level framework is given in figure 4.11. Because of time constraint, the optimal solution of the final sequence did not converge to the desired tolerance. The switching time sets $\{t_0, t_2, t_4, t_6\}$ and $\{t_1, t_3, t_5\}$ correspond to the initial time of the cruise modes and descent modes, respectively, of the final mode sequence. The normalized flight time and climate cost for all mode sequence calculated within this section is given in table 4.3.

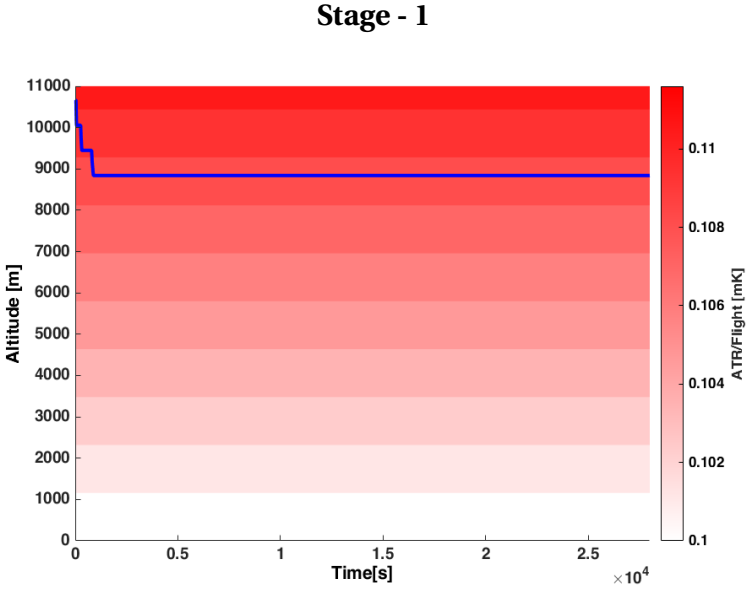

Switching Time (s)						
t_1	t_2	t_3	t_4	t_5	t_6	$t_7(t_f)$
0	252	252	615	615	1,115	27,985

Figure 4.11: **Altitude-real flight time plot for a constant altitude cruise with three step-descent and switching times calculated in stage 1 of the bi-level framework.**

Table 4.3: **Normalized climate cost, fuel and flight time for mode sequence calculated within TOM for calculating the climate cost optimal cruise trajectory within Climate Model A.**

Optimal Sequence	ATR [-]	Fuel [-]	Time [-]
Reference Trajectory	1	1	1
Initial Sequence	1.050	0.828	1.033
Cruise + 1 Descent	1.033	0.861	1.024
Cruise + 2 Descent	1.024	0.904	1.015
Cruise + 3 Descent	1.008	0.955	1.006

The optimal mode sequence of the considered optimal control problem consists of descent modes which are sequenced one after the other. Though the definition of the mode sequence used in this study does not allow for two adjacent mode insertions, the optimal duration of the cruise mode which is mandated between two mode insertions is calculated to be zero, see switching times in figure 4.10 and 4.11. Based on this, it is concluded that the rule discussed in figure 3.3 allows zero entries (duration of mode equals zero), and the algorithm efficiently captures these zero entries.

4.2.2. MODE SEQUENCE FOR CLIMATE MODEL B

This study so far considered control problems in which the optimal mode sequence was calculated by inserting either a climb or descent mode. The optimal sequences of these control problems are homogeneous and the modes were periodically sequenced. However, the optimal mode sequence for minimizing cruise phase climate impact can have non periodic mode sequence mainly because of the non-linear spatial dependency of the CCFs estimated in advanced climate models. Because of the latter characteristics of the CCFs, the mode sequence calculated for minimizing climate impact may simultaneously comprise both climb and de-

scent modes. Thus calculating the optimal mode sequence for such control problems will require careful consideration because each iteration of the bi-level framework may have more than one feasible mode insertion which lowers the overall cost.

In this section, the mode sequence for minimizing the fictitious climate cost during cruise is calculated using the bi-level framework. For understanding the characteristics of the bi-level framework with respect to non-linear CCFs, the climate cost is represented with fictitious CCFs of Climate model B, see figure 3.1. The arbitrary constants, k_{11}, k_{12}, k_{21} and k_{22} in eq. 3.8, are chosen to represent distinct feasible regions for climb and descent mode, where they individually lower the overall climate impact. The reference trajectory is calculated by solving a single phase cruise optimal control problem for the flight route between ORD - FRA. The cruise phase is initiated at FL 350 (10,668 m) assuming free flight conditions and constant Mach number of 0.82. Since the climate cost is lowered with altitude in the first half of the total flight time ($t <$ 14170 seconds), the flight path descends to the minimum cruise flight level (FL 270). For flight time greater than 14170 seconds the flight path swiftly climbs to the maximum cruise altitude (FL 410), as the conditions become favourable to fly at higher altitudes. The reference cruise trajectory is shown in figure 4.12. The values of the arbitrary constants are given in Appendix C.

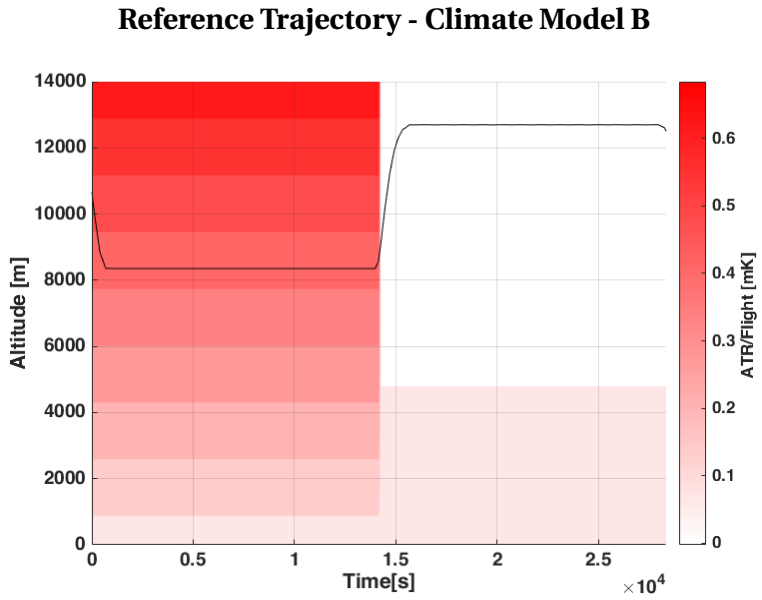

Figure 4.12: **Absolute minimal climate cost reference cruise trajectory calculated within climate model B.**

Similar to previous sections, the bi-level framework is initiated by solving a single phase optimal control problem for the initial sequence and selecting a set of candidate insertion times. The database for interpolating the climate cost of the final cruise mode in stage 2 is created by simulating cruise flight at different flight levels. The data stored for cruise at different flight levels is given in Appendix F. In the first iteration of stage 2, the directional derivative is evaluated for both climb and descent mode insertions. The directional derivative plots of both modes is given in figure 4.13. From the directional derivative plots it can be observed that both climb and descent mode have a feasible set of insertion times at which the overall cost is reduced. For a step-descent to lower the climate impact, the insertion times less than $\tau = 0.5$ (t = 14375 seconds) are found feasible, with the maximum cost reduction occurring for an insertion at $t = 0$. For insertion times greater than $\tau = 0.5$ climbing to higher altitude is found to be beneficial. The maximum cost reduction with climb mode insertion occurs at t = 14375 seconds.

Since the stage 2 iteration evaluates cost reduction with both climb and descent mode insertions, successive mode sequences are calculated considering two cases. In the first iteration of stage 2 two mode sequences are defined; cruise with step-climb and cruise with step-descent mode . For the mode sequence with climb mode the initial guess for insertion time of climb is set at t = 14375 seconds. The optimal switching times for this sequence is then calculated in stage 1. The optimal solution for the mode sequence with climb mode is shown in figure 4.14(A). Similarly the optimal switching times for mode sequence with descent mode is calculated in stage 1. The initial guess for insertion of descent mode is set at t = 0 seconds. The optimal solution obtained for this sequence is shown in figure 4.14(B).

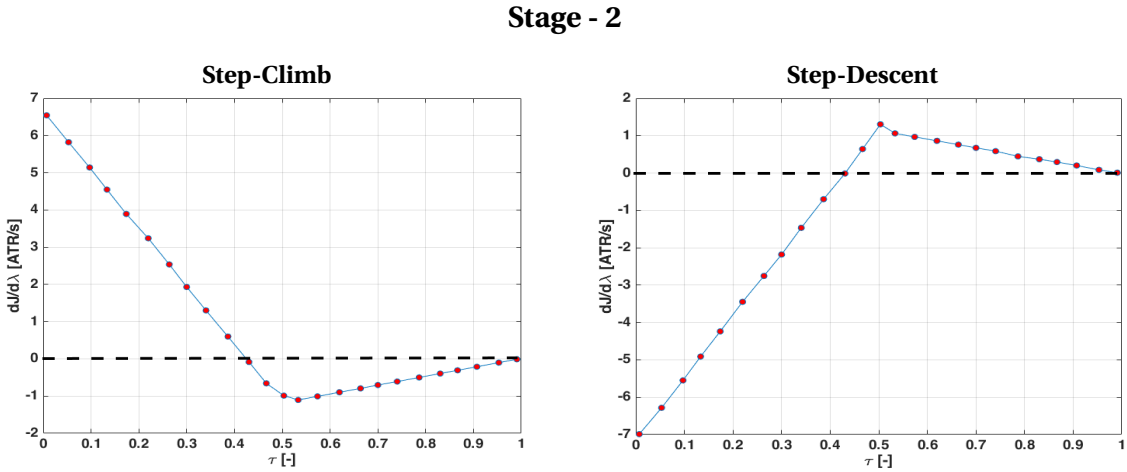

Figure 4.13: **Directional derivative- independent time plots for climb (left) and descent (right) mode insertions for lowering the climate cost of the cruise trajectory within climate model B.**

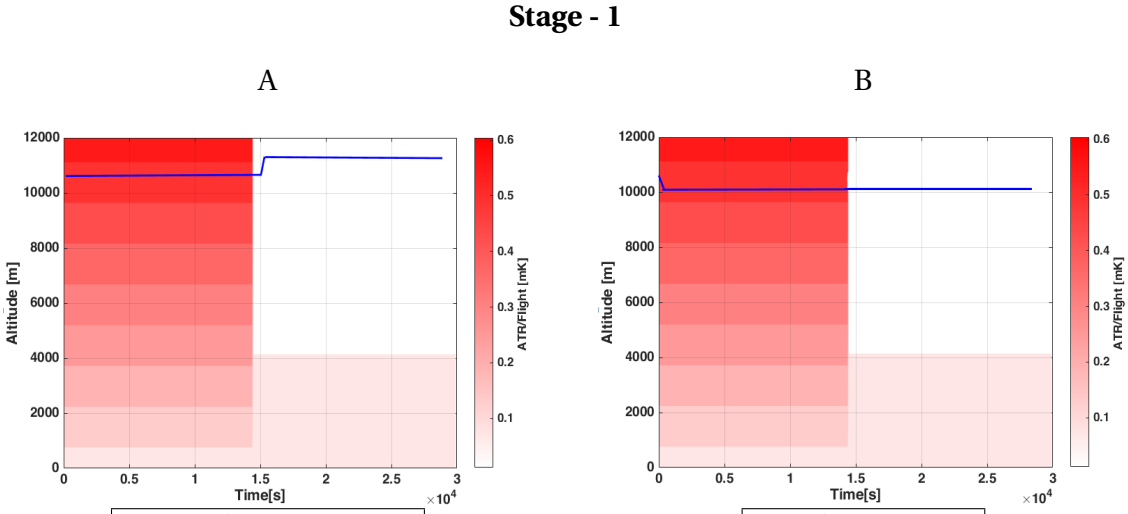

Switching Time (s)		
t_1	t_2	$t_3(t_f)$
15,033	15,533	28,837

Switching Time (s)		
t_1	t_2	$t_3(t_f)$
3	203	28,487

Figure 4.14: **Altitude-real flight time plots for a constant altitude cruise with one step-climb (left) and one step descent (right) and respective switching times calculated in stage 1 of the bi-level framework.**

In subsequent iterations of stage 2 the overall cost of the mode sequence shown 4.14(A) is observed to reduce further with climb mode insertions only. However, in case of the mode sequence shown in figure 4.14(B) the directional derivative is once again observed to be negative for both climb and descent mode insertion. The optimal solution calculated after inserting climb mode into the mode sequence 4.14(B) is shown in figure 4.15. As the directional derivative is evaluated only for mode insertions within the final mode of the previous sequence, the order in which the modes are inserted influences the mode sequence calculated in the subsequent iteration. Thus to calculate the optimal mode sequence, it is important that the modes be inserted in accordance to the insertion time at which the cost reduction is found to be maximum. Further, if two or more modes are found feasible within the stage 2 iteration then it is recommended to define the new sequence with the mode insertion for which the cost reduction is maximum. For the case considered in this section the cost reduction in the first iteration of stage 2 is found to be higher for descent mode insertion rather than for climb mode insertions, see table 4.4. In table 4.4 the normalized climate cost, fuel and flight time are given for all mode sequences discussed in this section.

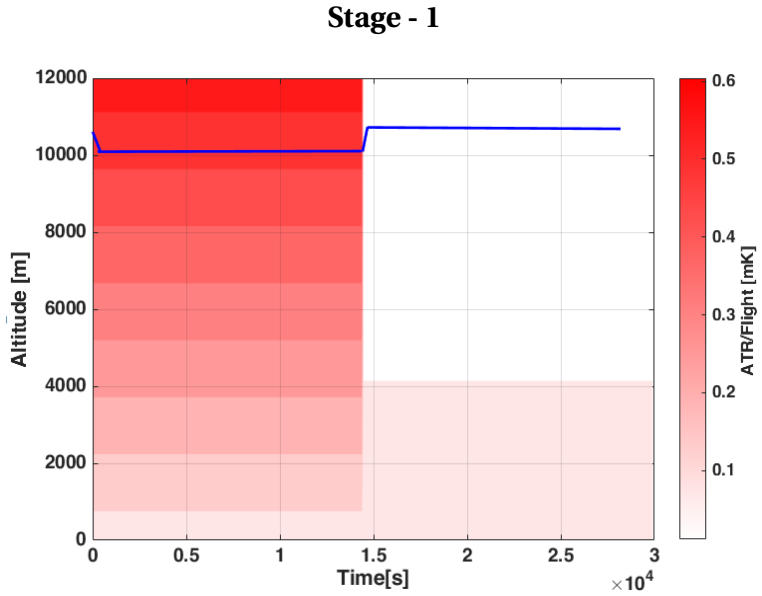

Switching Time (s)				
t_1	t_2	t_3	t_4	$t_5(t_f)$
0	452	14,247	14,747	28,626

Figure 4.15: **Altitude-real flight time plot of a constant altitude cruise with step-descent and climb mode along with their switching times calculated in stage 1 of the bi-level framework.**

Table 4.4: **Normalized climate cost, fuel and flight time for mode sequence calculated within TOM solved for minimizing the climate cost within Climate Model B.**

Optimal Sequence	ATR [-]	Fuel [-]	Time [-]
Reference Trajectory	1	1	1
Initial Sequence	1.252	0.923	1.014
Cruise + 1 Climb	1.244	0.908	1.018
Cruise + 1 Descent	1.185	0.959	1.005
Cruise + 1 Descent + 1 Climb	1.177	0.938	1.010

4.3. AIRCLIM CLIMATE OPTIMIZED TRAJECTORY

The trajectories calculated to minimize the climate cost based on the AirClim CCFs are influenced by the emission position. The cost functional measured for calculating such climate optimal trajectories are sensitive to deviations in all three dimensions of space. However, the bi-level framework designed in this study is only able to calculate the mode sequence based on the cost variation while accounting for deviations in one dimension, namely altitude. Thus the mode sequence calculated by the algorithm are sub-optimal solution. Further, additional errors will be introduced into the directional derivative as the algorithm does not account for lateral and directional deviations in flight path. To understand the limitation of the algorithm better, the optimal control problem to minimize the climate cost for Trans-Atlantic route from Lisbon (LIS) to Miami (MIA) is formulated and solved in this section.

4.3.1. PROBLEM DESCRIPTION AND REFERENCE TRAJECTORY

The single-mission assessment for the Trans-Atlantic route from Lisbon (LIS)- Miami (MIA) discussed in [40] is solved using the bi-level control algorithm for calculating cruise phase mode sequence with step-climb mode. The control problem for this mission is formulated with the mathematical model discussed in chapter 3. The cruise trajectory is optimized for minimizing the climate impact. In the performance criteria eq. 3.5 the weighing factor for climate impact is set to one. The trajectory is simulated with BADA 4.0 Airbus A330-200 aircraft performance model assuming ISA conditions. The flight conditions are constrained with ATM constraints.

The climate responses for aircraft emissions (m_i) are calculated within the model AirClim in dependency

of locus and time. For varying flight altitudes ($H_i \in$ [8500 m m,12500 m]) the cruise emissions are simulated and the resulting emission are distributed evenly into AirClim in 10° longitude and 10° latitude steps in corresponding height. The monthly climate impact per flight is expressed for each climate agent i as average temperature response over 100 years ($ATR_{100,i}$)), see eq. 3.9. The climate cost is expressed based on the annual average climate cost functions.

To validate the control problem formulated in this section, the cruise flight is optimized with free flight conditions. The cruise phase is simulated with the initial flight altitude fixed at FL 280 (8500 m), assuming 85% load factor and a constant Mach number of 0.82. The free flight climate optimal trajectory and the longitude-latitude plot for the cruise flight is shown in figure 4.16. The results calculated within TOM is in agreement with the results published in [40]. The free flight climate optimal trajectory reduced the climate impact by around 35% for 10% cash cost increase.

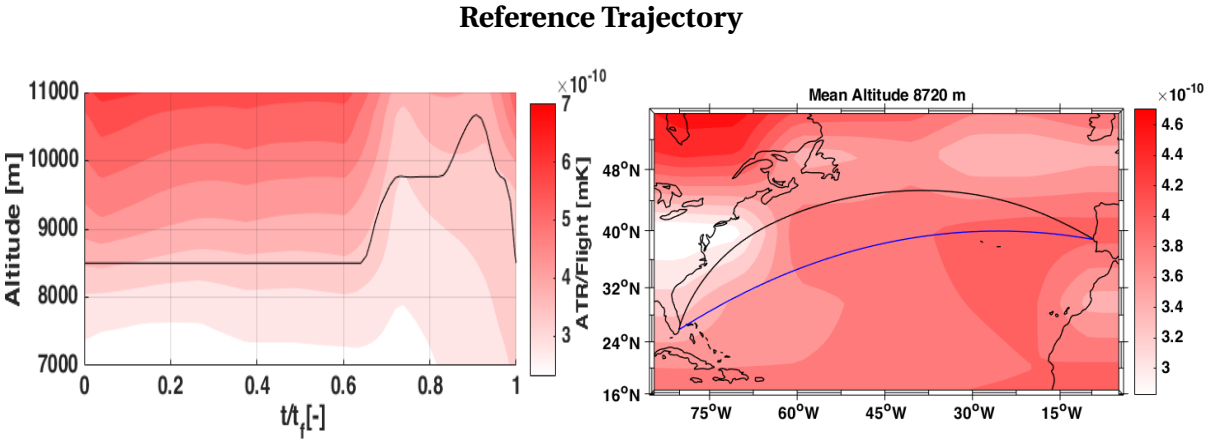

Figure 4.16: **Altitude-longitude plot (left) and latitude-longitude plot (right) of optimized trajectory on the trans-Atlantic route from Lisbon (LIS) to Miami (MIA). The trajectories are optimized to minimize the climate impact and flight conditions is assumed to be free.**

4.3.2. CLIMATE COST INTERPOLATION

As mentioned in the previous section, the emission is evenly distributed in steps of longitude and latitude for a corresponding height. The emission impact at a given longitude and latitude may vary with varying altitude. Therefore, the constant altitude cruise trajectories calculated for minimizing the climate cost at different flight levels may have different flight paths. This is clearly depicted in figure 4.17, where the longitude - latitude plots for climate optimal cruise are given with increasing flight levels. This increases the complexity of the problem especially while comparing trajectories which have the same initial and final position, but different mean altitude. In such cases the trajectories obtained from variations of a given mode sequence may be far from nominal and hence not comparable. Thus to determine the mode sequence the new mode sequence constructed in stage 2 should employ a single mode insertion technique on a flight path which is fixed with respect to the geographical coordinates i.e. constant in the longitude-latitude plane.

For calculating a feasible insertion in stage 2, it is important that the new mode sequence be comparable to the initial sequence. The new sequence is calculated by solving for an optimal path for the inserted mode and interpolating the cruise phase which follows after the inserted mode. To ensure consistency between the flight paths calculated in each iteration, the trajectory of the new sequence is made similar to the initial sequence trajectory in stage 2. To achieve such similarity the flight path is discritized into four parts as shown in figure 4.18. The first part represents the cruise phase till the insertion time $\hat{t}$, expressed as 1. The cost and flight path corresponding to first part is obtained from the solution of the initial sequence or previous sequence in subsequent iterations. The second part is the inserted mode which is obtained from solving the optimal control problem. For the final cruise phase, the flight path is split into two phases such that the flight path is converged into the trajectory of the initial sequence. From the final position $(\Lambda_{f_{mode}}, \phi_{f_{mode}})$, after the inserted mode, the closest coordinate (Λ_i, ϕ_i) in the trajectory of the initial sequence is determined by minimizing the distance between the coordinates. The flight path between the latter two coordinates is then interpolated as a constant altitude cruise mode. Since this mode is relatively small, the climate cost corresponding to this phase is neglected. However, the fuel burnt in this phase is calculated based on the weight

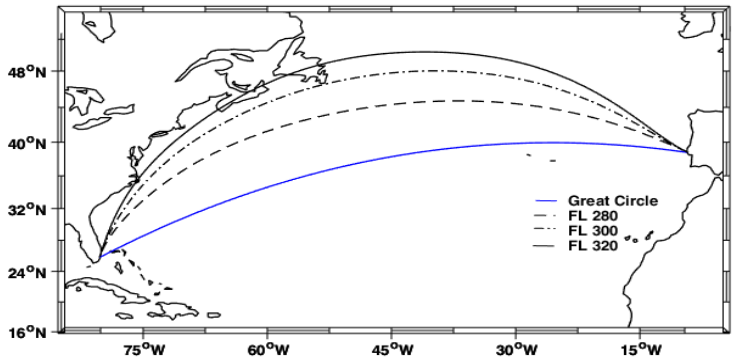

Figure 4.17: **Latitude-longitude plot of optimized constant altitude cruise trajectories calculated varying flight levels. The trajectories are optimized to lower the climate impact at each flight level.**

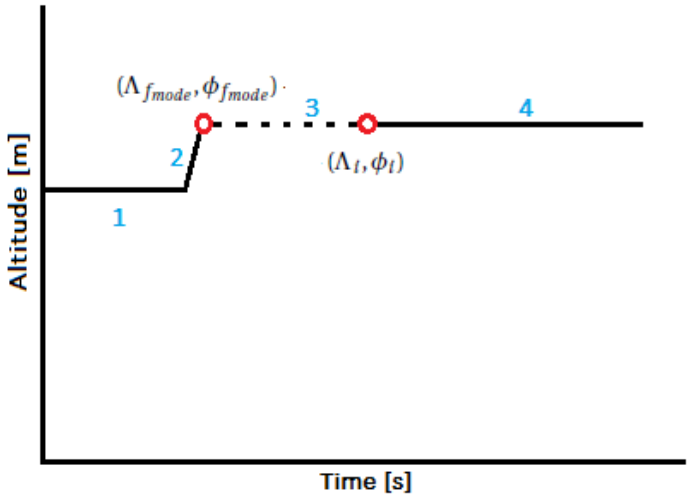

Figure 4.18: **Altitude- time plot describing the discritization of the cruise phase mode sequence in stage 2 of the algorithm.**

of the aircraft and distance between coordinates. The feasibility of the new sequence is then determined by calculating the available fuel and range for the fourth and final phase. For the final part the climate cost is again interpolated from the initial sequence solution. The final cost of the new sequence is finally expressed as the sum of all four parts. It is important to note that the new lower cost sequence calculated in stage 2 may not represent the global minimum. However, this method is expected to calculate the most optimal mode sequence for a given flight path.

4.3.3. AIRCLIM MODE SEQUENCE

The mode sequence for the flight route between LIS-MIA is calculated using the bi-level framework to minimize the climate cost. The cost variation in stage 2 is calculated using the method described in the previous section. The main objective of solving this hybrid problem in this section is to measure the accuracy and adequacy of the algorithm to estimate mode insertions. For convenience, the maximum number of mode insertions is limited to one and the set of discrete modes is restricted to climb modes. The initial cruise sequence for calculating the optimal flight route is initiated at FL 280. In stage 2 the new mode sequence with climb mode sequence is constructed for a set of insertion times (30% of the overall time steps) and the overall variation in cost is measured. The directional derivative plot evaluated to measure the climate cost reduction from modifying the sequence with climb mode is shown in figure 4.19.

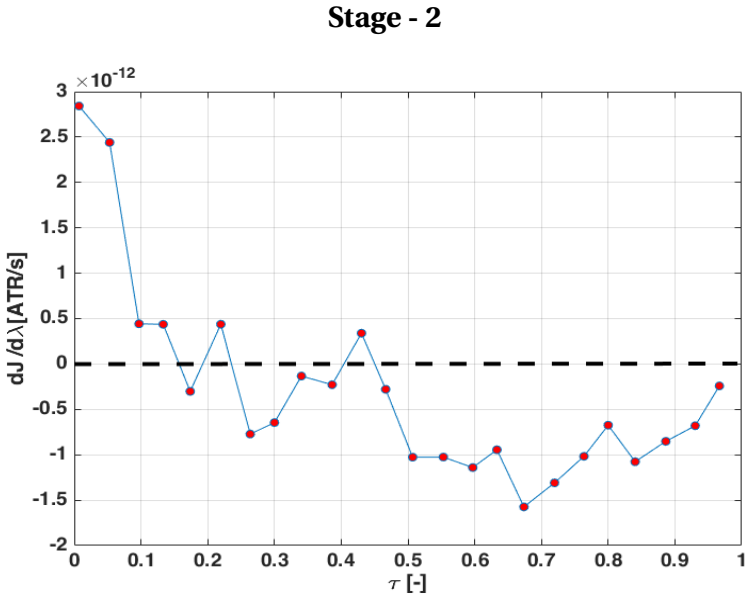

Figure 4.19: **Directional derivative- independent time plot for climb mode insertions for lowering the climate cost of the cruise trajectory within AirClim climate model.**

Based on the directional derivative plot it is observed that the maximum cost reduction occurs for a climb mode insertion at t = 18,511 seconds (τ = 0.6737). Since in stage 2 the evaluated directional derivative was found to be less than zero at more than one insertion time, the algorithm calculated a cruise phase sequence with 2000 ft. step-climb. The initial guess for the inserted climb is specified at the time in which cost reduction is observed to be maximum. The optimal switching times and climate cost for the new sequence is then calculated in stage 1. The optimal solution calculated after the first iteration of the algorithm is shown in figure 4.20 and normalized operating cost, climate cost, fuel and flight time for all sequence calculated is shown in table 4.5. Upon comparing the reference solution and the solution obtained from the first iteration of the algorithm it is observed that the overall climate impact of the first iteration mode sequence already approaches the reference climate cost. Although the mean altitudes of both trajectories are different, the climate impact is found almost similar because both trajectories are designed to minimize climate cost by flying different routes on the longitude-latitude plane. Thus unlike previously considered control problems it may not be always possible to compare the results of the algorithm with the reference trajectory.

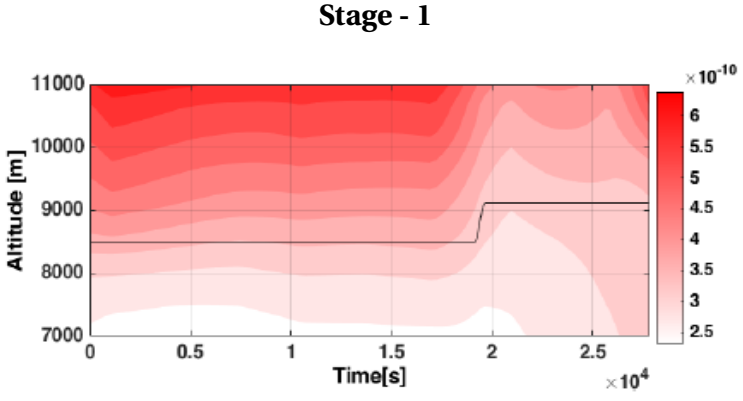

Switching Time (s)		
t_1	t_2	$t_3(t_f)$
19,179	19,679	27,762

Figure 4.20: **Altitude- real time plot of optimized cruise trajectory with step climb and switching times calculated in stage 1 of the bi-level framework.**

Table 4.5: **Normalized operating cost, climate cost, fuel and flight time for mode sequence calculated within TOM solved for minmizing the climate cost of cruise phase between LIS - MIA.**

Optimal Sequence	COC [-]	ATR [-]	Fuel [-]	Time [-]
Reference Trajectory	1	1	1	1
Initial Sequence	1.003	1.017	1.026	0.976
Cruise + 1 Climb	1.002	1.009	1.016	0.986

Table 4.6: **Table to express the differences between the stage 2 and stage 1 calculations for optimal switching time and cost reduction for trajectory shown in figure 4.20.**

Trajectory	Estimated Switching Time (s)	Optimal Switching Time (s)	Estimated Cost Reduction (ATR) $(dJ(\rho^{\eta}(\tilde{\lambda})))$	Actual Cost Reduction (ATR) (dJ)	Error in Cost Reduction (%)
Cruise + 1 Climb	18,511	19,179	3.15e-10	2e-10	57.5

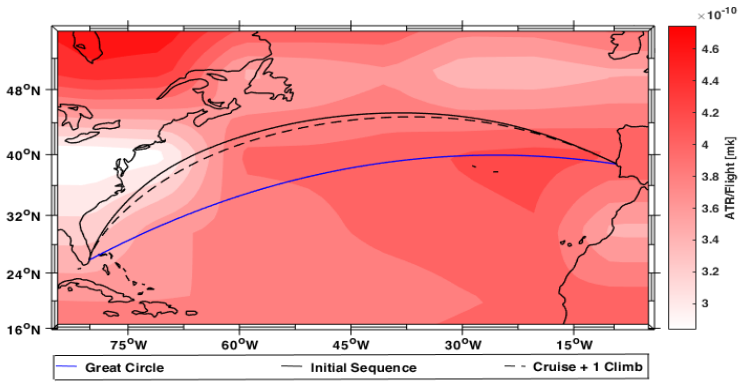

Figure 4.21: **Latitude-longitude plot of optimized cruise trajectories calculated with the initial mode sequence and for mode sequence with step-climb mode.**

To measure the accuracy of the algorithm the percentage error between the estimated cost reduction and actual cost reduction is calculated in table 4.6. The error in stage 2 solution is because of interpolation of the flight path discussed in previous section and the differences between the trajectories calculated in both stages which results in higher percentage overall error. This error can be minimized by selecting advanced interpolation techniques which can estimate the flight path and climate cost of the new mode sequence precisely . However, the maximum contribution to the overall error occurs from the difference in trajectories calculated in both stages. As the solver is free to optimize the flight path between the initial and final position, it is hard to completely remove this error. Figure 4.21 shows the optimal flight path calculated by the solver for the initial and first iteration mode sequence. Improving the accuracy of the algorithm would require the solver to ensure consistency between trajectories. This can possibly be attained by discritizting the flight route such that the aircraft is forced to pass through specific way-points.

5

CONCLUSION

With estimated increase in air traffic, there is an increased interest in finding climate optimized trajectories to reduce the overall climate impact of the aviation industry. From current understanding of the climate system, the non-CO_2 emissions from aircraft are estimated to contribute significantly to the global RF. The climate impact from these emissions are expected to be sensitive to locus and time of emission. Based on this, studies have identified large potential to mitigate climate impact from optimizing ideal 3D cruise trajectories. To extend this assessment further, this study considers inclusion of operational regulations while designing trajectories, as real flight paths are constrained with ATM regulations. The trajectories calculated in this study are limited to the cruise phase of the flight, as cruise is the longest phase of a long-haul flight. Since the free flight cruise trajectories were observed to vary in altitude, while reducing climate sensitivity along the trajectory, inclusion of ATM restricted step-climb and descent flight modes are considered essential to design climate optimized cruise trajectories.

Due to the dependency of the emissions on location and time, the resulting control problems in this study are formulated as a hybrid optimal control problem with variable mode sequence. Since a hybrid system comprises of both a continuous and discrete system, an optimal control technique based on the bi-level algorithm is designed to optimize both systems individually. The algorithm worked in two stages, the first stage calculates continuous inputs and optimal switching times for a given mode sequence and, the second stage updates the mode sequence from inserting a mode which lowers the overall cost. The algorithm iterates between the two stages until no further mode insertion is found feasible to decrease the cost. The feasibility of a mode to lower cost is determined by evaluating the directional derivative of the cost functional. The directional derivative is evaluated for a mode insertion of fixed duration. However, from available literature the bi-level technique is only known to efficiently solve control problems in which the trajectories are optimized to avoid specific target points. As defining climate sensitive target locations using advanced climate model is hard to do, the possibilities of extending this control technique to solve climate optimal cruise hybrid control problems cannot be coherently established. Since the understanding of the algorithm is limited, the objective of this study is defined to investigate the performance of the bi-level optimal control algorithm and to determine its suitability to calculate ATM regulated climate optimal trajectories.

To study the algorithm's performance, optimal control problems with performance criteria which individually account for the fuel consumption and locus of the trajectory are considered, since climate cost is a function of fuel flow and locus. For measuring the fuel consumption, a monetary cost function is defined as an objective function and to define a measure with respect to locus, fictitious Climate Cost Functions (CCF) with spatial variability in altitude are introduced. The objective of solving these optimal control problems is to calculate cruise trajectories with step-climb and/or descent modes such that the performance criterion is minimized. The cruise phase is initiated with a constant pressure altitude cruise mode and change in altitude is brought about by inserting a climb or descent mode. The altitude variation per climb/descent is limited to $\pm$ 2000 ft. (609.6 m), respectively, as per semi-circular rule. Both climb and descent modes are initiated in vertical speed mode with no bounds on Mach number. The dynamics of the aircraft were defined assuming a point mass model with variable aircraft mass and three degrees of freedom. The equations of motions, state, control and path variables are defined individually for each flight mode (cruise, climb and descent). All trajectories are simulated with a BADA 4.0 Airbus A330-200 aircraft performance model. The limitations on the climb and descent mode duration and vertical speed are calculated from ADS-B data of flightradar24.

To solve the optimal control problems with the bi-level control algorithm, a bi-level framework within the Trajectory Optimization Module (TOM) is designed. To initiate the bi-level framework, an optimal cruise trajectory with a single phase constant altitude cruise mode is obtained. With the latter solution the algorithm is initiated in stage 2, where insertions with climb and/or descent mode are calculated by solving a control problem at each insertion time. The overall cost of the new mode sequence calculated in stage 2 is expressed by combining the cost of the inserted mode and interpolating the cost of the final cruise phase. For each insertion the cost variation is calculated by evaluating the directional derivative. Subsequently, the optimal switching times and continuous inputs of the new mode sequence is calculated in stage 1. The framework iterates between stage 1 and 2 until the directional derivatives evaluated in stage 2 are observed to be greater than or equal to zero.

To validate the bi-level framework formulated in this study, the extensively studied control problem to minimize the cruise phase operating cost is solved. The cruise phase is initiated as a single phase constant altitude cruise mode and in each iteration of stage 2 a step-climb mode is inserted at all insertion times for constructing a new mode sequence. The cost variation and directional derivative both are evaluated in the first iteration of stage 2. As expected the climb mode insertion is found to lower the overall cost at all insertion times and the error between the actual cost reduction and estimated cost reduction is calculated to be less than 15%. Consequently, in the second iteration of stage 2 a mode sequence with two step-climb modes is constructed. As the thrust input of the climb mode calculated in stage 2 is over estimated, the maximum cost reduction estimated by evaluating the cost variation is found to be non reliable. This also influences the algorithm's ability to determine the feasibility of a mode insertion. Hence, significant difference between the estimated insertion time and optimal switching time is observed. However, the insertion time at which the the directional derivative is maximum approximately represents the optimal switching time of step-climb. Hence, evaluation of the directional derivative is considered to be an efficient tool in determining the feasibility of a mode insertion.

Since descent during cruise is an unconventional practice (excluding Top of Descent), optimal control problems with fictitious CCF are formulated and solved to calculate mode sequence with both climb and descent modes. The fictitious CCF with 1D spatial variability in altitude is defined such that the climate cost decreases with decreasing altitude. Within this model it is observed that the directional derivatives evaluated with descent mode lowered the climate cost at all insertion times and vice-verse with climb mode. The general rule to construct new mode sequence is defined such as to introduce a mandatory cruise mode after each inserted mode. Based on the reference trajectory the optimal mode sequence of the fictitious climate optimal cruise is observed to consist of descent modes in succession. Despite the general rule the optimal mode sequence calculated by the algorithm is found to represent a flight path similar to the reference trajectory. From this it is determined that the definition of mode sequence allow zero entries i.e. modes with zero duration. Additionally, a control problem with 2D (altitude and time) CCFs is solved to investigate the algorithm's performance in constructing an optimal sequence where both climb and descent modes are found to lower the overall cost. The CCFs for this fictitious model is defined with two distinct regions where climb and descent modes are individually found feasible. In each iteration of the stage 2 the directional derivative is evaluated to be negative for both climb and descent mode insertions. However, the final mode sequence calculated by the algorithm depends on the order in which the mode insertion is sequenced i.e. whether climb is inserted before descent or vice-verse. For calculating the optimal mode sequence it is recommended to first insert the mode which is evaluated to have maximum cost reduction. Further, when two or more mode insertions are evaluated to lower the overall cost, it is advised to give preference to the mode insertion which is found feasible at the earliest insertion time.

After understanding the characteristics of the bi-level control technique with fictitious climate models, the study is extended to calculate climate optimal cruise phase between Lisbon - Miami. The climate cost for the latter cruise phase is calculated using the AirClim CCFs. The AirClim CCFs are dependent on longitude, latitude and altitude. Because of this, the climate optimal cruise trajectories obtained at different flight levels are calculated to fly different flight paths i.e. the trajectory varies on the longitude-latitude plane. To make the trajectories consistent and comparable in each iteration of the algorithm, the cost variation is calculated assuming a constant flight path on the longitude-latitude plane. In stage 2 the new sequence is constructed by inserting the climb mode into the initial sequence. As the directional derivative evaluated is found to be less than zero, a cruise phase trajectory with the new mode sequence is calculated in stage 1 of the algorithm. While measuring the accuracy of the algorithm it is observed that the error between the actual cost reduction and estimated cost reduction is significantly high. Since the solver is free to calculate the optimal route between initial and final position, achieving consistent flight path in all the trajectories is difficult. This

introduces significant differences between the trajectories calculated in either stage of the algorithm.

From all the above observations and conclusions, it can be said that the bi-level algorithm does provide a systematic technique to calculate the optimal mode sequence for a hybrid system. The algorithm's ability to include zero entries introduces a favourable flexibility while calculating the optimal mode sequence and may also help in building a robust computational system. The results of this study validate the utilization of a bi-level optimal control technique to calculate a mode sequence which lowers the overall cost in comparison to the initial sequence. Although, calculating the optimal mode sequence with this technique would require further considerations such as the order of the inserted mode, magnitude of the directional derivative and the insertion time. This increases the complexity of the computational framework especially with increasing the number of modes. Additionally, the algorithm can only calculate variations from modifying the original trajectory. Hence, the final solution calculated by the algorithm may not always be the optimal solution. Any inconsistency between trajectories calculated within the algorithm can make the mode sequence ineffective. This method can thus be most effective for solving control problems in which the flight routes are assigned to fly specific way-points. Due to limited computational resources, the potential of the bi-level algorithm cannot be completely realized at the moment. As future studies are expected to focus on finding optimal mode definitions for designing climate optimal trajectories, the bi-level optimal control algorithm can act as an intermediary tool with which the researchers can systematically investigate cost benefits along the trajectories.

Future Work

During the course of this study, it is observed that the climate cost calculated with real climate model CCFs are usually in the order of 10^{-8}. While the order of magnitude of state vectors is found to be in the range $[10^2, 10^6]$. Scaling the CCF derivatives to an order similar to the state derivatives was observed to improve the computation time. Further, there appeared to be a relation between the scaling factors and directional derivatives, which was also reflected in the magnitude of the derivatives. In order to improve the computational efficiency of the framework, the latter requires further investigation and possibly, require an analytical method which can determine the scaling factors without influencing the proportionality between the directional derivatives and cost functional.

The framework currently calculates mode inputs from solving a control problem at each insertion time. Calculating mode inputs constitutes a higher percentage of the overall computation time. The future work with bi-level control technique would thus need to focus on finding an approximate feasible set of inputs for each mode insertion such that the overall computation time is reduced by a significant margin. Also, the framework is being redefined to incorporate ADiGator, an automatic differentiation software. This is expected to lower the overall memory utilization and provide maximum efficiency within available computational resource.

Finally, to determine the limitations of the proposed algorithm, climate optimal cruise trajectories with ATM constraints are planned to be designed for flight routes passing through specific way-points. These trajectories will be designed with AirClim climate model and will be integrated with step climb and descent procedures. The assessment of climate impact potential are planned to consider both east- and westbound routes and will be extended for an entire network.

A

VERTICAL SPEEDS FROM ADS-B DATA

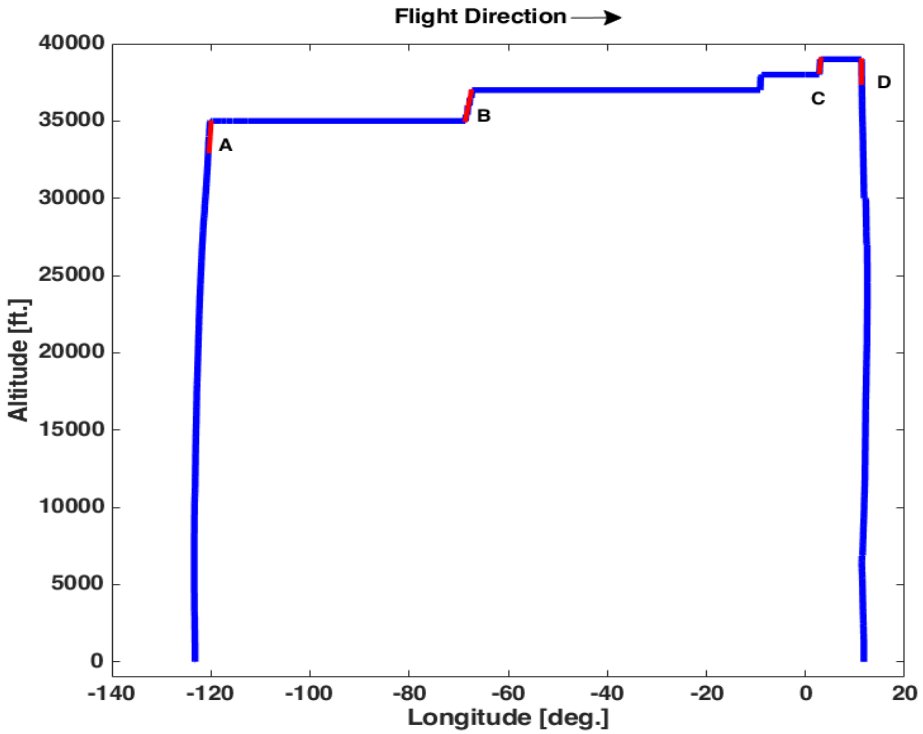

Figure A.1: **Altitude vs. longitutde plot for a flight route between Vancouver, Canada (YVR) - Munich, Germany (MUC) obtained from the ADS-B data of FlightRadar24.**

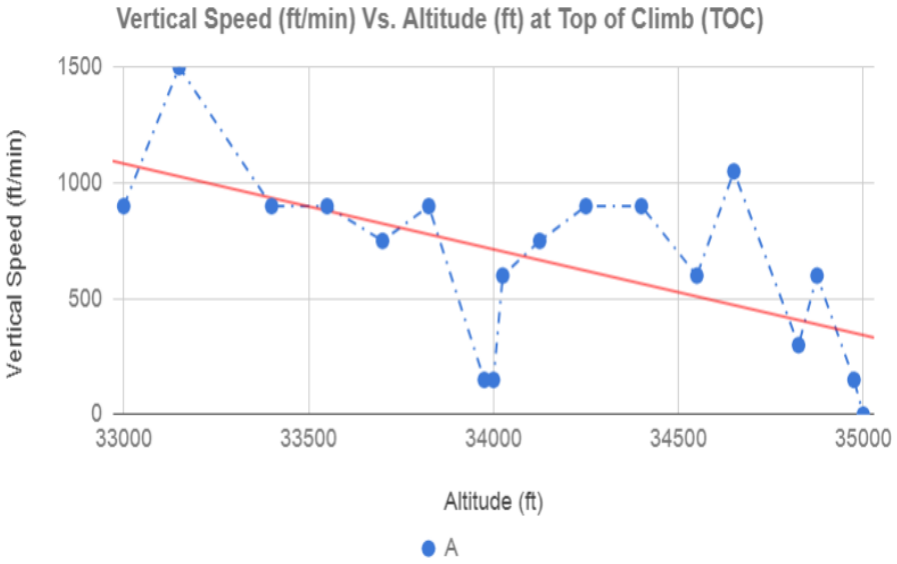
Vertical Speed (ft/min) Vs. Altitude (ft) at Top of Climb (TOC)
Vertical Speed (ft/min)
1500
1000
500
0
33000
33500
34000
34500
35000
Altitude (ft)
A

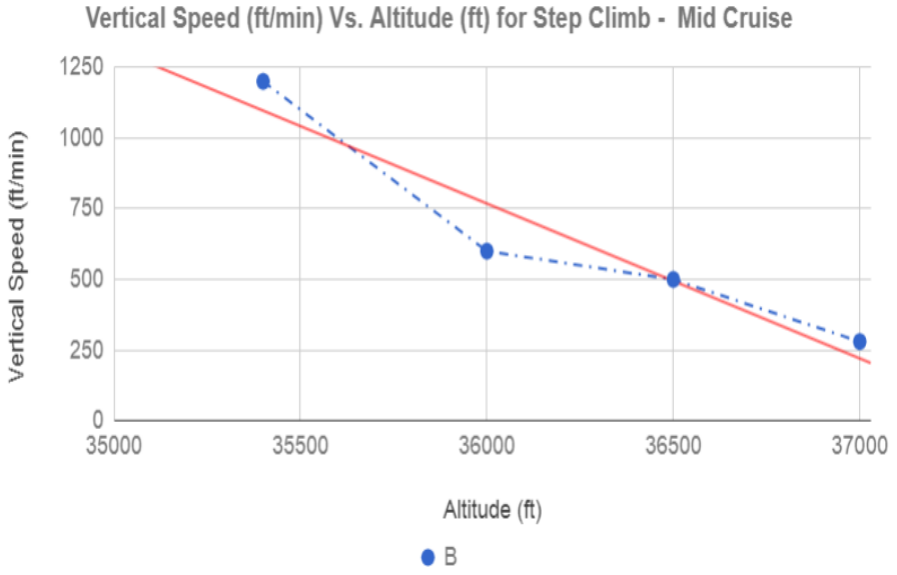
Vertical Speed (ft/min) Vs. Altitude (ft) for Step Climb - Mid Cruise
Vertical Speed (ft/min)
1250
1000
750
500
250
0
35000
35500
36000
36500
37000
Altitude (ft)
B

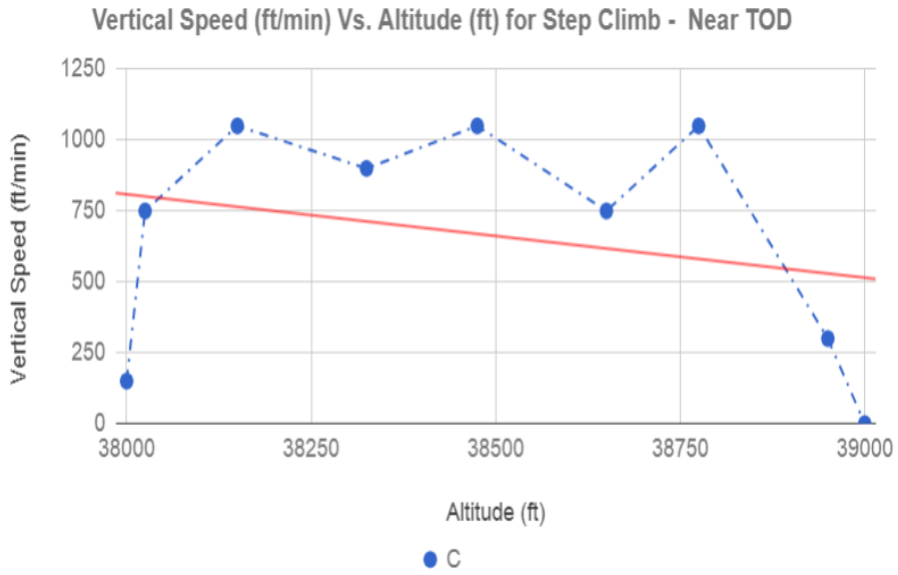
Vertical Speed (ft/min) Vs. Altitude (ft) for Step Climb - Near TOD
Vertical Speed (ft/min)
1250
1000
750
500
250
0
38000
38250
38500
38750
39000
Altitude (ft)
C

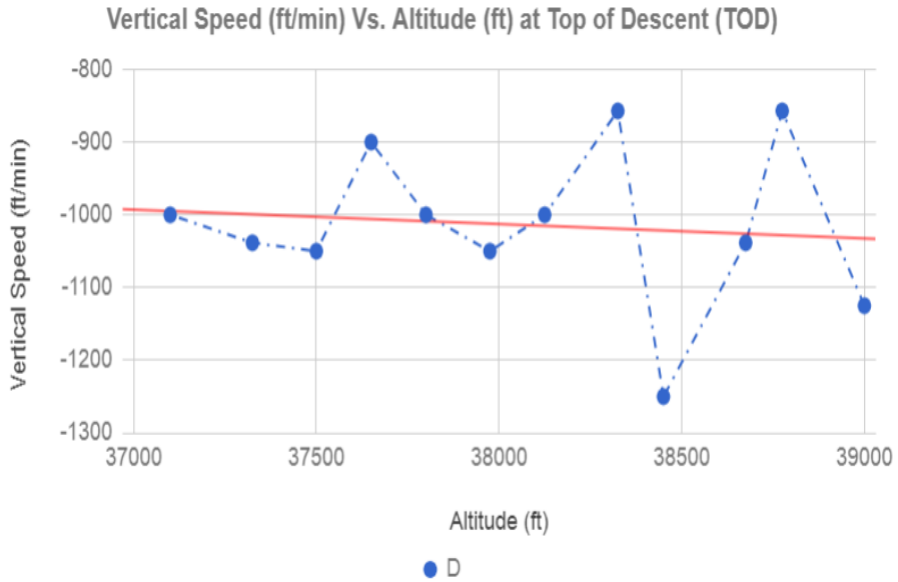
Vertical Speed (ft/min) Vs. Altitude (ft) at Top of Descent (TOD)
Vertical Speed (ft/min)
-800
-900
-1000
-1100
-1200
-1300
37000
37500
38000
38500
39000
Altitude (ft)
D

B

Boundary Conditions-I

State Variable Limits for Operating cost Control problem

Variable	Minimum Value	Maximum Value
Limitation of State Variables		
Initial Limits at τ = 0		
λ_0	λ_i^*	λ_i^*
ϕ_0	ϕ_i^*	ϕ_i^*
H_0	10,973 m	10, 973 m
$v_{TAS,0}$	200 m/s	270 m/s
m_0	1,63,085 kg	2,33,000 kg
$m_{i,0}$	0 kg	0 kg
Final Limits at τ = 1		
λ_f	λ_f^*	λ_f^*
ϕ_f	ϕ_f^*	ϕ_f^*
H_f	H_f^*	H_f^*
$v_{TAS,f}$	200 m/s	270 m/s
m_f	1,63,085 kg	2,33,000 kg
$m_{f,0}$	0 kg	0 kg
General Limits on State Variables		
λ	-180°	180°
ϕ	-90°	90°
H	8,500 m	12,700 m
v_{TAS}	200 m/s	270 m/s
m	1,63,085 kg	2,33,000 kg
m_i	0 kg	0 kg

CONSTANT ALTITUDE CONSTANT MACH CRUISE WITH STEP CLIMB

Variable	Minimum Value	Maximum Value
General Limitations of Path Variables for each mode		
Cruise Mode		
H_p	8,500 m	12,700 m
M_a	0.82	0.82
v_{CAS}	0 m/s	169.7 m/s
$C_{L,rel}$	0	1
γ	-0.05°	0.05°
Climb Mode		
H_p	H_i^*	$H_i^* + 610m$
M_a	0.72	0.84
v_{CAS}	0 m/s	169.7 m/s
$C_{L,rel}$	0	1
$\dot{H}$	0 m/s	5.08 m/s
γ	0°	10°

C

Boundary Conditions-II

State Variable Limits for Fictitious Climate Cost Control Problems

Variable	Minimum Value	Maximum Value
Limitation of State Variables		
Initial Limits at τ = 0		
λ_0	λ_i^*	λ_i^*
ϕ_0	ϕ_i^*	ϕ_i^*
H_0	10,973 m	10, 973 m
$\epsilon_{TAS,0}$	200 m/s	270 m/s
m_0	1,63,085 kg	2,33,000 kg
$m_{i,0}$	0 kg	10^7 kg
Final Limits at τ = 1		
λ_f	λ_f^*	λ_f^*
ϕ_f	ϕ_f^*	ϕ_f^*
H_f	H_f^*	H_f^*
$\epsilon_{TAS,f}$	200 m/s	270 m/s
m_f	1,63,085 kg	2,33,000 kg
$m_{f,0}$	0 kg	10^7
General Limits on State Variables		
λ	-180°	180°
ϕ	-90°	90°
H	8,500 m	12,700 m
ϵ_{TAS}	200 m/s	270 m/s
m	1,63,085 kg	2,33,000 kg
m_i	0 kg	10^7

CONSTANT ALTITUDE CONSTANT MACH CRUISE WITH CLIMB AND DESCENT MODE

Variable	Minimum Value	Maximum Value
General Limitations of Path Variables for each mode		
Cruise Mode		
H_p	8,500 m	12,700 m
M_a	0.82	0.82
v_{CAS}	0 m/s	169.7 m/s
$C_{L,rel}$	0	1
γ	-0.05°	0.05°
Climb Mode		
H_p	H_i^*	$H_i^* + 610m$
M_a	0.72	0.84
v_{CAS}	0 m/s	169.7 m/s
$C_{L,rel}$	0	1
$\dot{H}$	0 m/s	5.08 m/s
γ	0°	10°
Descent Mode		
H_p	H_i^*	$H_i^* - 610m$
M_a	0.72	0.84
v_{CAS}	0 m/s	169.7 m/s
$C_{L,rel}$	0	1
$\dot{H}$	-5.08 m/s	0 m/s
γ	-10°	0°

CLIMATE MODEL CONSTANTS

Constants	Value
k_{11}, k_{21}	1e-1
k_{12}	4e-5
k_{22}	-7e-6

D

Optimal Operating Cost Cruise Database

Cruise at Altitude 10973 m				
Weight in Kg.	Max Range (Km)	Max Flight Time (Sec.)	Available Fuel (Kg)	Fuel burnt per m (Kg/m)
204,892.60	6,680	27,577.66	41,807.60	0.0069
204,568.83	6,630	27,382.61	41,483.83	0.0068
203,993.42	6,540	27,035.13	40,908.42	0.0068
203,506.44	6,470	26,740.27	40,421.44	0.0068
203,372.19	6,450	26,658.85	40,287.19	0.0068
203,050.75	6,410	26,463.70	39,965.75	0.0068
202,479.46	6,320	26,116.10	39,394.46	0.0068
201,995.94	6,250	25,821.16	38,910.94	0.0068
201,862.65	6,230	25,739.73	38,777.65	0.0068
201,543.48	6,180	25,544.54	38,458.48	0.0067
200,976.20	6,100	25,196.90	37,891.20	0.0067
200,496.06	6,030	24,901.93	37,411.06	0.0067
200,363.69	6,010	24,820.49	37,278.69	0.0067
200,046.73	5,960	24,625.30	36,961.73	0.0067
199,483.36	5,880	24,277.63	36,398.36	0.0067
199,006.50	5,810	23,982.66	35,921.50	0.0067
198,875.03	5,790	23,901.22	35,790.03	0.0067
198,560.23	5,740	23,706.02	35,475.23	0.0066
198,000.66	5,650	23,358.35	34,915.66	0.0066
197,527.00	5,580	23,063.37	34,442.00	0.0066
197,396.41	5,560	22,981.93	34,311.41	0.0066
197,083.71	5,520	22,786.73	33,998.71	0.0066
196,527.85	5,430	22,439.06	33,442.85	0.0066
196,057.30	5,360	22,144.08	32,972.30	0.0066
195,927.57	5,340	22,062.64	32,842.57	0.0066
195,616.91	5,290	21,867.43	32,531.91	0.0066
195,064.66	5,210	21,519.76	31,979.66	0.0065
194,597.16	5,140	21,224.78	31,512.16	0.0065
194,468.26	5,120	21,143.34	31,383.26	0.0065
194,159.59	5,070	20,948.14	31,074.59	0.0065
193,610.87	4,990	20,600.47	30,525.87	0.0065
193,146.33	4,910	20,305.48	30,061.33	0.0065
193,018.25	4,900	20,224.04	29,933.25	0.0065
192,711.52	4,850	20,028.84	29,626.52	0.0065
192,166.24	4,760	19,681.17	29,081.24	0.0065
191,704.59	4,690	19,386.19	28,619.59	0.0065
191,577.30	4,670	19,304.75	28,492.30	0.0065
191,272.47	4,630	19,109.54	28,187.47	0.0064
190,730.54	4,540	18,761.87	27,645.54	0.0064
190,271.71	4,470	18,466.89	27,186.71	0.0064
190,145.20	4,450	18,385.45	27,060.20	0.0064
189,842.22	4,400	18,190.25	26,757.22	0.0064
189,303.56	4,320	17,842.58	26,218.56	0.0064

188,847.49	4,250	17,547.60	25,762.49	0.0064
188,721.73	4,230	17,466.16	25,636.73	0.0064
188,420.57	4,180	17,270.96	25,335.57	0.0064
187,885.10	4,100	16,923.29	24,800.10	0.0063
187,431.72	4,020	16,628.31	24,346.72	0.0063
187,306.70	4,010	16,546.87	24,221.70	0.0063
187,007.30	3,960	16,351.67	23,922.30	0.0063
186,474.96	3,870	16,004.00	23,389.96	0.0063
186,024.20	3,800	15,709.02	22,939.20	0.0063
185,899.90	3,780	15,627.58	22,814.90	0.0063
185,602.23	3,740	15,432.38	22,517.23	0.0063
185,072.94	3,650	15,084.71	21,987.94	0.0063
184,624.75	3,580	14,789.73	21,539.75	0.0063
184,501.16	3,560	14,708.29	21,416.16	0.0063
184,205.16	3,510	14,513.09	21,120.16	0.0063
183,678.85	3,430	14,165.42	20,593.85	0.0062
183,233.17	3,360	13,870.44	20,148.17	0.0062
183,110.27	3,340	13,789.00	20,025.27	0.0062
182,815.93	3,290	13,593.80	19,730.93	0.0062
182,292.53	3,210	13,246.13	19,207.53	0.0062
181,849.30	3,130	12,951.15	18,764.30	0.0062
181,727.07	3,120	12,869.71	18,642.07	0.0062
181,434.34	3,070	12,674.51	18,349.34	0.0062
180,913.79	2,980	12,326.84	17,828.79	0.0062
180,472.97	2,910	12,031.86	17,387.97	0.0062
180,351.40	2,890	11,950.42	17,266.40	0.0062
180,060.24	2,850	11,755.22	16,975.24	0.0062
179,542.48	2,760	11,407.55	16,457.48	0.0061
179,104.00	2,690	11,112.57	16,019.00	0.0061
178,983.07	2,670	11,031.13	15,898.07	0.0061
178,693.45	2,620	10,835.93	15,608.45	0.0061
178,178.42	2,540	10,488.26	15,093.42	0.0061
177,742.24	2,470	10,193.28	14,657.24	0.0061
177,621.94	2,450	10,111.84	14,536.94	0.0061
177,333.83	2,400	9,916.64	14,248.83	0.0061
176,821.47	2,320	9,568.97	13,736.47	0.0061
176,387.53	2,240	9,273.99	13,302.53	0.0061
176,267.86	2,230	9,192.56	13,182.86	0.0061
175,981.22	2,180	8,997.36	12,896.22	0.0061
175,471.47	2,090	8,649.69	12,386.47	0.0060
175,039.73	2,020	8,354.71	11,954.73	0.0060
174,920.66	2,000	8,273.27	11,835.66	0.0060
174,635.47	1,960	8,078.07	11,550.47	0.0060
174,128.28	1,870	7,730.41	11,043.28	0.0060
173,698.70	1,800	7,435.43	10,613.70	0.0060

173,580.22	1,780	7,353.99	10,495.22	0.0060
173,296.44	1,730	7,158.79	10,211.44	0.0060
172,791.76	1,650	6,811.13	9,706.76	0.0060
172,364.28	1,580	6,516.16	9,279.28	0.0060
172,246.39	1,560	6,434.72	9,161.39	0.0060
171,964.00	1,510	6,239.52	8,879.00	0.0060
171,461.76	1,430	5,891.87	8,376.76	0.0060
171,036.36	1,350	5,596.90	7,951.36	0.0060
170,919.03	1,340	5,515.46	7,834.03	0.0059
170,638.00	1,290	5,320.27	7,553.00	0.0059
170,138.17	1,200	4,972.61	7,053.17	0.0059
169,714.79	1,130	4,677.65	6,629.79	0.0059
169,598.01	1,110	4,596.21	6,513.01	0.0059
169,318.31	1,070	4,401.02	6,233.31	0.0059
168,820.84	981	4,053.38	5,735.84	0.0059
168,399.45	910	3,758.42	5,314.45	0.0059
168,283.22	890	3,676.99	5,198.22	0.0059
168,004.82	843	3,481.80	4,919.82	0.0059
167,509.66	759	3,134.16	4,424.66	0.0059
167,090.21	687	2,839.21	4,005.21	0.0059
166,974.52	668	2,757.78	3,889.52	0.0059
166,697.40	620	2,562.59	3,612.40	0.0059
166,204.50	536	2,214.95	3,119.50	0.0058
165,786.96	465	1,920.00	2,701.96	0.0058
165,671.79	445	1,838.57	2,586.79	0.0058
165,395.93	398	1,643.38	2,310.93	0.0058
164,905.25	314	1,295.73	1,820.25	0.0058
164,489.58	242	1,000.76	1,404.58	0.0058
164,374.93	223	919.32	1,289.93	0.0058
164,194.14	191	790.84	1,109.14	0.0058
163,836.60	130	536.52	751.60	0.0058
163,440.68	62	254.51	355.68	0.0058
163,157.39	13	52.50	72.39	0.0057

Cruise at Altitude 11582 m				
Weight in Kg.	Max. Range (Km)	Max Flight Time (Sec.)	Available Fuel (Kg)	Fuel burnt per m (Kg/m)
204,198.32	6,675	27,588.91	41,113.32	0.0069
203,871.94	6,628	27,393.78	40,786.94	0.0069
203,292.27	6,544	27,046.16	40,207.27	0.0069
202,802.09	6,472	26,751.18	39,717.09	0.0069
202,667.02	6,453	26,669.73	39,582.02	0.0068
202,343.73	6,406	26,474.50	39,258.73	0.0068
201,769.53	6,321	26,126.75	38,684.53	0.0068
201,283.93	6,250	25,831.69	38,198.93	0.0068
201,150.12	6,230	25,750.23	38,065.12	0.0068
200,829.82	6,183	25,554.96	37,744.82	0.0068
200,260.90	6,099	25,207.18	37,175.90	0.0067
199,779.72	6,028	24,912.09	36,694.72	0.0067
199,647.13	6,008	24,830.62	36,562.13	0.0067
199,329.73	5,961	24,635.34	36,244.73	0.0067
198,765.92	5,876	24,287.53	35,680.92	0.0067
198,289.03	5,805	23,992.43	35,204.03	0.0067
198,157.61	5,785	23,910.96	35,072.61	0.0067
197,843.02	5,738	23,715.68	34,758.02	0.0066
197,284.15	5,654	23,367.87	34,199.15	0.0066
196,811.41	5,582	23,072.76	33,726.41	0.0066
196,681.13	5,563	22,991.29	33,596.13	0.0066
196,369.25	5,516	22,796.01	33,284.25	0.0066
195,815.18	5,431	22,448.19	32,730.18	0.0066
195,346.47	5,360	22,153.09	32,261.47	0.0066
195,217.29	5,340	22,071.62	32,132.29	0.0065
194,908.04	5,293	21,876.33	31,823.04	0.0065
194,358.62	5,209	21,528.52	31,273.62	0.0065
193,893.80	5,137	21,233.41	30,808.80	0.0065
193,765.69	5,118	21,151.94	30,680.69	0.0065
193,459.00	5,070	20,956.66	30,374.00	0.0065
192,914.08	4,986	20,608.84	29,829.08	0.0065
192,453.05	4,915	20,313.74	29,368.05	0.0064
192,325.98	4,895	20,232.27	29,240.98	0.0064
192,021.76	4,848	20,036.99	28,936.76	0.0064
191,481.21	4,764	19,689.17	28,396.21	0.0064
191,023.85	4,692	19,394.07	27,938.85	0.0064
190,897.79	4,673	19,312.60	27,812.79	0.0064
190,595.98	4,625	19,117.32	27,510.98	0.0064
190,059.67	4,541	18,769.50	26,974.67	0.0064
189,605.87	4,470	18,474.40	26,520.87	0.0063
189,480.79	4,450	18,392.93	26,395.79	0.0063

189,181.31	4,403	18,197.65	26,096.31	0.0063
188,649.13	4,319	17,849.84	25,564.13	0.0063
188,198.79	4,247	17,554.74	25,113.79	0.0063
188,074.66	4,228	17,473.27	24,989.66	0.0063
187,777.45	4,180	17,277.98	24,692.45	0.0063
187,249.27	4,096	16,930.17	24,164.27	0.0063
186,802.31	4,025	16,635.07	23,717.31	0.0063
186,679.10	4,005	16,553.60	23,594.10	0.0062
186,384.09	3,958	16,358.32	23,299.09	0.0062
185,859.81	3,874	16,010.51	22,774.81	0.0062
185,416.11	3,802	15,715.41	22,331.11	0.0062
185,293.80	3,783	15,633.93	22,208.80	0.0062
185,000.94	3,735	15,438.65	21,915.94	0.0062
184,480.45	3,651	15,090.84	21,395.45	0.0062
184,039.94	3,580	14,795.74	20,954.94	0.0062
183,918.50	3,560	14,714.27	20,833.50	0.0062
183,627.72	3,513	14,518.99	20,542.72	0.0061
183,110.92	3,429	14,171.17	20,025.92	0.0061
182,673.50	3,357	13,876.07	19,588.50	0.0061
182,552.91	3,338	13,794.60	19,467.91	0.0061
182,264.17	3,290	13,599.32	19,179.17	0.0061
181,750.95	3,206	13,251.51	18,665.95	0.0061
181,316.55	3,135	12,956.41	18,231.55	0.0061
181,196.79	3,115	12,874.94	18,111.79	0.0061
180,910.03	3,068	12,679.66	17,825.03	0.0061
180,400.30	2,984	12,331.85	17,315.30	0.0060
179,968.84	2,912	12,036.74	16,883.84	0.0060
179,849.89	2,893	11,955.27	16,764.89	0.0060
179,565.05	2,845	11,759.99	16,480.05	0.0060
179,058.72	2,761	11,412.18	15,973.72	0.0060
178,630.13	2,690	11,117.08	15,545.13	0.0060
178,511.96	2,670	11,035.61	15,426.96	0.0060
178,229.00	2,623	10,840.33	15,144.00	0.0060
177,725.99	2,539	10,492.52	14,640.99	0.0060
177,300.18	2,467	10,197.42	14,215.18	0.0060
177,182.78	2,448	10,115.95	14,097.78	0.0060
176,901.65	2,400	9,920.67	13,816.65	0.0059
176,401.88	2,316	9,572.86	13,316.88	0.0059
175,978.79	2,245	9,277.76	12,893.79	0.0059
175,862.13	2,225	9,196.29	12,777.13	0.0059
175,582.79	2,178	9,001.01	12,497.79	0.0059
175,086.17	2,094	8,653.20	12,001.17	0.0059
174,665.73	2,022	8,358.10	11,580.73	0.0059

174,549.81	2,003	8,276.63	11,464.81	0.0059
174,272.20	1,955	8,081.35	11,187.20	0.0059
173,778.66	1,871	7,733.54	10,693.66	0.0059
173,360.81	1,800	7,438.45	10,275.81	0.0058
173,245.60	1,780	7,356.98	10,160.60	0.0058
172,969.69	1,733	7,161.70	9,884.69	0.0058
172,479.16	1,649	6,813.90	9,394.16	0.0058
172,063.84	1,577	6,518.80	8,978.84	0.0058
171,949.32	1,558	6,437.33	8,864.32	0.0058
171,675.06	1,510	6,242.06	8,590.06	0.0058
171,187.46	1,426	5,894.26	8,102.46	0.0058
170,774.61	1,355	5,599.17	7,689.61	0.0058
170,660.77	1,335	5,517.70	7,575.77	0.0058
170,388.13	1,288	5,322.43	7,303.13	0.0058
169,903.39	1,204	4,974.63	6,818.39	0.0057
169,492.95	1,132	4,679.55	6,407.95	0.0057
169,379.77	1,113	4,598.08	6,294.77	0.0057
169,108.72	1,065	4,402.81	6,023.72	0.0057
168,626.78	981	4,055.02	5,541.78	0.0057
168,218.69	910	3,759.94	5,133.69	0.0057
168,106.16	890	3,678.48	5,021.16	0.0057
167,836.65	843	3,483.21	4,751.65	0.0057
167,357.44	759	3,135.43	4,272.44	0.0057
166,951.65	687	2,840.35	3,866.65	0.0057
166,839.75	668	2,758.89	3,754.75	0.0057
166,571.76	620	2,563.63	3,486.76	0.0057
166,095.22	536	2,215.85	3,010.22	0.0057
165,691.68	465	1,920.77	2,606.68	0.0056
165,580.40	445	1,839.31	2,495.40	0.0056
165,313.88	398	1,644.04	2,228.88	0.0056
164,839.95	314	1,296.25	1,754.95	0.0056
164,438.62	242	1,001.16	1,353.62	0.0056
164,327.94	223	919.69	1,242.94	0.0056
164,062.85	175	724.41	977.85	0.0056
163,591.49	91	376.59	506.49	0.0056
163,192.28	20	81.48	107.28	0.0054

E

Optimal Climate Cost Cruise Database - Climate Model A

Cruise at Altitude 9449 m					
Weight in Kg.	Max Range (Km)	Max Flight Time (Sec.)	Available Fuel (Kg)	Fuel burnt per m (Kg/m)	CCF (ATR)
215,048.51	6,971	27,587.62	51,963.51	0.0080	0.00
214,653.35	6,922	27,300.32	51,568.35	0.0080	373.02
213,950.85	6,834	26,952.91	50,865.85	0.0080	1,037.38
213,357.85	6,759	26,660.17	50,272.85	0.0080	1,601.06
213,193.81	6,739	26,577.08	50,108.81	0.0079	1,756.69
212,801.70	6,689	26,383.35	49,716.70	0.0079	2,129.70
212,104.54	6,602	26,036.64	49,019.54	0.0079	2,794.07
211,514.25	6,527	25,743.07	48,429.25	0.0079	3,357.75
211,351.61	6,506	25,665.12	48,266.61	0.0079	3,513.37
210,961.76	6,457	25,466.87	47,876.76	0.0079	3,886.39
210,268.56	6,369	25,120.16	47,183.56	0.0079	4,550.75
209,681.69	6,295	24,826.56	46,596.69	0.0079	5,114.44
209,519.97	6,274	24,748.64	46,434.97	0.0079	5,270.06
209,132.32	6,225	24,550.39	46,047.32	0.0078	5,643.07
208,443.01	6,137	24,203.67	45,358.01	0.0078	6,307.44
207,859.41	6,062	23,910.07	44,774.41	0.0078	6,871.12
207,698.59	6,042	23,832.30	44,613.59	0.0078	7,026.74
207,313.07	5,992	23,633.90	44,228.07	0.0078	7,399.76
206,627.53	5,904	23,287.19	43,542.53	0.0078	8,064.12
206,047.08	5,830	22,993.57	42,962.08	0.0078	8,627.81
205,887.13	5,809	22,915.79	42,802.13	0.0078	8,783.43
205,503.67	5,760	22,717.42	42,418.67	0.0078	9,156.44
204,821.77	5,672	22,370.71	41,736.77	0.0077	9,820.81
204,244.38	5,597	22,077.08	41,159.38	0.0077	10,384.49
204,085.26	5,577	21,999.26	41,000.26	0.0077	10,540.11
203,703.81	5,528	21,800.94	40,618.81	0.0077	10,913.13
203,025.43	5,440	21,454.24	39,940.43	0.0077	11,577.49
202,451.00	5,365	21,160.59	39,366.00	0.0077	12,141.18
202,292.69	5,345	21,082.64	39,207.69	0.0077	12,296.80
201,913.17	5,295	20,884.46	38,828.17	0.0077	12,669.81
201,238.20	5,207	20,537.76	38,153.20	0.0077	13,334.18
200,666.63	5,133	20,244.10	37,581.63	0.0077	13,897.86
200,509.11	5,112	20,166.04	37,424.11	0.0077	14,053.48
200,131.47	5,063	19,967.98	37,046.47	0.0076	14,426.50
199,459.81	4,975	19,621.28	36,374.81	0.0076	15,090.86
198,891.01	4,900	19,327.61	35,806.01	0.0076	15,654.55
198,734.25	4,880	19,249.29	35,649.25	0.0076	15,810.17
198,358.42	4,830	19,051.50	35,273.42	0.0076	16,183.18
197,689.97	4,743	18,704.80	34,604.97	0.0076	16,847.55
197,123.86	4,668	18,411.11	34,038.86	0.0076	17,411.23
196,967.84	4,647	18,332.89	33,882.84	0.0076	17,566.85
196,593.77	4,598	18,135.02	33,508.77	0.0076	17,939.87
195,928.42	4,510	17,788.32	32,843.42	0.0076	18,604.24
195,364.92	4,436	17,494.61	32,279.92	0.0075	19,167.92

195,209.62	4,415	17,416.30	32,124.62	0.0075	19,323.54
194,837.26	4,366	17,218.53	31,752.26	0.0075	19,696.56
194,174.92	4,278	16,871.85	31,089.92	0.0075	20,360.92
193,613.95	4,203	16,578.12	30,528.95	0.0075	20,924.60
193,459.34	4,183	16,499.57	30,374.34	0.0075	21,080.23
193,088.63	4,133	16,302.05	30,003.63	0.0075	21,453.24
192,429.22	4,045	15,955.37	29,344.22	0.0075	22,117.61
191,870.71	3,971	15,661.62	28,785.71	0.0075	22,681.29
191,716.77	3,950	15,582.96	28,631.77	0.0075	22,836.91
191,347.67	3,901	15,385.57	28,262.67	0.0075	23,209.93
190,691.10	3,813	15,038.89	27,606.10	0.0075	23,874.29
190,134.96	3,739	14,745.12	27,049.96	0.0074	24,437.98
189,981.68	3,718	14,666.31	26,896.68	0.0074	24,593.60
189,614.14	3,669	14,469.09	26,529.14	0.0074	24,966.61
188,960.32	3,581	14,122.41	25,875.32	0.0074	25,630.98
188,406.50	3,506	13,828.62	25,321.50	0.0074	26,194.66
188,253.85	3,486	13,749.59	25,168.85	0.0074	26,350.28
187,887.83	3,436	13,552.61	24,802.83	0.0074	26,723.30
187,236.69	3,348	13,205.94	24,151.69	0.0074	27,387.66
186,685.11	3,274	12,912.11	23,600.11	0.0074	27,951.35
186,533.08	3,253	12,833.03	23,448.08	0.0074	28,106.97
186,168.53	3,204	12,636.13	23,083.53	0.0074	28,479.98
185,519.99	3,116	12,289.46	22,434.99	0.0074	29,144.35
184,970.60	3,041	11,995.62	21,885.60	0.0074	29,708.03
184,819.16	3,021	11,916.34	21,734.16	0.0074	29,863.65
184,456.05	2,971	11,719.65	21,371.05	0.0074	30,236.67
183,810.04	2,884	11,372.98	20,725.04	0.0073	30,901.03
183,262.77	2,809	11,079.11	20,177.77	0.0073	31,464.72
183,111.92	2,788	10,999.86	20,026.92	0.0073	31,620.34
182,750.20	2,739	10,803.17	19,665.20	0.0073	31,993.35
182,106.64	2,651	10,456.50	19,021.64	0.0073	32,657.72
181,561.45	2,577	10,162.63	18,476.45	0.0073	33,221.40
181,411.16	2,556	10,083.12	18,326.16	0.0073	33,377.02
181,050.79	2,507	9,886.68	17,965.79	0.0073	33,750.04
180,409.63	2,419	9,540.02	17,324.63	0.0073	34,414.40
179,866.43	2,344	9,246.12	16,781.43	0.0073	34,978.09
179,716.69	2,324	9,166.41	16,631.69	0.0073	35,133.71
179,357.64	2,274	8,970.20	16,272.64	0.0073	35,506.72
178,718.81	2,186	8,623.55	15,633.81	0.0073	36,171.09
178,177.57	2,112	8,329.63	15,092.57	0.0072	36,734.77
178,028.36	2,091	8,249.73	14,943.36	0.0073	36,890.39
177,670.59	2,042	8,053.72	14,585.59	0.0072	37,263.41
177,034.02	1,954	7,707.07	13,949.02	0.0072	37,927.78
176,494.69	1,880	7,413.13	13,409.69	0.0072	38,491.46
176,345.99	1,859	7,333.07	13,260.99	0.0072	38,647.08
175,989.48	1,810	7,137.24	12,904.48	0.0072	39,020.10

175,355.11	1,722	6,790.59	12,270.11	0.0072	39,684.46
174,817.63	1,647	6,496.64	11,732.63	0.0072	40,248.14
174,669.44	1,627	6,416.43	11,584.44	0.0072	40,403.77
174,314.14	1,577	6,220.76	11,229.14	0.0072	40,776.78
173,681.93	1,489	5,874.11	10,596.93	0.0072	41,441.15
173,146.25	1,415	5,580.14	10,061.25	0.0072	42,004.83
172,998.56	1,394	5,499.80	9,913.56	0.0072	42,160.45
172,644.44	1,345	5,304.27	9,559.44	0.0072	42,533.47
172,014.31	1,257	4,957.63	8,929.31	0.0072	43,197.83
171,480.39	1,182	4,663.65	8,395.39	0.0072	43,761.52
171,333.19	1,162	4,583.17	8,248.19	0.0072	43,917.14
170,980.23	1,113	4,387.79	7,895.23	0.0071	44,290.15
170,352.14	1,025	4,041.16	7,267.14	0.0071	44,954.52
169,819.93	950	3,747.16	6,734.93	0.0071	45,518.20
169,673.19	929	3,666.53	6,588.19	0.0071	45,673.82
169,321.36	880	3,471.31	6,236.36	0.0071	46,046.84
168,695.25	792	3,124.68	5,610.25	0.0071	46,711.20
168,164.72	718	2,830.66	5,079.72	0.0071	47,274.89
168,018.43	697	2,749.89	4,933.43	0.0071	47,430.51
167,667.69	648	2,554.83	4,582.69	0.0071	47,803.52
167,043.53	560	2,208.20	3,958.53	0.0071	48,467.89
166,514.62	485	1,914.17	3,429.62	0.0071	49,031.57
166,368.78	465	1,833.25	3,283.78	0.0071	49,187.19
166,019.11	415	1,638.35	2,934.11	0.0071	49,560.21
165,396.84	328	1,291.73	2,311.84	0.0071	50,224.57
164,869.52	253	997.68	1,784.52	0.0071	50,788.26
164,724.12	232	916.63	1,639.12	0.0071	50,943.88
164,375.49	183	721.88	1,290.49	0.0071	51,316.89
163,755.06	95	375.27	670.06	0.0071	51,981.26
163,229.28	21	81.19	144.28	0.0070	52,544.94

Cruise at Altitude 10058 m					
Weight in Kg.	Max Range (Km)	Max Flight Time (Sec.)	Available Fuel (Kg)	Fuel burnt per m (Kg/m)	CCF (ATR)
212,699.26	6,971	27,767.09	49,614.26	0.0078	0.00
212,445.60	6,939	27,608.29	49,360.60	0.0078	260.34
211,944.83	6,874	27,352.16	48,859.83	0.0078	775.68
211,391.42	6,803	27,068.71	48,306.42	0.0078	1,347.08
210,995.54	6,752	26,865.39	47,910.54	0.0077	1,756.40
210,892.96	6,739	26,815.64	47,807.96	0.0077	1,862.77
210,511.36	6,689	26,616.31	47,426.36	0.0077	2,258.31
209,833.24	6,601	26,266.59	46,748.24	0.0077	2,962.80
209,259.53	6,527	25,970.14	46,174.53	0.0077	3,560.52
209,101.41	6,506	25,889.01	46,016.41	0.0077	3,725.54
208,722.77	6,457	25,691.74	45,637.77	0.0077	4,121.09
208,049.89	6,369	25,342.02	44,964.89	0.0076	4,825.57
207,480.52	6,295	25,045.56	44,395.52	0.0076	5,423.30
207,323.60	6,274	24,964.31	44,238.60	0.0076	5,588.31
206,947.81	6,225	24,767.16	43,862.81	0.0076	5,983.86
206,279.94	6,137	24,417.44	43,194.94	0.0076	6,688.34
205,714.77	6,062	24,120.98	42,629.77	0.0076	7,286.07
205,558.99	6,042	24,039.76	42,473.99	0.0076	7,451.09
205,185.94	5,992	23,842.59	42,100.94	0.0075	7,846.63
204,522.89	5,904	23,492.87	41,437.89	0.0075	8,551.11
203,961.76	5,830	23,196.40	40,876.76	0.0075	9,148.84
203,807.09	5,809	23,115.19	40,722.09	0.0075	9,313.86
203,436.67	5,760	22,918.01	40,351.67	0.0075	9,709.40
202,778.26	5,672	22,568.30	39,693.26	0.0075	10,413.89
202,221.01	5,597	22,271.82	39,136.01	0.0075	11,011.61
202,067.41	5,577	22,190.60	38,982.41	0.0075	11,176.63
201,699.53	5,528	21,993.44	38,614.53	0.0074	11,572.17
201,045.59	5,440	21,643.72	37,960.59	0.0074	12,276.66
200,492.09	5,365	21,347.24	37,407.09	0.0074	12,874.38
200,339.52	5,344	21,266.01	37,254.52	0.0074	13,039.40
199,974.08	5,295	21,068.86	36,889.08	0.0074	13,434.94
199,324.46	5,207	20,719.15	36,239.46	0.0074	14,139.43
198,774.56	5,133	20,422.66	35,689.56	0.0074	14,737.15
198,622.98	5,112	20,341.42	35,537.98	0.0074	14,902.17
198,259.90	5,063	20,144.29	35,174.90	0.0073	15,297.71
197,614.43	4,975	19,794.58	34,529.43	0.0073	16,002.20
197,068.02	4,900	19,498.08	33,983.02	0.0073	16,599.93
196,917.39	4,880	19,416.81	33,832.39	0.0073	16,764.94
196,556.59	4,830	19,219.71	33,471.59	0.0073	17,160.49
195,915.13	4,743	18,870.00	32,830.13	0.0073	17,864.97
195,372.08	4,668	18,573.50	32,287.08	0.0073	18,462.70
195,222.37	4,647	18,492.24	32,137.37	0.0073	18,627.72
194,863.76	4,598	18,295.14	31,778.76	0.0073	19,023.26
194,226.18	4,510	17,945.43	31,141.18	0.0072	19,727.74

193,686.38	4,436	17,648.92	30,601.38	0.0072	20,325.47
193,537.56	4,415	17,567.68	30,452.56	0.0072	20,490.49
193,181.07	4,366	17,370.57	30,096.07	0.0072	20,886.03
192,547.23	4,278	17,020.86	29,462.23	0.0072	21,590.52
192,010.56	4,203	16,724.34	28,925.56	0.0072	22,188.24
191,862.59	4,183	16,642.94	28,777.59	0.0072	22,353.26
191,508.16	4,133	16,445.99	28,423.16	0.0072	22,748.80
190,877.93	4,045	16,096.29	27,792.93	0.0072	23,453.29
190,344.29	3,971	15,799.76	27,259.29	0.0071	24,051.01
190,197.15	3,950	15,718.31	27,112.15	0.0071	24,216.03
189,844.70	3,901	15,521.41	26,759.70	0.0071	24,611.57
189,217.97	3,813	15,171.71	26,132.97	0.0071	25,316.06
188,687.26	3,738	14,875.17	25,602.26	0.0071	25,913.78
188,540.93	3,718	14,793.78	25,455.93	0.0071	26,078.80
188,190.39	3,669	14,596.84	25,105.39	0.0071	26,474.34
187,567.03	3,581	14,247.14	24,482.03	0.0071	27,178.83
187,039.16	3,506	13,950.59	23,954.16	0.0071	27,776.56
186,893.61	3,486	13,869.17	23,808.61	0.0071	27,941.57
186,544.92	3,436	13,672.26	23,459.92	0.0071	28,337.12
185,924.84	3,348	13,322.56	22,839.84	0.0070	29,041.60
185,399.70	3,274	13,026.01	22,314.70	0.0070	29,639.33
185,254.91	3,253	12,944.59	22,169.91	0.0070	29,804.35
184,908.01	3,204	12,747.69	21,823.01	0.0070	30,199.89
184,291.09	3,116	12,397.99	21,206.09	0.0070	30,904.37
183,768.62	3,041	12,101.43	20,683.62	0.0070	31,502.10
183,624.55	3,021	12,019.96	20,539.55	0.0070	31,667.12
183,279.39	2,971	11,823.11	20,194.39	0.0070	32,062.66
182,665.54	2,884	11,473.42	19,580.54	0.0070	32,767.15
182,145.64	2,809	11,176.85	19,060.64	0.0070	33,364.87
182,002.27	2,788	11,095.37	18,917.27	0.0070	33,529.89
181,658.80	2,739	10,898.54	18,573.80	0.0070	33,925.43
181,047.92	2,651	10,548.85	17,962.92	0.0069	34,629.92
180,530.51	2,577	10,252.27	17,445.51	0.0069	35,227.64
180,387.83	2,556	10,170.73	17,302.83	0.0069	35,392.66
180,045.99	2,507	9,973.97	16,960.99	0.0069	35,788.20
179,437.99	2,419	9,624.27	16,352.99	0.0069	36,492.69
178,923.00	2,344	9,327.69	15,838.00	0.0069	37,090.41
178,780.98	2,324	9,246.10	15,695.98	0.0069	37,255.43
178,440.72	2,274	9,049.39	15,355.72	0.0069	37,650.97
177,835.51	2,186	8,699.70	14,750.51	0.0069	38,355.46
177,322.86	2,112	8,403.10	14,237.86	0.0069	38,953.18
177,181.49	2,091	8,321.50	14,096.49	0.0069	39,118.20
176,842.77	2,042	8,124.82	13,757.77	0.0069	39,513.75
176,240.27	1,954	7,775.13	13,155.27	0.0068	40,218.23
175,729.89	1,880	7,478.52	12,644.89	0.0068	40,815.96
175,589.14	1,859	7,396.89	12,504.14	0.0068	40,980.98

175,251.91	1,810	7,200.24	12,166.91	0.0068	41,376.52
174,652.03	1,722	6,850.56	11,567.03	0.0068	42,081.00
174,143.87	1,647	6,553.94	11,058.87	0.0068	42,678.73
174,003.72	1,627	6,472.27	10,918.72	0.0068	42,843.75
173,667.93	1,577	6,275.67	10,582.93	0.0068	43,239.29
173,070.61	1,489	5,925.98	9,985.61	0.0068	43,943.78
172,564.59	1,415	5,629.36	9,479.59	0.0068	44,541.50
172,425.03	1,394	5,547.65	9,340.03	0.0068	44,706.52
172,090.65	1,345	5,351.09	9,005.65	0.0068	45,102.06
171,495.80	1,257	5,001.41	8,410.80	0.0068	45,806.55
170,991.86	1,182	4,704.78	7,906.86	0.0068	46,404.27
170,852.87	1,162	4,623.04	7,767.87	0.0067	46,569.29
170,519.85	1,112	4,426.52	7,434.85	0.0067	46,964.83
169,927.42	1,025	4,076.84	6,842.42	0.0067	47,669.32
169,425.50	950	3,780.20	6,340.50	0.0067	48,267.04
169,287.06	929	3,698.42	6,202.06	0.0067	48,432.06
168,955.37	880	3,501.95	5,870.37	0.0067	48,827.60
168,365.27	792	3,152.27	5,280.27	0.0067	49,532.09
167,865.32	718	2,855.62	4,780.32	0.0067	50,129.81
167,727.42	697	2,773.81	4,642.42	0.0067	50,294.83
167,397.02	648	2,577.37	4,312.02	0.0067	50,690.38
166,809.20	560	2,227.70	3,724.20	0.0067	51,394.86
166,311.15	485	1,931.04	3,226.15	0.0067	51,992.59
166,173.82	465	1,849.31	3,088.82	0.0067	52,157.61
165,957.13	432	1,719.92	2,872.13	0.0067	52,417.95
165,528.55	368	1,464.13	2,443.55	0.0067	52,933.28
165,053.90	297	1,180.52	1,968.90	0.0067	53,504.68
164,714.22	246	977.37	1,629.22	0.0066	53,914.00
164,626.06	232	924.67	1,541.06	0.0066	54,020.38
164,473.82	209	833.47	1,388.82	0.0066	54,203.93
164,155.78	162	643.00	1,070.78	0.0066	54,587.66
163,758.61	102	404.94	673.61	0.0066	55,067.30
163,388.81	46	183.08	303.81	0.0066	55,514.29
163,145.17	9	36.81	60.17	0.0065	55,808.99

Cruise at Altitude 10668 m					
Weight in Kg.	Max Range (Km)	Max Flight Time (Sec.)	Available Fuel (Kg)	Fuel burnt per m (Kg/m)	CCF (ATR)
211,280.83	6,971	28,048.19	48,195.83	0.0079	0.00
211,026.00	6,939	27,864.51	47,941.00	0.0078	275.52
210,522.75	6,874	27,603.27	47,437.75	0.0078	820.92
209,967.72	6,803	27,318.15	46,882.72	0.0078	1,425.64
209,571.15	6,752	27,117.66	46,486.15	0.0077	1,858.84
209,468.83	6,739	27,073.83	46,383.83	0.0077	1,971.42
209,086.71	6,689	26,860.82	46,001.71	0.0077	2,390.03
208,407.81	6,601	26,507.02	45,322.81	0.0077	3,135.60
207,834.67	6,527	26,210.74	44,749.67	0.0076	3,768.19
207,677.67	6,506	26,152.97	44,592.67	0.0077	3,942.83
207,428.73	6,474	25,998.57	44,343.73	0.0076	4,218.36
206,936.93	6,410	25,737.31	43,851.93	0.0076	4,763.75
206,393.77	6,338	25,452.08	43,308.77	0.0076	5,368.48
206,005.95	6,287	25,251.75	42,920.95	0.0075	5,801.67
205,906.00	6,274	25,213.48	42,821.00	0.0076	5,914.25
205,659.69	6,242	25,064.92	42,574.69	0.0076	6,189.77
205,173.11	6,177	24,804.33	42,088.11	0.0075	6,735.17
204,635.55	6,106	24,518.98	41,550.55	0.0075	7,339.89
204,251.74	6,055	24,318.52	41,166.74	0.0075	7,773.09
204,152.63	6,042	24,275.29	41,067.63	0.0075	7,885.66
203,782.47	5,992	24,061.86	40,697.47	0.0075	8,304.28
203,124.64	5,904	23,708.00	40,039.64	0.0075	9,049.85
202,569.09	5,830	23,411.64	39,484.09	0.0074	9,682.44
202,416.50	5,809	23,341.98	39,331.50	0.0074	9,857.08
202,049.96	5,760	23,128.67	38,964.96	0.0074	10,275.69
201,398.53	5,672	22,775.01	38,313.53	0.0074	11,021.27
200,848.33	5,597	22,478.35	37,763.33	0.0073	11,653.85
200,697.21	5,577	22,408.83	37,612.21	0.0074	11,828.50
200,334.13	5,528	22,195.60	37,249.13	0.0073	12,247.11
199,688.84	5,440	21,841.96	36,603.84	0.0073	12,992.68
199,143.74	5,365	21,545.19	36,058.74	0.0073	13,625.27
198,994.02	5,345	21,475.14	35,909.02	0.0073	13,799.91
198,634.26	5,295	21,262.51	35,549.26	0.0073	14,218.52
197,994.84	5,207	20,908.91	34,909.84	0.0072	14,964.10
197,454.64	5,133	20,612.02	34,369.64	0.0072	15,596.69
197,306.24	5,112	20,541.37	34,221.24	0.0072	15,771.33
196,949.68	5,063	20,329.43	33,864.68	0.0072	16,189.94
196,315.89	4,975	19,975.86	33,230.89	0.0072	16,935.52
195,780.38	4,900	19,678.86	32,695.38	0.0071	17,568.10
195,633.26	4,880	19,607.68	32,548.26	0.0072	17,742.75
195,279.74	4,830	19,396.35	32,194.74	0.0071	18,161.36
194,651.35	4,743	19,042.82	31,566.35	0.0071	18,906.93
194,120.34	4,668	18,745.71	31,035.34	0.0071	19,539.52

193,974.45	4,647	18,673.97	30,889.45	0.0071	19,714.16
193,623.86	4,598	18,463.28	30,538.86	0.0071	20,132.77
193,000.65	4,510	18,109.78	29,915.65	0.0071	20,878.35
192,473.96	4,436	17,812.56	29,388.96	0.0070	21,510.93
192,329.25	4,415	17,740.27	29,244.25	0.0070	21,685.58
191,981.47	4,366	17,530.21	28,896.47	0.0070	22,104.19
191,363.24	4,278	17,176.74	28,278.24	0.0070	22,849.76
190,840.69	4,203	16,879.40	27,755.69	0.0070	23,482.35
190,697.11	4,183	16,806.57	27,612.11	0.0070	23,656.99
190,352.04	4,133	16,597.14	27,267.04	0.0070	24,075.61
189,738.59	4,045	16,243.70	26,653.59	0.0070	24,821.18
189,220.03	3,971	15,946.25	26,135.03	0.0069	25,453.77
189,077.53	3,950	15,872.87	25,992.53	0.0069	25,628.41
188,735.06	3,901	15,664.07	25,650.06	0.0069	26,047.02
188,126.21	3,813	15,310.66	25,041.21	0.0069	26,792.60
187,611.49	3,738	15,013.10	24,526.49	0.0069	27,425.18
187,470.03	3,718	14,939.18	24,385.03	0.0069	27,599.83
187,130.06	3,669	14,731.00	24,045.06	0.0069	28,018.44
186,525.63	3,581	14,377.62	23,440.63	0.0069	28,764.01
186,014.60	3,506	14,079.95	22,929.60	0.0068	29,396.60
185,874.16	3,486	14,005.48	22,789.16	0.0068	29,571.24
185,536.59	3,436	13,797.93	22,451.59	0.0068	29,989.85
184,936.42	3,348	13,444.58	21,851.42	0.0068	30,735.43
184,428.95	3,274	13,146.79	21,343.95	0.0068	31,368.02
184,289.47	3,253	13,071.77	21,204.47	0.0068	31,542.66
183,954.23	3,204	12,864.86	20,869.23	0.0068	31,961.27
183,358.15	3,116	12,511.54	20,273.15	0.0068	32,706.85
182,854.11	3,041	12,213.64	19,769.11	0.0067	33,339.43
182,715.56	3,021	12,138.08	19,630.56	0.0068	33,514.08
182,382.56	2,971	11,931.79	19,297.56	0.0067	33,932.69
181,790.44	2,884	11,578.50	18,705.44	0.0067	34,678.26
181,289.69	2,809	11,280.49	18,204.69	0.0067	35,310.85
181,152.05	2,788	11,204.38	18,067.05	0.0067	35,485.49
180,821.20	2,739	10,998.72	17,736.20	0.0067	35,904.10
180,232.89	2,651	10,645.46	17,147.89	0.0067	36,649.68
179,735.33	2,577	10,347.33	16,650.33	0.0066	37,282.26
179,598.56	2,556	10,270.68	16,513.56	0.0067	37,456.91
179,269.79	2,507	10,065.65	16,184.79	0.0067	37,875.52
178,685.16	2,419	9,712.41	15,600.16	0.0066	38,621.09
178,190.67	2,344	9,414.17	15,105.67	0.0066	39,253.68
178,054.74	2,324	9,336.97	14,969.74	0.0066	39,428.32
177,727.98	2,274	9,132.57	14,642.98	0.0066	39,846.94
177,146.90	2,186	8,779.36	14,061.90	0.0066	40,592.51
176,655.38	2,112	8,480.99	13,570.38	0.0066	41,225.10
176,520.25	2,091	8,403.25	13,435.25	0.0066	41,399.74

176,195.43	2,042	8,199.48	13,110.43	0.0066	41,818.35
175,617.79	1,954	7,846.30	12,532.79	0.0066	42,563.93
175,129.14	1,880	7,547.82	12,044.14	0.0065	43,196.51
174,994.79	1,859	7,469.53	11,909.79	0.0065	43,371.16
174,671.85	1,810	7,266.39	11,586.85	0.0065	43,789.77
174,097.51	1,722	6,913.24	11,012.51	0.0065	44,535.34
173,611.63	1,647	6,614.64	10,526.63	0.0065	45,167.93
173,478.04	1,627	6,535.81	10,393.04	0.0065	45,342.57
173,156.91	1,577	6,333.30	10,071.91	0.0065	45,761.18
172,585.78	1,489	5,980.17	9,500.78	0.0065	46,506.76
172,102.58	1,415	5,681.48	9,017.58	0.0065	47,139.34
171,969.73	1,394	5,602.10	8,884.73	0.0065	47,313.99
171,650.35	1,345	5,400.22	8,565.35	0.0065	47,732.60
171,082.32	1,257	5,047.14	7,997.32	0.0064	48,478.18
170,601.71	1,182	4,748.33	7,516.71	0.0064	49,110.76
170,469.56	1,162	4,668.41	7,384.56	0.0064	49,285.40
170,151.88	1,112	4,467.15	7,066.88	0.0064	49,704.02
169,586.85	1,025	4,114.09	6,501.85	0.0064	50,449.59
169,108.75	950	3,815.16	6,023.75	0.0064	51,082.18
168,977.28	929	3,734.70	5,892.28	0.0064	51,256.82
168,661.25	880	3,534.07	5,576.25	0.0064	51,675.43
168,099.12	792	3,181.03	5,014.12	0.0064	52,421.01
167,623.45	718	2,881.97	4,538.45	0.0064	53,053.59
167,492.65	697	2,800.95	4,407.65	0.0064	53,228.24
167,178.21	648	2,600.96	4,093.21	0.0064	53,646.85
166,618.89	560	2,247.95	3,533.89	0.0063	54,392.42
166,145.57	485	1,948.80	3,060.57	0.0063	55,025.01
166,015.41	465	1,867.24	2,930.41	0.0063	55,199.65
165,702.51	415	1,667.88	2,617.51	0.0063	55,618.26
165,145.91	327	1,314.91	2,060.91	0.0063	56,363.84
164,674.88	253	1,015.65	1,589.88	0.0063	56,996.43
164,545.57	232	933.85	1,460.57	0.0063	57,171.07
164,400.91	209	841.23	1,315.91	0.0063	57,365.32
164,098.97	162	648.83	1,013.97	0.0063	57,771.44
163,722.17	102	408.58	637.17	0.0063	58,279.05
163,371.34	46	184.66	286.34	0.0063	58,752.12
163,141.43	9	37.14	56.43	0.0061	59,064.00

Cruise at Altitude 11278 m					
Weight in Kg.	Max Range (Km)	Max Flight Time (Sec.)	Available Fuel (Kg)	Fuel burnt per m (Kg/m)	CCF (ATR)
211,445.47	6,971	28,230.31	48,360.47	0.0081	0.00
211,048.18	6,922	28,032.36	47,963.18	0.0081	0.23
210,340.05	6,834	27,653.69	47,255.05	0.0081	1,224.26
209,739.26	6,760	27,346.52	46,654.26	0.0081	1,889.49
209,573.62	6,739	27,249.17	46,488.62	0.0081	2,073.15
209,176.10	6,690	27,045.32	46,091.10	0.0081	2,513.36
208,467.36	6,602	26,668.08	45,382.36	0.0081	3,297.41
207,866.08	6,528	26,359.02	44,781.08	0.0081	3,962.64
207,700.26	6,507	26,264.88	44,615.26	0.0081	4,146.30
207,302.30	6,458	26,059.98	44,217.30	0.0080	4,586.51
206,596.03	6,370	25,702.59	43,511.03	0.0080	5,370.56
206,000.64	6,295	25,405.28	42,915.64	0.0080	6,035.79
205,836.83	6,275	25,318.81	42,751.83	0.0079	6,219.44
205,444.92	6,225	25,120.37	42,359.92	0.0079	6,659.66
204,750.07	6,138	24,764.90	41,665.07	0.0079	7,443.71
204,163.85	6,063	24,465.61	41,078.85	0.0078	8,108.93
204,002.84	6,042	24,388.16	40,917.84	0.0078	8,292.59
203,617.14	5,993	24,182.18	40,532.14	0.0078	8,732.80
202,932.77	5,905	23,827.19	39,847.77	0.0077	9,516.85
202,355.58	5,831	23,527.58	39,270.58	0.0077	10,182.08
202,196.97	5,810	23,451.04	39,111.97	0.0077	10,365.74
201,817.04	5,761	23,244.41	38,732.04	0.0077	10,805.95
201,142.77	5,673	22,889.46	38,057.77	0.0076	11,590.00
200,574.01	5,598	22,589.75	37,489.01	0.0076	12,255.23
200,417.67	5,578	22,512.76	37,332.67	0.0076	12,438.89
200,043.18	5,528	22,306.66	36,958.18	0.0076	12,879.10
199,378.50	5,440	21,951.72	36,293.50	0.0075	13,663.15
198,817.68	5,366	21,651.96	35,732.68	0.0075	14,328.38
198,663.51	5,345	21,574.59	35,578.51	0.0075	14,512.03
198,294.17	5,296	21,368.91	35,209.17	0.0075	14,952.25
197,638.55	5,208	21,013.98	34,553.55	0.0074	15,736.30
197,085.27	5,133	20,714.17	34,000.27	0.0074	16,401.53
196,933.14	5,113	20,636.52	33,848.14	0.0074	16,585.18
196,568.68	5,063	20,431.17	33,483.68	0.0074	17,025.39
195,921.66	4,976	20,076.24	32,836.66	0.0073	17,809.44
195,375.52	4,901	19,776.39	32,290.52	0.0073	18,474.67
195,225.34	4,880	19,698.48	32,140.34	0.0073	18,658.33
194,865.51	4,831	19,493.42	31,780.51	0.0073	19,098.54
194,226.64	4,743	19,138.50	31,141.64	0.0072	19,882.59
193,687.28	4,669	18,838.61	30,602.28	0.0072	20,547.82
193,538.95	4,648	18,760.46	30,453.95	0.0072	20,731.48
193,183.52	4,599	18,555.67	30,098.52	0.0072	21,171.69
192,552.40	4,511	18,200.75	29,467.40	0.0071	21,955.74
192,019.48	4,436	17,900.83	28,934.48	0.0071	22,620.97

191,872.92	4,416	17,822.43	28,787.92	0.0071	22,804.62
191,521.67	4,366	17,617.92	28,436.67	0.0071	23,244.84
190,897.91	4,278	17,263.01	27,812.91	0.0071	24,028.89
190,371.13	4,204	16,963.05	27,286.13	0.0070	24,694.12
190,226.23	4,183	16,884.41	27,141.23	0.0070	24,877.77
189,878.97	4,134	16,680.17	26,793.97	0.0070	25,317.99
189,262.23	4,046	16,325.27	26,177.23	0.0070	26,102.03
188,741.28	3,971	16,025.26	25,656.28	0.0070	26,767.26
188,597.99	3,951	15,946.38	25,512.99	0.0070	26,950.92
188,254.52	3,901	15,742.42	25,169.52	0.0069	27,391.13
187,644.47	3,814	15,387.52	24,559.47	0.0069	28,175.18
187,129.09	3,739	15,087.47	24,044.09	0.0069	28,840.41
186,987.32	3,718	15,008.35	23,902.32	0.0069	29,024.07
186,647.47	3,669	14,804.66	23,562.47	0.0069	29,464.28
186,043.80	3,581	14,449.78	22,958.80	0.0068	30,248.33
185,533.74	3,507	14,149.69	22,448.74	0.0068	30,913.56
185,393.42	3,486	14,070.33	22,308.42	0.0068	31,097.22
185,057.03	3,437	13,866.92	21,972.03	0.0068	31,537.43
184,459.45	3,349	13,512.04	21,374.45	0.0068	32,321.48
183,954.47	3,274	13,211.90	20,869.47	0.0067	32,986.71
183,815.53	3,254	13,132.30	20,730.53	0.0068	33,170.36
183,482.45	3,204	12,929.17	20,397.45	0.0067	33,610.58
182,890.69	3,116	12,574.30	19,805.69	0.0067	34,394.63
182,390.57	3,042	12,274.11	19,305.57	0.0067	35,059.85
182,252.96	3,021	12,194.27	19,167.96	0.0067	35,243.51
181,923.03	2,972	11,991.41	18,838.03	0.0067	35,683.72
181,336.85	2,884	11,636.56	18,251.85	0.0066	36,467.77
180,841.37	2,809	11,336.31	17,756.37	0.0066	37,133.00
180,705.04	2,789	11,256.22	17,620.04	0.0066	37,316.66
180,378.14	2,739	11,053.64	17,293.14	0.0066	37,756.87
179,797.28	2,652	10,698.80	16,712.28	0.0066	38,540.92
179,306.26	2,577	10,398.50	16,221.26	0.0066	39,206.15
179,171.14	2,556	10,318.17	16,086.14	0.0066	39,389.81
178,847.14	2,507	10,115.87	15,762.14	0.0065	39,830.02
178,271.40	2,419	9,761.05	15,186.40	0.0065	40,614.07
177,784.64	2,345	9,460.70	14,699.64	0.0065	41,279.30
177,650.68	2,324	9,380.13	14,565.68	0.0065	41,462.95
177,329.46	2,275	9,178.12	14,244.46	0.0065	41,903.17
176,758.62	2,187	8,823.31	13,673.62	0.0065	42,687.22
176,275.96	2,112	8,522.91	13,190.96	0.0065	43,352.45
176,143.12	2,092	8,442.09	13,058.12	0.0065	43,536.10
175,824.56	2,042	8,240.37	12,739.56	0.0064	43,976.31
175,258.42	1,954	7,885.58	12,173.42	0.0064	44,760.36
174,779.69	1,880	7,585.12	11,694.69	0.0064	45,425.59
174,647.92	1,859	7,504.05	11,562.92	0.0064	45,609.25
174,331.93	1,810	7,302.62	11,246.93	0.0064	46,049.46

173,770.31	1,722	6,947.84	10,685.31	0.0064	46,833.51
173,295.34	1,647	6,647.33	10,210.34	0.0063	47,498.74
173,164.61	1,627	6,566.01	10,079.61	0.0064	47,682.40
172,851.07	1,577	6,364.87	9,766.07	0.0063	48,122.61
172,293.79	1,490	6,010.10	9,208.79	0.0063	48,906.66
171,822.45	1,415	5,709.54	8,737.45	0.0063	49,571.89
171,692.71	1,394	5,627.97	8,607.71	0.0063	49,755.54
171,381.54	1,345	5,427.11	8,296.54	0.0063	50,195.76
170,828.43	1,257	5,072.36	7,743.43	0.0063	50,979.81
170,360.58	1,183	4,771.74	7,275.58	0.0063	51,645.04
170,231.79	1,162	4,689.92	7,146.79	0.0063	51,828.69
169,922.89	1,113	4,489.36	6,837.89	0.0062	52,268.91
169,373.80	1,025	4,134.62	6,288.80	0.0062	53,052.95
168,909.31	950	3,833.95	5,824.31	0.0062	53,718.18
168,781.43	930	3,751.88	5,696.43	0.0062	53,901.84
168,474.73	880	3,551.60	5,389.73	0.0062	54,342.05
167,929.50	792	3,196.88	4,844.50	0.0062	55,126.10
167,468.24	718	2,896.15	4,383.24	0.0062	55,791.33
167,341.25	697	2,813.83	4,256.25	0.0062	55,974.99
167,036.65	648	2,613.84	3,951.65	0.0062	56,415.20
166,495.14	560	2,259.13	3,410.14	0.0061	57,199.25
166,036.99	485	1,958.35	2,951.99	0.0061	57,864.48
165,910.86	465	1,875.78	2,825.86	0.0061	58,048.14
165,608.29	415	1,676.09	2,523.29	0.0061	58,488.35
165,070.38	327	1,321.40	1,985.38	0.0061	59,272.40
164,615.22	253	1,020.56	1,530.22	0.0061	59,937.63
164,489.98	232	937.84	1,404.98	0.0061	60,121.28
164,350.38	209	845.14	1,265.38	0.0061	60,325.56
164,058.92	162	651.90	973.92	0.0061	60,752.63
163,695.32	102	410.45	610.32	0.0061	61,286.44
163,356.76	46	185.40	271.76	0.0060	61,783.92
163,137.01	9	37.30	52.01	0.0056	62,111.90

Cruise at Altitude 11887 m					
Weight in Kg.	Max Range (Km)	Max Flight Time (Sec.)	Available Fuel (Kg)	Fuel burnt per m (Kg/m)	CCF (ATR)
211,577.51	6,971	28,152.15	48,492.51	0.0074	0.00
211,452.41	6,954	28,559.40	48,367.41	0.0075	158.91
211,181.89	6,918	28,495.35	48,096.89	0.0075	501.98
210,821.30	6,870	28,382.37	47,736.30	0.0075	960.01
210,441.50	6,819	28,082.34	47,356.50	0.0075	1,442.23
210,117.79	6,776	27,989.01	47,032.79	0.0075	1,853.16
209,914.58	6,749	27,766.84	46,829.58	0.0075	2,111.50
209,864.34	6,742	27,804.48	46,779.34	0.0075	2,175.27
209,625.14	6,710	27,655.65	46,540.14	0.0075	2,479.28
209,150.71	6,647	27,373.84	46,065.71	0.0075	3,081.07
208,624.68	6,577	27,072.13	45,539.68	0.0075	3,748.32
208,247.80	6,527	26,852.51	45,162.80	0.0075	4,226.32
208,149.95	6,514	26,800.52	45,064.95	0.0075	4,350.53
207,785.97	6,465	26,588.68	44,700.97	0.0075	4,812.43
207,136.63	6,378	26,209.31	44,051.63	0.0075	5,635.10
206,585.82	6,305	25,897.79	43,500.82	0.0075	6,333.10
206,433.74	6,284	25,803.64	43,348.74	0.0075	6,525.80
206,069.38	6,236	25,599.27	42,984.38	0.0075	6,987.70
205,419.45	6,149	25,219.99	42,334.45	0.0075	7,810.36
204,868.14	6,075	24,911.52	41,783.14	0.0075	8,508.36
204,715.94	6,055	24,813.56	41,630.94	0.0075	8,701.06
204,351.24	6,006	24,612.10	41,266.24	0.0075	9,162.96
203,700.74	5,919	24,233.22	40,615.74	0.0075	9,985.63
203,148.94	5,845	23,926.38	40,063.94	0.0075	10,683.63
202,996.63	5,825	23,826.68	39,911.63	0.0075	10,876.33
202,631.59	5,776	23,626.78	39,546.59	0.0075	11,338.23
201,980.52	5,689	23,248.65	38,895.52	0.0075	12,160.90
201,428.24	5,615	22,942.67	38,343.24	0.0075	12,858.89
201,275.80	5,594	22,842.33	38,190.80	0.0075	13,051.60
200,910.42	5,545	22,643.25	37,825.42	0.0075	13,513.49
200,258.81	5,458	22,266.10	37,173.81	0.0075	14,336.16
199,706.04	5,384	21,960.43	36,621.04	0.0075	15,034.16
199,553.47	5,363	21,860.18	36,468.47	0.0075	15,226.86
199,187.73	5,314	21,661.40	36,102.73	0.0075	15,688.76
198,535.58	5,227	21,285.46	35,450.58	0.0075	16,511.43
197,982.32	5,152	20,979.59	34,897.32	0.0074	17,209.43
197,829.62	5,132	20,880.14	34,744.62	0.0074	17,402.13
197,463.51	5,083	20,681.16	34,378.51	0.0074	17,864.03
196,810.83	4,995	20,306.66	33,725.83	0.0074	18,686.70
196,257.08	4,921	20,000.23	33,172.08	0.0074	19,384.69
196,104.25	4,900	19,902.44	33,019.25	0.0074	19,577.39
195,737.77	4,851	19,702.60	32,652.77	0.0074	20,039.29
195,084.55	4,763	19,329.57	31,999.55	0.0074	20,861.96
194,530.35	4,689	19,022.56	31,445.35	0.0074	21,559.96

194,377.41	4,668	18,926.95	31,292.41	0.0074	21,752.66
194,010.60	4,619	18,725.78	30,925.60	0.0074	22,214.56
193,356.83	4,531	18,354.06	30,271.83	0.0074	23,037.23
192,802.11	4,456	18,046.15	29,717.11	0.0074	23,735.22
192,649.00	4,436	17,952.26	29,564.00	0.0074	23,927.93
192,281.85	4,386	17,750.64	29,196.85	0.0074	24,389.82
191,627.56	4,298	17,380.03	28,542.56	0.0074	25,212.49
191,072.29	4,223	17,071.46	27,987.29	0.0074	25,910.49
190,919.02	4,203	16,979.08	27,834.02	0.0074	26,103.19
190,551.66	4,153	16,777.43	27,466.66	0.0074	26,565.09
189,896.56	4,065	16,407.20	26,811.56	0.0074	27,387.76
189,343.31	3,990	16,112.70	26,258.31	0.0073	28,085.76
189,192.25	3,969	16,033.03	26,107.25	0.0073	28,278.46
188,953.68	3,937	15,898.50	25,868.68	0.0073	28,582.47
188,479.79	3,872	15,623.83	25,394.79	0.0073	29,184.26
187,955.26	3,801	15,335.18	24,870.26	0.0073	29,851.52
187,581.90	3,749	15,128.66	24,496.90	0.0072	30,329.51
187,486.02	3,736	15,092.86	24,401.02	0.0072	30,453.72
187,127.24	3,686	14,875.01	24,042.24	0.0072	30,915.62
186,489.15	3,598	14,517.40	23,404.15	0.0072	31,738.29
185,951.84	3,523	14,215.71	22,866.84	0.0072	32,436.29
185,803.91	3,502	14,134.98	22,718.91	0.0071	32,628.99
185,450.09	3,453	13,931.57	22,365.09	0.0071	33,090.89
184,822.47	3,364	13,575.30	21,737.47	0.0071	33,913.56
184,293.16	3,290	13,273.50	21,208.16	0.0070	34,611.55
184,147.70	3,269	13,193.57	21,062.70	0.0070	34,804.26
183,799.30	3,219	12,989.47	20,714.30	0.0070	35,266.15
183,181.11	3,131	12,633.11	20,096.11	0.0070	36,088.82
182,659.70	3,056	12,331.37	19,574.70	0.0069	36,786.82
182,516.38	3,035	12,251.25	19,431.38	0.0069	36,979.52
182,173.09	2,986	12,047.36	19,088.09	0.0069	37,441.42
181,563.84	2,897	11,690.93	18,478.84	0.0069	38,264.09
181,049.85	2,823	11,389.20	17,964.85	0.0068	38,962.09
180,908.57	2,802	11,308.95	17,823.57	0.0068	39,154.79
180,570.11	2,752	11,105.23	17,485.11	0.0068	39,616.69
179,969.30	2,664	10,748.73	16,884.30	0.0068	40,439.36
179,462.34	2,589	10,446.98	16,377.34	0.0067	41,137.35
179,323.00	2,568	10,366.72	16,238.00	0.0067	41,330.06
178,989.09	2,519	10,163.05	15,904.09	0.0067	41,791.95
178,396.28	2,430	9,806.54	15,311.28	0.0067	42,614.62
177,895.97	2,356	9,504.76	14,810.97	0.0066	43,312.62
177,758.45	2,335	9,424.34	14,673.45	0.0066	43,505.32
177,428.86	2,285	9,220.87	14,343.86	0.0066	43,967.22
176,843.63	2,197	8,864.35	13,758.63	0.0066	44,789.89
176,349.64	2,122	8,562.51	13,264.64	0.0066	45,487.89
176,213.84	2,101	8,481.87	13,128.84	0.0066	45,680.59

175,888.34	2,052	8,278.65	12,803.34	0.0065	46,142.48
175,310.32	1,963	7,922.13	12,225.32	0.0065	46,965.15
174,822.32	1,888	7,620.23	11,737.32	0.0065	47,663.15
174,688.16	1,868	7,539.29	11,603.16	0.0065	47,855.85
174,366.55	1,818	7,336.41	11,281.55	0.0065	48,317.75
173,795.37	1,730	6,979.93	10,710.37	0.0064	49,140.42
173,313.07	1,655	6,677.98	10,228.07	0.0064	49,838.42
173,180.46	1,634	6,596.71	10,095.46	0.0064	50,031.12
172,862.55	1,585	6,394.21	9,777.55	0.0064	50,493.02
172,297.90	1,496	6,037.75	9,212.90	0.0064	51,315.69
171,821.02	1,421	5,735.75	8,736.02	0.0063	52,013.68
171,689.89	1,401	5,654.15	8,604.89	0.0063	52,206.39
171,375.49	1,351	5,452.01	8,290.49	0.0063	52,668.28
170,817.06	1,263	5,095.55	7,732.06	0.0063	53,490.95
170,345.34	1,188	4,793.49	7,260.34	0.0063	54,188.95
170,215.62	1,167	4,711.56	7,130.62	0.0063	54,381.65
169,904.59	1,118	4,509.78	6,819.59	0.0063	54,843.55
169,352.08	1,029	4,153.35	6,267.08	0.0062	55,666.22
168,885.30	954	3,851.24	5,800.30	0.0062	56,364.22
168,756.92	934	3,769.02	5,671.92	0.0062	56,556.92
168,449.10	884	3,567.59	5,364.10	0.0062	57,018.81
167,902.24	796	3,211.18	4,817.24	0.0062	57,841.48
167,440.17	721	2,909.02	4,355.17	0.0061	58,539.48
167,313.07	700	2,826.44	4,228.07	0.0061	58,732.18
167,008.30	651	2,625.40	3,923.30	0.0061	59,194.08
166,466.85	562	2,269.00	3,381.85	0.0061	60,016.75
166,009.28	487	1,966.77	2,924.28	0.0061	60,714.75
165,883.57	467	1,884.31	2,798.57	0.0061	60,907.45
165,684.73	434	1,751.63	2,599.73	0.0061	61,211.46
165,291.99	369	1,490.90	2,206.99	0.0061	61,813.25
164,857.94	298	1,201.90	1,772.94	0.0060	62,480.51
164,547.79	247	994.95	1,462.79	0.0060	62,958.50
164,467.70	233	941.60	1,382.70	0.0060	63,082.72
164,328.57	210	848.17	1,243.57	0.0060	63,297.06
164,038.55	162	654.13	953.55	0.0060	63,745.16
163,677.45	102	411.55	592.45	0.0060	64,305.27
163,340.61	46	185.37	255.61	0.0057	64,827.25
163,132.41	9	37.39	47.41	0.0052	65,171.39

F

Optimal Climate Cost Cruise Database - Climate Model B

Cruise at Altitude 9449 m					
Weight in Kg.	Max Range (Km)	Max Flight Time (Sec.)	Available Fuel (Kg)	Fuel burnt per m (Kg/m)	CCF (ATR)
214,250.58	6,971	28,221.94	51,165.58	0.0082	0.00
213,986.97	6,939	27,553.15	50,901.97	0.0080	71.11
213,474.81	6,875	27,169.24	50,389.81	0.0078	211.87
212,915.07	6,803	26,936.19	49,830.07	0.0078	367.94
212,517.82	6,752	26,789.69	49,432.82	0.0077	479.75
212,415.57	6,739	26,748.86	49,330.57	0.0078	508.80
212,028.81	6,690	26,483.67	48,943.81	0.0079	616.84
211,337.04	6,602	26,095.96	48,252.04	0.0078	809.26
210,757.66	6,527	25,887.82	47,672.66	0.0077	972.53
210,599.92	6,506	25,829.60	47,514.92	0.0078	1,017.60
210,215.17	6,457	25,562.25	47,130.17	0.0078	1,125.64
209,527.58	6,369	25,181.09	46,442.58	0.0077	1,318.06
208,951.67	6,294	24,966.98	45,866.67	0.0076	1,481.33
208,794.96	6,274	24,914.22	45,709.96	0.0078	1,526.40
208,412.52	6,224	24,645.97	45,327.52	0.0078	1,634.44
207,728.91	6,136	24,264.12	44,643.91	0.0077	1,826.87
207,156.49	6,062	24,050.25	44,071.49	0.0076	1,990.13
207,000.71	6,041	23,995.45	43,915.71	0.0077	2,035.20
206,620.46	5,992	23,728.51	43,535.46	0.0077	2,143.24
205,940.66	5,904	23,346.70	42,855.66	0.0076	2,335.67
205,371.55	5,829	23,132.36	42,286.55	0.0075	2,498.93
205,216.67	5,809	23,075.81	42,131.67	0.0077	2,544.00
204,838.51	5,760	22,810.45	41,753.51	0.0077	2,652.04
204,162.35	5,672	22,428.72	41,077.35	0.0076	2,844.47
203,596.29	5,597	22,212.37	40,511.29	0.0075	3,007.73
203,442.22	5,576	22,154.21	40,357.22	0.0076	3,052.80
203,066.05	5,527	21,891.35	39,981.05	0.0076	3,160.84
202,393.39	5,439	21,510.45	39,308.39	0.0075	3,353.27
201,830.19	5,364	21,291.05	38,745.19	0.0075	3,516.53
201,676.88	5,344	21,231.74	38,591.88	0.0076	3,561.60
201,302.60	5,295	20,971.67	38,217.60	0.0076	3,669.64
200,633.32	5,207	20,591.97	37,548.32	0.0075	3,862.07
200,072.86	5,132	20,369.06	36,987.86	0.0074	4,025.33
199,920.27	5,111	20,308.80	36,835.27	0.0076	4,070.40
199,547.81	5,062	20,051.61	36,462.81	0.0076	4,178.44
198,881.78	4,974	19,673.34	35,796.78	0.0075	4,370.87
198,323.95	4,900	19,446.68	35,238.95	0.0074	4,534.13
198,172.06	4,879	19,385.59	35,087.06	0.0075	4,579.20
197,801.35	4,830	19,131.32	34,716.35	0.0075	4,687.24
197,138.47	4,742	18,754.59	34,053.47	0.0074	4,879.67
196,583.16	4,667	18,524.05	33,498.16	0.0074	5,042.93
196,431.94	4,647	18,462.19	33,346.94	0.0075	5,088.01
196,062.93	4,597	18,210.83	32,977.93	0.0075	5,196.04
195,403.09	4,509	17,835.73	32,318.09	0.0074	5,388.47

194,850.22	4,435	17,601.32	31,765.22	0.0073	5,551.73
194,699.66	4,414	17,538.74	31,614.66	0.0075	5,596.81
194,332.28	4,365	17,290.24	31,247.28	0.0075	5,704.84
193,675.40	4,277	16,916.78	30,590.40	0.0074	5,897.27
193,124.91	4,202	16,678.60	30,039.91	0.0073	6,060.53
192,974.98	4,182	16,615.33	29,889.98	0.0074	6,105.61
192,609.20	4,133	16,369.60	29,524.20	0.0074	6,213.65
191,955.17	4,045	15,997.75	28,870.17	0.0073	6,406.07
191,406.99	3,970	15,755.94	28,321.99	0.0073	6,569.33
191,257.70	3,949	15,691.99	28,172.70	0.0074	6,614.41
190,893.46	3,900	15,448.94	27,808.46	0.0074	6,722.45
190,242.21	3,812	15,078.66	27,157.21	0.0073	6,914.87
189,696.29	3,738	14,833.34	26,611.29	0.0072	7,078.13
189,547.61	3,717	14,768.69	26,462.61	0.0074	7,123.21
189,184.87	3,668	14,528.28	26,099.87	0.0074	7,231.25
188,536.33	3,580	14,159.50	25,451.33	0.0073	7,423.67
187,992.60	3,505	13,910.76	24,907.60	0.0072	7,586.93
187,844.51	3,485	13,845.38	24,759.51	0.0073	7,632.01
187,483.25	3,435	13,607.59	24,398.25	0.0073	7,713.74
186,837.32	3,347	13,240.29	23,752.32	0.0073	7,818.58
186,295.72	3,273	12,988.17	23,210.72	0.0072	7,920.10
186,148.22	3,252	12,922.04	23,063.22	0.0073	7,944.56
185,788.39	3,203	12,686.89	22,703.39	0.0073	8,008.15
185,145.01	3,115	12,321.04	22,060.01	0.0072	8,121.40
184,605.48	3,040	12,065.57	21,520.48	0.0072	8,217.49
184,458.55	3,020	11,998.69	21,373.55	0.0073	8,244.02
184,100.11	2,970	11,766.17	21,015.11	0.0073	8,307.61
183,459.21	2,882	11,401.76	20,374.21	0.0072	8,420.87
182,921.70	2,808	11,143.00	19,836.70	0.0071	8,516.96
182,775.33	2,787	11,075.36	19,690.33	0.0072	8,543.49
182,418.24	2,738	10,845.44	19,333.24	0.0073	8,607.08
181,779.75	2,650	10,482.45	18,694.75	0.0072	8,720.33
181,244.23	2,575	10,220.58	18,159.23	0.0071	8,816.43
181,098.42	2,555	10,152.12	18,013.42	0.0072	8,842.95
180,742.65	2,506	9,924.81	17,657.65	0.0072	8,906.54
180,106.51	2,418	9,563.11	17,021.51	0.0072	9,019.80
179,572.90	2,343	9,298.05	16,487.90	0.0071	9,115.89
179,427.62	2,322	9,228.68	16,342.62	0.0072	9,142.42
179,073.14	2,273	9,004.07	15,988.14	0.0072	9,206.01
178,439.28	2,185	8,643.75	15,354.28	0.0071	9,319.26
177,907.53	2,111	8,375.47	14,822.53	0.0070	9,415.36
177,762.77	2,090	8,305.22	14,677.77	0.0072	9,441.89
177,409.54	2,041	8,083.33	14,324.54	0.0072	9,505.47
176,777.91	1,953	7,724.36	13,692.91	0.0071	9,618.73
176,247.96	1,878	7,452.92	13,162.96	0.0070	9,714.82
176,103.71	1,858	7,381.75	13,018.71	0.0071	9,741.35

175,751.70	1,808	7,162.60	12,666.70	0.0072	9,804.94
175,122.22	1,720	6,804.95	12,037.22	0.0071	9,918.20
174,594.04	1,646	6,530.41	11,509.04	0.0070	10,014.29
174,450.29	1,625	6,458.25	11,365.29	0.0071	10,040.82
174,099.47	1,576	6,241.88	11,014.47	0.0071	10,104.41
173,472.11	1,488	5,885.53	10,387.11	0.0071	10,217.66
172,945.64	1,413	5,607.93	9,860.64	0.0070	10,313.75
172,802.38	1,393	5,534.73	9,717.38	0.0071	10,340.28
172,452.72	1,343	5,321.17	9,367.72	0.0071	10,403.87
171,827.41	1,255	4,966.10	8,742.41	0.0070	10,517.13
171,302.63	1,181	4,685.52	8,217.63	0.0070	10,613.22
171,159.84	1,160	4,611.16	8,074.84	0.0071	10,639.75
170,811.32	1,111	4,400.51	7,726.32	0.0071	10,703.34
170,188.01	1,023	4,046.66	7,103.01	0.0070	10,816.59
169,664.85	948	3,763.13	6,579.85	0.0069	10,912.69
169,522.55	928	3,687.62	6,437.55	0.0070	10,939.21
169,175.21	879	3,479.98	6,090.21	0.0071	11,002.80
168,553.73	791	3,127.13	5,468.73	0.0070	11,116.06
168,033.12	716	2,842.84	4,948.12	0.0069	11,212.15
167,892.41	695	2,768.51	4,807.41	0.0070	11,238.68
167,666.80	663	2,634.22	4,581.80	0.0070	11,280.53
167,215.18	599	2,370.20	4,130.18	0.0070	11,363.38
166,715.46	528	2,090.26	3,630.46	0.0069	11,455.24
166,363.64	477	1,895.01	3,278.64	0.0068	11,521.05
166,273.32	463	1,844.91	3,188.32	0.0069	11,538.15
166,049.57	431	1,713.82	2,964.57	0.0070	11,580.00
165,600.07	367	1,452.07	2,515.07	0.0070	11,662.85
165,102.13	295	1,171.05	2,017.13	0.0069	11,754.71
164,752.77	245	973.31	1,667.77	0.0068	11,820.51
164,663.14	231	922.06	1,578.14	0.0069	11,837.61
164,506.26	209	830.22	1,421.26	0.0070	11,867.12
164,173.85	161	637.51	1,088.85	0.0070	11,928.81
163,756.67	101	399.91	671.67	0.0068	12,005.92
163,378.79	45	181.04	293.79	0.0065	12,077.78
163,142.86	9	36.58	57.86	0.0064	12,125.16

Cruise at Altitude 10058 m					
Weight in Kg.	Max Range (Km)	Max Flight Time (Sec.)	Available Fuel (Kg)	Fuel burnt per m (Kg/m)	CCF (ATR)
212,692.86	6,971	27,887.26	49,607.86	0.0078	0.00
212,307.63	6,922	27,543.07	49,222.63	0.0078	110.43
211,622.19	6,834	27,191.93	48,537.19	0.0077	307.11
211,045.34	6,759	26,896.87	47,960.34	0.0078	473.98
210,885.49	6,739	26,813.63	47,800.49	0.0077	520.06
210,503.88	6,689	26,616.71	47,418.88	0.0077	630.48
209,825.87	6,602	26,267.90	46,740.87	0.0077	827.17
209,252.21	6,527	25,970.85	46,167.21	0.0077	994.04
209,094.34	6,506	25,896.80	46,009.34	0.0077	1,040.11
208,715.72	6,457	25,692.77	45,630.72	0.0077	1,150.54
208,042.81	6,369	25,343.06	44,957.81	0.0076	1,347.22
207,473.61	6,295	25,046.99	44,388.61	0.0076	1,514.09
207,316.83	6,274	24,969.57	44,231.83	0.0076	1,560.17
206,941.05	6,225	24,768.07	43,856.05	0.0076	1,670.59
206,273.19	6,137	24,418.46	43,188.19	0.0076	1,867.28
205,708.15	6,062	24,122.25	42,623.15	0.0076	2,034.15
205,552.57	6,042	24,045.79	42,467.57	0.0076	2,080.22
205,179.51	5,992	23,843.43	42,094.51	0.0075	2,190.65
204,516.45	5,904	23,493.82	41,431.45	0.0075	2,387.33
203,955.46	5,830	23,197.63	40,870.46	0.0075	2,554.21
203,800.97	5,809	23,121.00	40,715.97	0.0075	2,600.28
203,430.55	5,760	22,918.81	40,345.55	0.0075	2,710.70
202,772.13	5,672	22,569.20	39,687.13	0.0075	2,907.39
202,215.02	5,598	22,273.00	39,130.02	0.0075	3,074.26
202,061.60	5,577	22,196.25	38,976.60	0.0075	3,120.33
201,693.71	5,528	21,994.19	38,608.71	0.0074	3,230.76
201,039.76	5,440	21,644.57	37,954.76	0.0074	3,427.44
200,486.39	5,365	21,348.38	37,401.39	0.0074	3,594.32
200,334.00	5,345	21,271.52	37,249.00	0.0074	3,640.39
199,968.56	5,295	21,069.58	36,883.56	0.0074	3,750.82
199,318.91	5,207	20,719.95	36,233.91	0.0074	3,947.50
198,769.15	5,133	20,423.76	35,684.15	0.0074	4,114.37
198,617.74	5,112	20,346.54	35,532.74	0.0074	4,160.44
198,254.66	5,063	20,144.98	35,169.66	0.0073	4,270.87
197,609.17	4,975	19,795.33	34,524.17	0.0073	4,467.55
197,062.89	4,900	19,499.16	33,977.89	0.0073	4,634.43
196,912.44	4,880	19,421.76	33,827.44	0.0073	4,680.50
196,551.63	4,830	19,220.36	33,466.63	0.0073	4,790.93
195,910.15	4,743	18,870.72	32,825.15	0.0073	4,987.61
195,367.24	4,668	18,574.63	32,282.24	0.0073	5,154.48
195,217.69	4,647	18,496.70	32,132.69	0.0073	5,200.55
194,859.08	4,598	18,295.82	31,774.08	0.0073	5,310.98
194,221.48	4,510	17,946.09	31,136.48	0.0072	5,507.66
193,681.81	4,436	17,650.00	30,596.81	0.0072	5,674.54

193,533.16	4,415	17,571.90	30,448.16	0.0072	5,720.61
193,176.67	4,366	17,371.21	30,091.67	0.0072	5,831.04
192,542.81	4,278	17,021.48	29,457.81	0.0072	6,027.72
192,006.27	4,203	16,725.40	28,921.27	0.0072	6,194.59
191,858.50	4,183	16,647.48	28,773.50	0.0072	6,240.66
191,504.05	4,133	16,446.58	28,419.05	0.0072	6,351.09
190,873.80	4,045	16,096.87	27,788.80	0.0072	6,547.77
190,340.29	3,971	15,800.73	27,255.29	0.0071	6,714.65
190,193.35	3,950	15,722.74	27,108.35	0.0071	6,760.72
189,840.88	3,901	15,521.98	26,755.88	0.0071	6,871.15
189,214.12	3,813	15,172.26	26,129.12	0.0071	7,067.83
188,683.54	3,739	14,876.10	25,598.54	0.0071	7,234.70
188,537.40	3,718	14,797.83	25,452.40	0.0071	7,280.77
188,186.85	3,669	14,597.38	25,101.85	0.0071	7,391.20
187,563.46	3,581	14,247.64	24,478.46	0.0071	7,587.88
187,035.72	3,506	13,951.46	23,950.72	0.0071	7,754.76
186,890.36	3,486	13,873.14	23,805.36	0.0071	7,800.83
186,541.66	3,436	13,672.76	23,456.66	0.0071	7,883.13
185,921.54	3,348	13,323.03	22,836.54	0.0070	7,986.17
185,396.54	3,274	13,026.84	22,311.54	0.0070	8,087.04
185,251.92	3,253	12,947.99	22,166.92	0.0070	8,111.06
184,905.02	3,204	12,748.18	21,820.02	0.0070	8,173.97
184,288.08	3,116	12,398.42	21,203.08	0.0070	8,286.01
183,765.73	3,041	12,102.23	20,680.73	0.0070	8,381.06
183,621.82	3,021	12,023.00	20,536.82	0.0070	8,407.31
183,276.66	2,971	11,823.53	20,191.66	0.0070	8,470.21
182,662.79	2,884	11,473.82	19,577.79	0.0070	8,582.25
182,143.00	2,809	11,177.49	19,058.00	0.0070	8,677.31
181,999.81	2,788	11,098.33	18,914.81	0.0070	8,703.55
181,656.33	2,739	10,898.93	18,571.33	0.0070	8,766.46
181,045.42	2,651	10,549.20	17,960.42	0.0069	8,878.50
180,528.13	2,577	10,252.86	17,443.13	0.0069	8,973.56
180,385.62	2,556	10,173.50	17,300.62	0.0069	8,999.80
180,043.77	2,507	9,974.31	16,958.77	0.0069	9,062.71
179,435.74	2,419	9,624.59	16,350.74	0.0069	9,174.74
178,920.87	2,344	9,328.22	15,835.87	0.0069	9,269.80
178,779.01	2,324	9,248.48	15,694.01	0.0069	9,296.05
178,438.75	2,274	9,049.71	15,353.75	0.0069	9,358.95
177,833.52	2,186	8,699.97	14,748.52	0.0069	9,470.99
177,320.98	2,112	8,403.55	14,235.98	0.0069	9,566.05
177,179.80	2,091	8,323.98	14,094.80	0.0069	9,592.29
176,841.06	2,042	8,125.09	13,756.06	0.0069	9,655.20
176,238.52	1,954	7,775.35	13,153.52	0.0068	9,767.24
175,728.27	1,880	7,478.95	12,643.27	0.0068	9,862.30
175,587.69	1,859	7,398.89	12,502.69	0.0068	9,888.54
175,250.45	1,810	7,200.47	12,165.45	0.0068	9,951.44

174,650.55	1,722	6,850.74	11,565.55	0.0068	10,063.48
174,142.49	1,647	6,554.29	11,057.49	0.0068	10,158.54
174,002.53	1,627	6,474.07	10,917.53	0.0068	10,184.79
173,666.73	1,577	6,275.86	10,581.73	0.0068	10,247.69
173,069.38	1,489	5,926.13	9,984.38	0.0068	10,359.73
172,563.47	1,415	5,629.66	9,478.47	0.0068	10,454.79
172,424.09	1,394	5,549.20	9,339.09	0.0068	10,481.03
172,089.69	1,345	5,351.25	9,004.69	0.0068	10,543.94
171,494.82	1,257	5,001.53	8,409.82	0.0068	10,655.98
170,990.99	1,182	4,705.02	7,905.99	0.0067	10,751.03
170,852.18	1,162	4,624.34	7,767.18	0.0068	10,777.28
170,519.15	1,112	4,426.64	7,434.15	0.0067	10,840.18
169,926.68	1,025	4,076.93	6,841.68	0.0067	10,952.22
169,424.88	950	3,780.39	6,339.88	0.0067	11,047.28
169,286.63	929	3,699.48	6,201.63	0.0067	11,073.52
168,954.92	880	3,502.05	5,869.92	0.0067	11,136.43
168,364.79	792	3,152.34	5,279.79	0.0067	11,248.47
167,864.96	718	2,855.78	4,779.96	0.0067	11,343.53
167,727.24	697	2,774.62	4,642.24	0.0067	11,369.77
167,396.83	648	2,577.46	4,311.83	0.0067	11,432.68
166,808.97	560	2,227.76	3,723.97	0.0067	11,544.71
166,311.04	485	1,931.17	3,226.04	0.0067	11,639.77
166,173.86	465	1,849.78	3,088.86	0.0067	11,666.02
165,844.70	415	1,652.89	2,759.70	0.0067	11,728.92
165,259.05	328	1,303.20	2,174.05	0.0067	11,840.96
164,762.99	253	1,006.57	1,677.99	0.0066	11,936.02
164,626.25	232	924.84	1,541.25	0.0066	11,962.26
164,298.31	183	728.31	1,213.31	0.0066	12,025.17
163,714.84	95	378.62	629.84	0.0066	12,137.21
163,220.45	21	81.92	135.45	0.0066	12,232.27

Cruise at Altitude 10668 m					
Weight in Kg.	Max Range (Km)	Max Flight Time (Sec.)	Available Fuel (Kg)	Fuel burnt per m (Kg/m)	CCF (ATR)
211,311.26	6,971	28,189.86	48,226.26	0.0078	0.00
210,925.14	6,922	27,794.28	47,840.14	0.0078	113.38
210,235.12	6,834	27,438.36	47,150.12	0.0078	315.31
209,657.15	6,759	27,142.17	46,572.15	0.0077	486.64
209,498.02	6,739	27,098.36	46,413.02	0.0077	533.95
209,115.92	6,689	26,860.58	46,030.92	0.0077	647.32
208,436.23	6,602	26,505.48	45,351.23	0.0077	849.26
207,863.09	6,527	26,210.03	44,778.09	0.0077	1,020.59
207,705.56	6,506	26,141.67	44,620.56	0.0077	1,067.89
207,327.50	6,457	25,927.16	44,242.50	0.0076	1,181.27
206,655.58	6,369	25,572.49	43,570.58	0.0076	1,383.20
206,088.32	6,295	25,276.93	43,003.32	0.0076	1,554.53
205,932.43	6,274	25,204.60	42,847.43	0.0076	1,601.84
205,558.29	6,225	24,993.70	42,473.29	0.0076	1,715.21
204,893.45	6,137	24,639.52	41,808.45	0.0075	1,917.15
204,331.95	6,062	24,343.09	41,246.95	0.0075	2,088.48
204,177.63	6,042	24,270.42	41,092.63	0.0075	2,135.78
203,807.31	5,992	24,060.74	40,722.31	0.0075	2,249.16
203,149.20	5,905	23,706.49	40,064.20	0.0075	2,451.09
202,593.29	5,830	23,410.06	39,508.29	0.0074	2,622.42
202,440.51	5,809	23,337.25	39,355.51	0.0074	2,669.73
202,073.80	5,760	23,127.46	38,988.80	0.0074	2,783.10
201,422.09	5,672	22,773.53	38,337.09	0.0074	2,985.04
200,871.52	5,598	22,476.74	37,786.52	0.0074	3,156.37
200,720.19	5,577	22,403.57	37,635.19	0.0074	3,203.67
200,356.92	5,528	22,194.09	37,271.92	0.0073	3,317.05
199,711.35	5,440	21,840.60	36,626.35	0.0073	3,518.98
199,165.88	5,365	21,543.32	36,080.88	0.0073	3,690.31
199,015.94	5,345	21,470.24	35,930.94	0.0073	3,737.62
198,655.98	5,295	21,260.85	35,570.98	0.0073	3,850.99
198,016.28	5,207	20,907.63	34,931.28	0.0072	4,052.93
197,475.74	5,133	20,610.23	34,390.74	0.0072	4,224.26
197,327.08	5,112	20,535.34	34,242.08	0.0072	4,271.56
196,970.30	5,063	20,327.78	33,885.30	0.0072	4,384.94
196,336.27	4,975	19,974.59	33,251.27	0.0072	4,586.87
195,800.42	4,900	19,677.14	32,715.42	0.0072	4,758.20
195,653.04	4,880	19,601.77	32,568.04	0.0072	4,805.51
195,299.33	4,831	19,394.77	32,214.33	0.0072	4,918.88
194,670.71	4,743	19,041.60	31,585.71	0.0071	5,120.82
194,139.35	4,668	18,743.96	31,054.35	0.0071	5,292.15
193,993.22	4,647	18,668.62	30,908.22	0.0071	5,339.45
193,642.44	4,598	18,461.71	30,557.44	0.0071	5,452.83
193,019.00	4,510	18,108.63	29,934.00	0.0071	5,654.76
192,491.98	4,436	17,810.93	29,406.98	0.0070	5,826.09

192,347.00	4,415	17,734.69	29,262.00	0.0071	5,873.40
191,999.05	4,366	17,528.75	28,914.05	0.0070	5,986.77
191,380.60	4,278	17,175.63	28,295.60	0.0070	6,188.71
190,857.73	4,203	16,877.83	27,772.73	0.0070	6,360.04
190,713.88	4,183	16,801.13	27,628.88	0.0070	6,407.34
190,368.64	4,133	16,595.76	27,283.64	0.0070	6,520.72
189,754.99	4,046	16,242.66	26,669.99	0.0070	6,722.65
189,236.11	3,971	15,944.75	26,151.11	0.0069	6,893.98
189,093.35	3,950	15,867.72	26,008.35	0.0069	6,941.29
188,750.72	3,901	15,662.75	25,665.72	0.0069	7,054.66
188,141.66	3,813	15,309.69	25,056.66	0.0069	7,256.60
187,626.63	3,739	15,011.67	24,541.63	0.0069	7,427.93
187,484.91	3,718	14,934.24	24,399.91	0.0069	7,475.23
187,144.79	3,669	14,729.75	24,059.79	0.0069	7,588.61
186,540.17	3,581	14,376.71	23,455.17	0.0069	7,790.54
186,028.83	3,506	14,078.61	22,943.83	0.0068	7,961.87
185,888.12	3,486	14,000.80	22,803.12	0.0068	8,009.18
185,550.41	3,436	13,796.75	22,465.41	0.0068	8,092.45
184,950.06	3,348	13,443.74	21,865.06	0.0068	8,194.15
184,442.28	3,274	13,145.54	21,357.28	0.0068	8,294.84
184,302.54	3,253	13,067.40	21,217.54	0.0068	8,318.54
183,967.16	3,204	12,863.76	20,882.16	0.0068	8,381.06
183,370.91	3,116	12,510.77	20,285.91	0.0068	8,492.40
182,866.57	3,041	12,212.46	19,781.57	0.0067	8,586.86
182,727.78	3,021	12,134.11	19,642.78	0.0068	8,612.94
182,394.64	2,972	11,930.79	19,309.64	0.0067	8,675.45
181,802.35	2,884	11,577.80	18,717.35	0.0067	8,786.79
181,301.31	2,809	11,279.41	18,216.31	0.0067	8,881.26
181,163.43	2,789	11,200.81	18,078.43	0.0067	8,907.34
180,832.45	2,739	10,997.80	17,747.45	0.0067	8,969.85
180,243.98	2,651	10,644.82	17,158.98	0.0067	9,081.19
179,746.11	2,577	10,346.22	16,661.11	0.0067	9,175.66
179,609.12	2,556	10,267.61	16,524.12	0.0067	9,201.74
179,280.22	2,507	10,064.81	16,195.22	0.0067	9,264.25
178,695.42	2,419	9,711.85	15,610.42	0.0066	9,375.59
178,200.67	2,344	9,413.32	15,115.67	0.0066	9,470.05
178,064.50	2,324	9,334.08	14,979.50	0.0066	9,496.13
177,737.62	2,274	9,131.84	14,652.62	0.0066	9,558.65
177,156.39	2,187	8,778.87	14,071.39	0.0066	9,669.99
176,664.60	2,112	8,480.24	13,579.60	0.0066	9,764.45
176,529.25	2,091	8,400.72	13,444.25	0.0066	9,790.53
176,204.32	2,042	8,198.86	13,119.32	0.0066	9,853.04
175,626.52	1,954	7,845.90	12,541.52	0.0066	9,964.38
175,137.60	1,880	7,547.18	12,052.60	0.0065	10,058.85
175,003.04	1,859	7,467.31	11,918.04	0.0065	10,084.93
174,679.98	1,810	7,265.88	11,594.98	0.0065	10,147.44

174,105.50	1,722	6,912.93	11,020.50	0.0065	10,258.78
173,619.36	1,647	6,614.12	10,534.36	0.0065	10,353.25
173,485.55	1,627	6,533.91	10,400.55	0.0065	10,379.33
173,164.31	1,577	6,332.89	10,079.31	0.0065	10,441.84
172,593.04	1,489	5,979.95	9,508.04	0.0065	10,553.18
172,109.58	1,415	5,681.03	9,024.58	0.0065	10,647.64
171,976.51	1,394	5,600.49	8,891.51	0.0065	10,673.72
171,657.03	1,345	5,399.89	8,572.03	0.0065	10,736.24
171,088.85	1,257	5,046.95	8,003.85	0.0064	10,847.57
170,607.99	1,182	4,747.94	7,522.99	0.0064	10,942.04
170,475.62	1,162	4,667.05	7,390.62	0.0064	10,968.12
170,157.84	1,113	4,466.88	7,072.84	0.0064	11,030.63
169,592.67	1,025	4,113.96	6,507.67	0.0064	11,141.97
169,114.31	950	3,814.85	6,029.31	0.0064	11,236.44
168,982.63	930	3,733.63	5,897.63	0.0064	11,262.52
168,666.49	880	3,533.89	5,581.49	0.0064	11,325.03
168,104.23	792	3,180.98	5,019.23	0.0064	11,436.37
167,628.29	718	2,881.79	4,543.29	0.0064	11,530.84
167,497.28	697	2,800.22	4,412.28	0.0064	11,556.92
167,182.74	648	2,600.89	4,097.74	0.0064	11,619.43
166,623.29	560	2,248.00	3,538.29	0.0064	11,730.77
166,149.71	485	1,948.74	3,064.71	0.0063	11,825.23
166,019.34	465	1,866.83	2,934.34	0.0063	11,851.31
165,706.34	415	1,667.91	2,621.34	0.0063	11,913.83
165,149.63	328	1,315.03	2,064.63	0.0063	12,025.16
164,678.22	253	1,015.65	1,593.22	0.0063	12,119.63
164,548.47	232	933.43	1,463.47	0.0063	12,145.71
164,236.95	183	734.92	1,151.95	0.0063	12,208.22
163,682.89	95	382.05	597.89	0.0063	12,319.56
163,213.64	21	82.66	128.64	0.0062	12,414.03

Cruise at Altitude 11278 m					
Weight in Kg.	Max Range (Km)	Max Flight Time (Sec.)	Available Fuel (Kg)	Fuel burnt per m (Kg/m)	CCF (ATR)
211,398.70	6,971	28,256.81	48,313.70	0.0081	0.00
211,002.79	6,922	28,039.47	47,917.79	0.0081	115.93
210,296.01	6,834	27,660.61	47,211.01	0.0081	322.42
209,696.77	6,760	27,350.93	46,611.77	0.0080	497.61
209,532.13	6,739	27,277.42	46,447.13	0.0080	545.98
209,136.10	6,690	27,052.88	46,051.10	0.0081	661.91
208,428.66	6,602	26,675.48	45,343.66	0.0080	868.40
207,830.03	6,528	26,372.17	44,745.03	0.0080	1,043.59
207,666.12	6,507	26,308.68	44,581.12	0.0080	1,091.96
207,271.29	6,458	26,076.91	44,186.29	0.0080	1,207.89
206,565.98	6,370	25,704.67	43,480.98	0.0080	1,414.38
205,972.46	6,296	25,420.23	42,887.46	0.0079	1,589.57
205,810.90	6,275	25,364.47	42,725.90	0.0079	1,637.94
205,422.03	6,226	25,137.62	42,337.03	0.0079	1,753.87
204,728.37	6,138	24,769.06	41,643.37	0.0078	1,960.36
204,143.60	6,063	24,475.71	41,058.60	0.0078	2,135.55
203,983.39	6,043	24,403.72	40,898.39	0.0078	2,183.92
203,598.42	5,993	24,187.22	40,513.42	0.0078	2,299.85
202,914.71	5,905	23,832.16	39,829.71	0.0077	2,506.33
202,338.50	5,831	23,532.56	39,253.50	0.0077	2,681.53
202,180.42	5,810	23,465.38	39,095.42	0.0077	2,729.90
201,801.12	5,761	23,249.06	38,716.12	0.0077	2,845.83
201,127.39	5,673	22,893.92	38,042.39	0.0076	3,052.31
200,559.50	5,599	22,594.62	37,474.50	0.0076	3,227.51
200,403.61	5,578	22,524.76	37,318.61	0.0076	3,275.87
200,029.61	5,529	22,310.72	36,944.61	0.0076	3,391.81
199,365.40	5,441	21,955.92	36,280.40	0.0075	3,598.29
198,805.34	5,366	21,656.38	35,720.34	0.0075	3,773.49
198,651.56	5,346	21,585.19	35,566.56	0.0075	3,821.85
198,282.63	5,296	21,372.64	35,197.63	0.0075	3,937.79
197,627.44	5,208	21,017.91	34,542.44	0.0074	4,144.27
197,074.81	5,134	20,718.15	33,989.81	0.0074	4,319.46
196,923.01	5,113	20,645.67	33,838.01	0.0074	4,367.83
196,558.90	5,064	20,434.61	33,473.90	0.0074	4,483.77
195,912.26	4,976	20,079.93	32,827.26	0.0073	4,690.25
195,366.75	4,901	19,780.54	32,281.75	0.0073	4,865.44
195,216.96	4,881	19,708.31	32,131.96	0.0073	4,913.81
194,857.53	4,831	19,497.22	31,772.53	0.0073	5,029.74
194,219.03	4,743	19,141.95	31,134.03	0.0072	5,236.23
193,680.26	4,669	18,842.75	30,595.26	0.0072	5,411.42
193,532.29	4,648	18,769.34	30,447.29	0.0072	5,459.79
193,177.23	4,599	18,559.39	30,092.23	0.0072	5,575.72
192,546.46	4,511	18,204.00	29,461.46	0.0071	5,782.21
192,014.07	4,436	17,904.72	28,929.07	0.0071	5,957.40

191,867.82	4,416	17,830.18	28,782.82	0.0071	6,005.77
191,516.89	4,367	17,621.37	28,431.89	0.0071	6,121.70
190,893.45	4,279	17,266.07	27,808.45	0.0071	6,328.19
190,367.15	4,204	16,966.74	27,282.15	0.0070	6,503.38
190,222.56	4,183	16,891.55	27,137.56	0.0070	6,551.75
189,875.59	4,134	16,683.44	26,790.59	0.0070	6,667.68
189,259.13	4,046	16,328.14	26,174.13	0.0070	6,874.17
188,738.63	3,972	16,028.74	25,653.63	0.0069	7,049.36
188,595.60	3,951	15,952.76	25,510.60	0.0070	7,097.73
188,252.39	3,902	15,745.45	25,167.39	0.0069	7,213.66
187,642.60	3,814	15,390.22	24,557.60	0.0069	7,420.15
187,127.63	3,739	15,090.70	24,042.63	0.0069	7,595.34
186,986.09	3,719	15,014.05	23,901.09	0.0069	7,643.71
186,646.47	3,669	14,807.47	23,561.47	0.0069	7,759.64
186,043.03	3,581	14,452.31	22,958.03	0.0068	7,966.12
185,533.34	3,507	14,152.72	22,448.34	0.0068	8,141.32
185,393.25	3,486	14,075.62	22,308.25	0.0068	8,189.69
185,057.07	3,437	13,869.55	21,972.07	0.0068	8,273.63
184,459.69	3,349	13,514.39	21,374.69	0.0068	8,373.59
183,955.06	3,274	13,214.69	20,870.06	0.0067	8,473.69
183,816.32	3,254	13,136.93	20,731.32	0.0067	8,496.99
183,483.41	3,204	12,931.57	20,398.41	0.0067	8,558.86
182,891.85	3,117	12,576.48	19,806.85	0.0067	8,669.06
182,392.05	3,042	12,276.73	19,307.05	0.0067	8,762.56
182,254.64	3,021	12,198.69	19,169.64	0.0067	8,788.38
181,924.88	2,972	11,993.68	18,839.88	0.0067	8,850.25
181,338.86	2,884	11,638.56	18,253.86	0.0066	8,960.45
180,843.69	2,810	11,338.78	17,758.69	0.0066	9,053.95
180,707.54	2,789	11,260.21	17,622.54	0.0066	9,079.77
180,380.79	2,740	11,055.74	17,295.79	0.0066	9,141.64
179,800.09	2,652	10,700.65	16,715.09	0.0066	9,251.84
179,309.35	2,577	10,400.77	16,224.35	0.0066	9,345.34
179,174.40	2,557	10,321.71	16,089.40	0.0066	9,371.16
178,850.53	2,507	10,117.80	15,765.53	0.0065	9,433.03
178,274.92	2,419	9,762.74	15,189.92	0.0065	9,543.23
177,788.42	2,345	9,462.77	14,703.42	0.0065	9,636.73
177,654.63	2,324	9,383.36	14,569.63	0.0065	9,662.55
177,333.53	2,275	9,179.89	14,248.53	0.0065	9,724.42
176,762.81	2,187	8,824.84	13,677.81	0.0065	9,834.62
176,280.37	2,112	8,524.74	13,195.37	0.0064	9,928.12
176,147.68	2,092	8,444.88	13,062.68	0.0065	9,953.93
175,829.23	2,042	8,241.95	12,744.23	0.0064	10,015.81
175,263.20	1,954	7,886.94	12,178.20	0.0064	10,126.01
174,784.68	1,880	7,586.75	11,699.68	0.0064	10,219.51
174,653.06	1,859	7,506.56	11,568.06	0.0064	10,245.32
174,337.16	1,810	7,304.01	11,252.16	0.0064	10,307.20

173,775.63	1,722	6,949.05	10,690.63	0.0064	10,417.40
173,300.87	1,648	6,648.80	10,215.87	0.0063	10,510.90
173,170.27	1,627	6,568.15	10,085.27	0.0064	10,536.71
172,856.81	1,578	6,366.08	9,771.81	0.0063	10,598.59
172,299.61	1,490	6,011.16	9,214.61	0.0063	10,708.79
171,828.45	1,415	5,710.81	8,743.45	0.0063	10,802.29
171,698.85	1,394	5,629.84	8,613.85	0.0063	10,828.10
171,387.75	1,345	5,428.18	8,302.75	0.0063	10,889.98
170,834.70	1,257	5,073.29	7,749.70	0.0063	11,000.18
170,367.02	1,183	4,772.86	7,282.02	0.0062	11,093.68
170,238.36	1,162	4,691.54	7,153.36	0.0063	11,119.49
169,929.53	1,113	4,490.30	6,844.53	0.0062	11,181.37
169,380.48	1,025	4,135.45	6,295.48	0.0062	11,291.57
168,916.15	950	3,834.93	5,831.15	0.0062	11,385.07
168,788.40	930	3,753.25	5,703.40	0.0062	11,410.88
168,481.75	880	3,552.43	5,396.75	0.0062	11,472.76
167,936.56	792	3,197.60	4,851.56	0.0062	11,582.96
167,475.45	718	2,896.96	4,390.45	0.0062	11,676.46
167,348.58	697	2,814.93	4,263.58	0.0062	11,702.27
167,044.03	648	2,614.53	3,959.03	0.0062	11,764.15
166,502.55	560	2,259.72	3,417.55	0.0061	11,874.35
166,044.54	485	1,958.98	2,959.54	0.0061	11,967.85
165,918.52	465	1,876.58	2,833.52	0.0061	11,993.66
165,616.02	415	1,676.64	2,531.02	0.0061	12,055.54
165,078.10	328	1,321.85	1,993.10	0.0061	12,165.74
164,623.16	253	1,021.11	1,538.16	0.0061	12,259.24
164,498.14	232	938.55	1,413.14	0.0061	12,285.05
164,197.49	183	738.77	1,112.49	0.0061	12,346.93
163,663.00	95	384.05	578.00	0.0061	12,457.13

Cruise at Altitude 11887 m					
Weight in Kg.	Max Range (Km)	Max Flight Time (Sec.)	Available Fuel (Kg)	Fuel burnt per m (Kg/m)	CCF (ATR)
211,641.06	6,971	28,191.75	48,556.06	0.0075	0.00
211,515.20	6,954	28,553.60	48,430.20	0.0075	40.74
211,244.63	6,918	28,502.97	48,159.63	0.0075	128.69
210,883.72	6,870	28,373.52	47,798.72	0.0075	246.12
210,503.83	6,819	28,090.76	47,418.83	0.0075	369.75
210,179.87	6,776	27,977.33	47,094.87	0.0075	475.10
209,976.44	6,749	27,775.21	46,891.44	0.0075	541.33
209,926.07	6,742	27,797.92	46,841.07	0.0075	557.68
209,686.47	6,710	27,651.75	46,601.47	0.0075	635.62
209,211.94	6,647	27,375.69	46,126.94	0.0075	789.90
208,685.67	6,577	27,070.93	45,600.67	0.0075	960.97
208,308.57	6,527	26,854.01	45,223.57	0.0075	1,083.51
208,210.58	6,514	26,796.64	45,125.58	0.0075	1,115.36
207,846.12	6,465	26,586.75	44,761.12	0.0075	1,233.78
207,196.73	6,378	26,211.73	44,111.73	0.0075	1,444.69
206,645.59	6,305	25,895.13	43,560.59	0.0075	1,623.64
206,493.41	6,284	25,806.40	43,408.41	0.0075	1,673.04
206,128.61	6,236	25,597.47	43,043.61	0.0075	1,791.46
205,478.62	6,149	25,223.14	42,393.62	0.0075	2,002.37
204,926.98	6,075	24,907.45	41,841.98	0.0075	2,181.32
204,774.65	6,055	24,818.48	41,689.65	0.0075	2,230.72
204,409.53	6,006	24,610.27	41,324.53	0.0075	2,349.14
203,758.94	5,919	24,236.63	40,673.94	0.0075	2,560.05
203,206.80	5,845	23,921.73	40,121.80	0.0075	2,739.00
203,054.34	5,825	23,832.63	39,969.34	0.0075	2,788.40
202,688.88	5,776	23,625.04	39,603.88	0.0075	2,906.82
202,037.71	5,689	23,252.08	38,952.71	0.0075	3,117.73
201,485.07	5,615	22,937.88	38,400.07	0.0075	3,296.68
201,332.48	5,594	22,848.72	38,247.48	0.0075	3,346.08
200,966.69	5,545	22,641.68	37,881.69	0.0075	3,464.50
200,314.95	5,458	22,269.41	37,229.95	0.0075	3,675.41
199,761.83	5,384	21,955.84	36,676.83	0.0075	3,854.36
199,609.10	5,363	21,866.69	36,524.10	0.0075	3,903.76
199,242.99	5,314	21,660.14	36,157.99	0.0075	4,022.18
198,590.67	5,227	21,288.55	35,505.67	0.0075	4,233.09
198,037.07	5,153	20,975.55	34,952.07	0.0075	4,412.04
197,884.21	5,132	20,886.50	34,799.21	0.0075	4,461.44
197,517.78	5,083	20,680.33	34,432.78	0.0075	4,579.86
196,864.91	4,995	20,309.44	33,779.91	0.0074	4,790.77
196,310.83	4,921	19,996.94	33,225.83	0.0074	4,969.72
196,157.85	4,900	19,908.11	33,072.85	0.0074	5,019.12
195,791.10	4,851	19,702.21	32,706.10	0.0074	5,137.54
195,137.67	4,763	19,332.03	32,052.67	0.0074	5,348.45
194,583.13	4,689	19,019.97	31,498.13	0.0074	5,527.40

194,430.01	4,668	18,931.47	31,345.01	0.0074	5,576.80
194,062.95	4,619	18,725.74	30,977.95	0.0074	5,695.22
193,408.97	4,531	18,356.28	30,323.97	0.0074	5,906.13
192,853.97	4,456	18,044.60	29,768.97	0.0074	6,085.08
192,700.73	4,436	17,956.57	29,615.73	0.0074	6,134.48
192,333.36	4,386	17,750.88	29,248.36	0.0074	6,252.90
191,678.84	4,298	17,382.14	28,593.84	0.0074	6,463.81
191,123.38	4,224	17,070.82	28,038.38	0.0074	6,642.76
190,970.04	4,203	16,983.46	27,885.04	0.0074	6,692.16
190,602.35	4,153	16,777.48	27,517.35	0.0074	6,810.58
189,947.22	4,065	16,409.57	26,862.22	0.0074	7,021.49
189,391.71	3,990	16,100.65	26,306.71	0.0074	7,200.44
189,238.63	3,970	16,016.10	26,153.63	0.0074	7,249.84
188,872.60	3,920	15,815.89	25,787.60	0.0073	7,368.26
188,223.93	3,832	15,459.57	25,138.93	0.0073	7,579.17
187,676.82	3,757	15,157.34	24,591.82	0.0073	7,758.12
187,526.33	3,736	15,074.55	24,441.33	0.0073	7,807.52
187,166.43	3,686	14,873.78	24,081.43	0.0072	7,925.94
186,528.42	3,598	14,517.45	23,443.42	0.0072	8,136.85
185,990.20	3,523	14,215.22	22,905.20	0.0072	8,315.80
185,842.12	3,503	14,132.29	22,757.12	0.0071	8,365.20
185,487.95	3,453	13,931.66	22,402.95	0.0071	8,449.74
184,860.00	3,365	13,575.33	21,775.00	0.0071	8,547.86
184,330.13	3,290	13,273.09	21,245.13	0.0070	8,647.31
184,184.33	3,269	13,190.10	21,099.33	0.0070	8,670.16
183,835.58	3,219	12,989.53	20,750.58	0.0070	8,731.34
183,217.11	3,131	12,633.21	20,132.11	0.0070	8,840.30
182,695.12	3,056	12,330.96	19,610.12	0.0069	8,932.75
182,551.46	3,036	12,247.91	19,466.46	0.0069	8,958.28
182,207.82	2,986	12,047.41	19,122.82	0.0069	9,019.45
181,598.31	2,898	11,691.09	18,513.31	0.0069	9,128.42
181,083.77	2,823	11,388.84	17,998.77	0.0068	9,220.87
180,942.15	2,802	11,305.74	17,857.15	0.0068	9,246.39
180,603.33	2,752	11,105.29	17,518.33	0.0068	9,307.57
180,002.30	2,664	10,748.97	16,917.30	0.0068	9,416.53
179,494.80	2,589	10,446.71	16,409.80	0.0068	9,508.98
179,355.10	2,569	10,363.57	16,270.10	0.0067	9,534.50
179,020.86	2,519	10,163.17	15,935.86	0.0067	9,595.68
178,427.84	2,431	9,806.85	15,342.84	0.0067	9,704.64
177,927.03	2,356	9,504.58	14,842.03	0.0067	9,797.09
177,789.15	2,335	9,421.40	14,704.15	0.0067	9,822.62
177,459.25	2,285	9,221.05	14,374.25	0.0066	9,883.80
176,873.84	2,197	8,864.73	13,788.84	0.0066	9,992.76
176,379.35	2,122	8,562.46	13,294.35	0.0066	10,085.21
176,243.21	2,102	8,479.24	13,158.21	0.0066	10,110.73
175,917.42	2,052	8,278.92	12,832.42	0.0065	10,171.91

175,339.23	1,964	7,922.61	12,254.23	0.0065	10,280.87
174,850.77	1,889	7,620.33	11,765.77	0.0065	10,373.32
174,716.26	1,868	7,537.09	11,631.26	0.0065	10,398.85
174,394.39	1,818	7,336.80	11,309.39	0.0065	10,460.02
173,823.07	1,730	6,980.49	10,738.07	0.0064	10,568.99
173,340.33	1,655	6,678.21	10,255.33	0.0064	10,661.44
173,207.39	1,635	6,594.93	10,122.39	0.0064	10,686.96
172,889.23	1,585	6,394.68	9,804.23	0.0064	10,748.14
172,324.45	1,497	6,038.37	9,239.45	0.0064	10,857.10
171,847.15	1,422	5,736.08	8,762.15	0.0064	10,949.55
171,715.70	1,401	5,652.78	8,630.70	0.0063	10,975.07
171,401.09	1,351	5,452.56	8,316.09	0.0063	11,036.25
170,842.53	1,263	5,096.25	7,757.53	0.0063	11,145.21
170,370.43	1,188	4,793.97	7,285.43	0.0063	11,237.66
170,240.39	1,168	4,710.63	7,155.39	0.0063	11,263.19
169,929.16	1,118	4,510.45	6,844.16	0.0063	11,324.37
169,376.53	1,030	4,154.14	6,291.53	0.0062	11,433.33
168,909.38	955	3,851.85	5,824.38	0.0062	11,525.78
168,780.70	934	3,768.49	5,695.70	0.0062	11,551.30
168,472.69	884	3,568.34	5,387.69	0.0062	11,612.48
167,925.73	796	3,212.04	4,840.73	0.0062	11,721.44
167,463.31	721	2,909.75	4,378.31	0.0062	11,813.89
167,335.92	700	2,826.36	4,250.92	0.0062	11,839.42
167,030.99	651	2,626.24	3,945.99	0.0061	11,900.59
166,489.44	563	2,269.94	3,404.44	0.0061	12,009.56
166,031.54	488	1,967.65	2,946.54	0.0061	12,102.01
165,905.39	467	1,884.24	2,820.39	0.0061	12,127.53
165,603.40	417	1,684.15	2,518.40	0.0061	12,188.71
165,067.03	329	1,327.86	1,982.03	0.0061	12,297.67
164,613.45	254	1,025.57	1,528.45	0.0060	12,390.12
164,488.52	234	942.18	1,403.52	0.0060	12,415.64
164,291.51	201	810.44	1,206.51	0.0060	12,455.91
163,902.33	136	549.81	817.33	0.0060	12,535.62
163,471.97	65	260.81	386.97	0.0060	12,624.00
163,164.50	13	53.80	79.50	0.0060	12,687.31

BIBLIOGRAPHY

[1] S. Lee, W. Fahey, P. Forster, P. Newton, and R. Wit. Aviation and global climate change in the 21^{st} century. Atmospheric Environment, Vol. 43, pp. 3520-3537, 2009.

[2] M. Niklaß, B. Lührs, V. Grewe, K. Dahlmann, T. Luchkova, F. Linke, and V. Gollnick. Potential to reduce the climate impact of aviation by climate restricted airspaces. 19^{th} Air Transport Research Society (ATRS) World Conference, Singapore, 2015.

[3] C. Frömming, V. Grewe, P. Jöckel, S. Brinkop, H. Dietmüller, S.; Garny, M. Ponater, E. Tsati, and S. Matthes. Climate Cost Functions as a Basis for Climate Optimized Flight Trajectories. 10^{th} USA/Europe ATM Res. and Dev. Seminar, 2013.

[4] B. Lührs, M. Niklaß, C. Frömming, V. Grewe, and V. Gollnick. Cost-Benefit Assessment of 2D and 3D Climate and Weather Optimized Trajectories. 16^{th} AIAA Aviation Technology, Integration and Operations Conference, 2016.

[5] M. Soler, A. Olivares, and E. Staffetti. Hybrid Optimal Control Approach to Commercial Aircrafts 3D Multiphases Trajectory Optimization. AIAA Guidance, Navigation, and Control Conference, 2010.

[6] IPCC. Climate Change 2013: The Physical Science Basis. Contribution of Working Group I to the Fifth Assessment Report of the Intergovernmental Panel on Climate Change. Cambridge University Press, Cambridge, United Kingdom and New York, NY, USA, 2013.

[7] D. Lee and G. Pitari. Transport impacts on atmosphere and climate: Aviation. Atmospheric Environment, Vol. 44, pp. 4678–4734, 2010.

[8] IATA. New IATA Passenger Forecast Reveals Fast-Growing Markets of the Future. http://www.iata.org/pressroom/pr/Pages/2014-10-16-01.aspx, 2014. Accessed: 26-Apr.-2017.

[9] J. Penner and D. Lister. Aviation and the Global Atmosphere. A Special Report of IPCC Working Groups I and III. Cambridge University Press, 1999.

[10] R. Oliveira and C. Büskens. Benefits of Optimal Flight Planning on Noise and Emissions Abatement at the Frankfurt Airport. AIAA Guidance, Navigation, and Control Conference, 2012.

[11] B. Sridhar, H. Ng, N. Chen, and J. Li. Three-Dimensional Trajectory Design for Reducing Climate Impact of Trans-Atlantic Flights. 14^{th} AIAA Aviation Technology, Integration, and Operations Conference, 2014-2289, 2014.

[12] S. Waitz, J. Townsend, J. Cutcher-Gershenfeld, E. Greitzer, and J. Kerrebrock. Report to the United States Congress: Aviation and the Environment, A National Vision, Framework for Goals and Recommended Actions, . Partnership for Air Transportation Noise and Emissions Reduction, MIT, Cambridge, MA., p. 18, 2014.

[13] K. Gierens, L. Lim, and K. Eleftheratos. A Review of Various Strategies for Contrail Avoidance. The Open Atmospheric Science Journal, Vol. 2, pp. 1-7, 2008.

[14] S. Hartjes, H. Visser, and T. Hendriks. Contrail Mitigation through 3D Aircraft Trajectory Optimization. 16^{th} AIAA Aviation Technology, Integration, and Operations Conference, 2016.

[15] B. Sridhar, H. Ng, and N. Chen. Aircraft Trajectory Optimization and Contrails Avoidance in the Presence of Winds. Journal of Guidance, Control, and Dynamics, Vol. 34, No. 5, pp. 1577-1584, 2011.

[16] S. Park and J. Clarke. Vertical Trajectory Optimization to Minimize Environmental Impact in the Presence of Wind. Journal of Aircraft, Vol. 53, No. 3, pp. 725-737, 2016.

[17] D. Pargett and M. Ardema. Flight Path Optimization at Constant Altitude. Journal of Guidance, Control and Dynamics, Vol. 30, No. 4, pp. 1197-1201, 2007.

[18] M. Ardema and B. Asuncion. Flight Path Optimization at Constant Altitude. Variational Analysis and Aerospace Engineering, Springer Optimization and Its Applications, Vol. 33, 2005.

[19] H. Ng, B. Sridhar, and S. Grabbe. A Practical Approach for Optimizing Aircraft Trajectories in Winds. 31^{st} Digital Avionics Systems Conference, pp. 3D6-1-3D6-14, 2012.

[20] V. Grewe and A. Stenke. AirClim: an efficient tool for climate evaluation of aircraft technology. Atmospheric Chemistry and Physics, Vol. 8, pp. 4621-4639, 2008.

[21] G. Volker, C. Frömming, and S. Matthes. Aircraft Routing with Minimal Climate Impact: The REACT4C Cost Function modelling approach. Geoscientific Model Development, pp. 175-201, 2014.

[22] International Virtual Aviation Organization. Semi-Circular Rule. IVAO HQ training department, 2015.

[23] ICAO. Best Practices for Fuel Economy. ICAO Operational Measures Workshop, Montreal, 2006.

[24] Airbus. A330 & A340 Flight Crew Training Manual. Airbus, 2004.

[25] H. Visser. Aircraft Performance Optimization. Delft University of Technology, Course AE-4447, 2014.

[26] H. Ng, B. Sridhar, and S. Grabbe. Optimizing Aircraft Trajectories with Multiple Cruise Altitudes in the Presence of Winds. Journal of Aerospace Information Systems, Vol. 11, No. 1, pp. 35-47, 2014.

[27] H. Gonzalez, R. Vasudevan, M. Kamgarpour, S. Sastry, R. Bajcsy, and C. Tomlin. A Descent Algorithm for the Optimal Control of Constrained Nonlinear Switched Dynamical Systems. 13^{th} ACM International Conference, Hybrid Systems: Computation and Control, pp. 51-60, 2010.

[28] X. Xu and P. Antsaklis. Results and Perspectives on Computational Methods for Optimal Control of Switched Systems. Hybrid Systems: Computation and Control, Springer, pp. 540–555., 2003.

[29] A. Harada and Y. Miyazawa. Dynamic Programming Applications to Flight Trajectory Optimization. 19^{th} IFAC Symposium on Automatic Control in Aerospace, Vol. 46, pp.441-446, 2013.

[30] M. Kamgarpour, M. Soler, C. Tomlin, A. Olivares, and J. Lygeros. Hybrid Optimal Control for Aircraft Trajectory Design with a Variable Sequence of Modes. 18^{th} IFAC World Congress Milano, Vol. 44, pp. 7238-7243, 2011.

[31] H. Visser and S. Hartjes. Economic and Environmental Optimization of Flight Trajectories Connecting a City-Pair. Journal of Aerospace Engineering, Vol. 228, No. 6, pp. 980-993, 2014.

[32] P. Bonami, A. Olivares, M. Soler, and E. Staffetti. Multiphase Mixed-Integer Optimal Control Approach to Aircraft Trajectory Optimization. Journal of Guidance, Control, and Dynamics, Vol. 36, No. 5, pp. 1267-1277, 2013.

[33] A. Wächter and L. Biegler. On the Implementation of an Interior-Point Filter Line-Search Algorithm for Large-Scale Nonlinear Programming. Mathematical Programming Ser. A 106, pp. 25-57, 2006.

[34] U. Boscain and B. Piccoli. An Introduction to Optimal Control. Technical Report, S.I.S.S.A, Trieste,Italy, 2004.

[35] D. DuBois and G. Paynter. Fuel Flow Method 2 for Estimating Aircraft Emissions. SAE Technical Paper 2006-01-1987, 2006.

[36] Eurocontrol Experimental Centre. Concept Document for the Base of Aircraft Data (BADA) Family 4. EEC Technical/Scientific Report No. 12/11/22-57, 2014.

[37] A. Nuic, M. Iagaru, E. Gallo, and F. Navarro. Advanced Aircraft Performance Modelling for ATM: BADA 4.0 Results. 24^{th} Digital Avionics System Conference, 2005.

[38] Airbus. Getting to Grips with Cost Index. Flight Operations Support & Line Assistance, Issue-II, 1998.

[39] R. Liebeck, D. Andrastek, J. Chau, R. Girvin, R. Lyon, B. Rawdon, P. Scott, and R. Wright. Advanced Subsonic Airplane Design & Economic Studies. National Aeronautics and Space Administration Lewis Research Center, NAS3-25965, 1995.

[40] M. Niklaß, K. Dahlmann, C. Frömming, V. Grewe, V. Gollnick, B. Lührs, and J. Manen. Are Climate Restricted Areas a Viable Interim Climate Mitigation Option over the North Atlantic? 16^{th} AIAA Aviation Technology, Integration, and Operations Conference, AIAA Aviation Forum, 2016.

[41] A. Rao, D. Benson, C. Darby, M. Patterson, C. Francolin, and I. Sanders. GPOPS, A MATLAB Software for Solving Multiple-Phase Optimal Control Problems Using the Gauss Pseudospectral Method. ACM Transactions on Mathematical Software, Vol. 37, No. 2, Article 22, 2010.

[42] C. Francolin, D. Benson, W. Hager, and A. Rao. Costate approximation in optimal control using integral Gaussian quadrature orthogonal collocation methods. Optimal Control Applications and Methods, Vol. 36, No. 4, pp. 381-397, 2014.